

1. The first part of the document discusses the importance of maintaining accurate records of all transactions and activities. It emphasizes the need for transparency and accountability in financial reporting.

2. The second part of the document outlines the various methods and techniques used to collect and analyze data. It includes a detailed description of the experimental procedures and the statistical tools employed.

3. The third part of the document presents the results of the study, including a comparison of the different methods and a discussion of the implications of the findings.

4. The fourth part of the document concludes the study and provides a summary of the key findings and recommendations for future research.

5. The fifth part of the document contains a list of references and a bibliography, providing a comprehensive overview of the literature related to the study.

6. The sixth part of the document includes a list of figures and tables, which are essential for understanding the data and results presented in the study.

7. The seventh part of the document contains a list of appendices, which provide additional information and data related to the study.

8. The eighth part of the document includes a list of footnotes and a glossary, which are useful for clarifying terms and providing additional context.

9. The ninth part of the document contains a list of acknowledgments, which recognize the contributions of individuals and organizations that supported the study.

10. The tenth part of the document includes a list of contact information and a list of authors, providing a way to reach the researchers and learn more about the study.

11. The eleventh part of the document contains a list of references and a bibliography, providing a comprehensive overview of the literature related to the study.

12. The twelfth part of the document includes a list of figures and tables, which are essential for understanding the data and results presented in the study.

13. The thirteenth part of the document contains a list of appendices, which provide additional information and data related to the study.

14. The fourteenth part of the document includes a list of footnotes and a glossary, which are useful for clarifying terms and providing additional context.

15. The fifteenth part of the document contains a list of acknowledgments, which recognize the contributions of individuals and organizations that supported the study.

16. The sixteenth part of the document includes a list of contact information and a list of authors, providing a way to reach the researchers and learn more about the study.

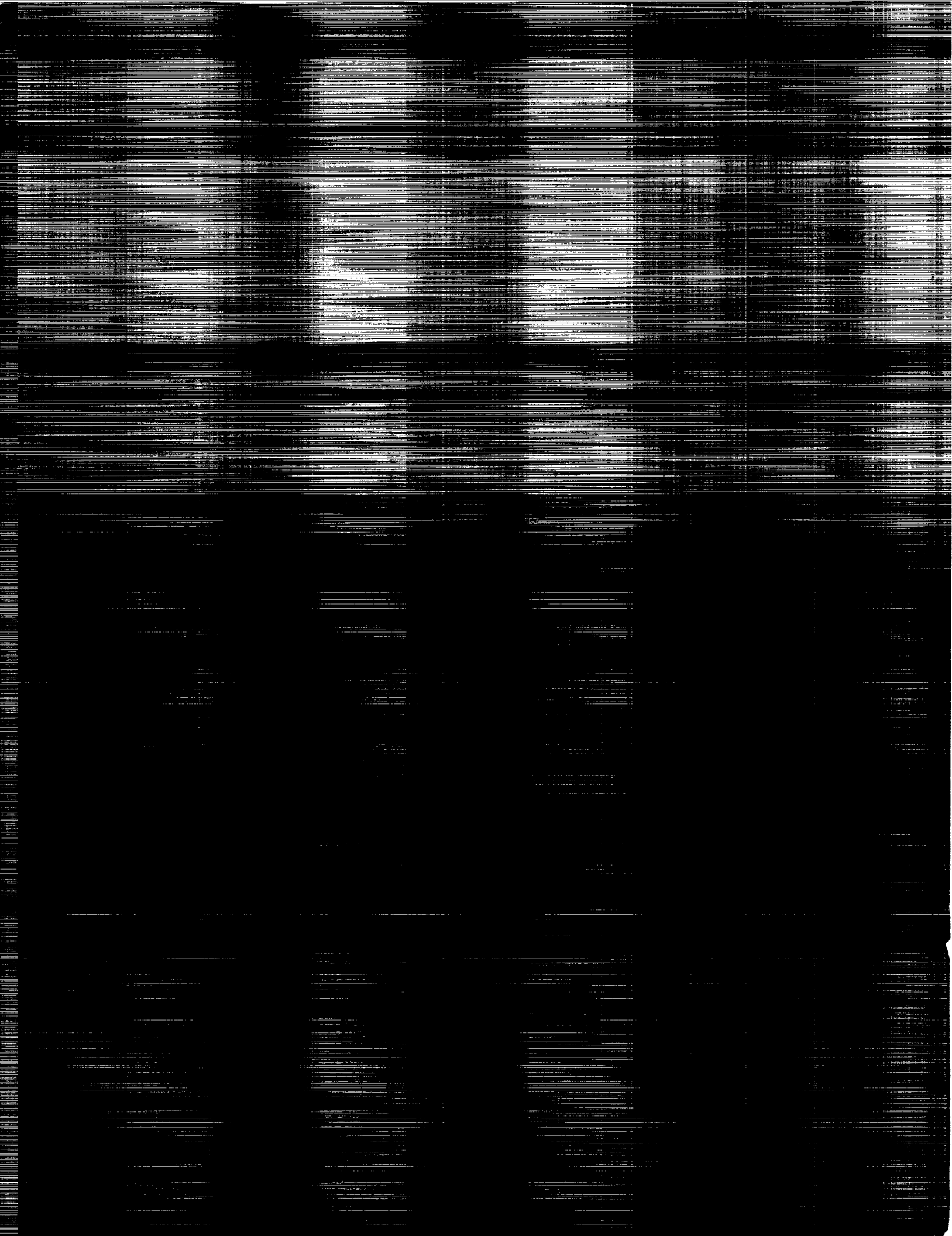
17. The seventeenth part of the document contains a list of references and a bibliography, providing a comprehensive overview of the literature related to the study.

18. The eighteenth part of the document includes a list of figures and tables, which are essential for understanding the data and results presented in the study.

19. The nineteenth part of the document contains a list of appendices, which provide additional information and data related to the study.

20. The twentieth part of the document includes a list of footnotes and a glossary, which are useful for clarifying terms and providing additional context.

ABSTRACT VOLUME



**First Landing Site Workshop for the
2003 Mars
Exploration Rovers**

January 24–25, 2001
NASA Ames Research Center
Mountain View, California

Sponsored by

National Aeronautics and Space Administration
NASA Ames Research Center
Lunar and Planetary Institute

Steering Committee

Matt Golombek, Co-Chair, *Jet Propulsion Laboratory*
John Grant, Co-Chair, *Smithsonian Institution*
Bruce Jakosky, *University of Colorado, Boulder*
Mike Carr, *U.S. Geological Survey, Menlo Park*
Phil Christensen, *Arizona State University*
Jack Farmer, *Arizona State University*
Virginia Gulick, *NASA Ames Research Center/SETI Institute*
Michael Malin, *Malin Space Science Systems, Inc.*
George McGill, *University of Massachusetts*
Richard Morris, *NASA Johnson Space Center*
Timothy Parker, *Jet Propulsion Laboratory*
Roger Phillips, *Washington University*
Mike Shepard, *Jet Propulsion Laboratory*
Kenneth Tanaka, *U.S. Geological Survey, Flagstaff*

Compiled in 2001 by
LUNAR AND PLANETARY INSTITUTE

The Institute is operated by the Universities Space Research Association under Contract No. NASW-4574 with the National Aeronautics and Space Administration.

Material in this volume may be copied without restraint for library, abstract service, education, or personal research purposes; however, republication of any paper or portion thereof requires the written permission of the authors as well as the appropriate acknowledgment of this publication.

Abstracts in this volume may be cited as

Author A. B. (2001) Title of abstract. In *First Landing Site Workshop for the 2003 Mars Exploration Rovers*, p. xx. LPI Contribution No. 1079, Lunar and Planetary Institute, Houston.

This report is distributed by

ORDER DEPARTMENT
Lunar and Planetary Institute
3600 Bay Area Boulevard
Houston TX 77058-1113
Phone: 281-486-2172
Fax: 281-486-2186
E-mail: order@lpi.usra.edu

Please contact the Order Department for ordering information.

Preface

This volume contains abstracts that have been accepted for presentation at the First Landing Site Workshop for the 2003 Mars Exploration Rovers, January 24–25, 2001. The Steering Committee consisted of Matt Golombek, Co-Chair (*Jet Propulsion Laboratory*), John Grant, Co-Chair (*Smithsonian Institution*), Bruce Jakosky (*University of Colorado, Boulder*), Mike Carr (*U.S. Geological Survey, Menlo Park*), Phil Christensen (*Arizona State University*), Jack Farmer (*Arizona State University*), Virginia Gulick (*NASA Ames Research Center/SETI Institute*), Michael Malin (*Malin Space Science Systems, Inc.*), George McGill (*University of Massachusetts*), Richard Morris (*NASA Johnson Space Center*), Timothy Parker (*Jet Propulsion Laboratory*), Roger Phillips (*Washington University*), Mike Shepard (*Jet Propulsion Laboratory*), and Kenneth Tanaka (*U.S. Geological Survey, Flagstaff*).

Logistics were provided by Virginia Gulick and the Lunar and Planetary Institute. Administrative and publications support were provided by the Publications and Program Services Department of the Lunar and Planetary Institute.



Contents

Exobiology at Sinus Meridiani — 2003 and Beyond <i>C. C. Allen, F. Westall, and R. T. Schelble</i>	1
Results from FIDO Prototype Mars Rover Field Trials <i>R. E. Arvidson</i>	3
Potential MER Landing Sites in the Terra Meridiani and Valles Marineris Regions of Mars <i>N. G. Barlow</i>	4
Mineralogy Considerations for 2003 MER Site Selection and the Importance for Astrobiology <i>J. L. Bishop</i>	6
Assessing Layered Materials in Gale Crater <i>N. T. Bridges</i>	8
Exploring Impact Crater Paleolakes in 2003 <i>N. A. Cabrol and E. A. Grin</i>	10
The TES Hematite-rich Region in Sinus Meridiani; A Proposed Landing Site for the 2003 Rover <i>P. R. Christensen, J. Bandfield, V. Hamilton, S. Ruff, R. Morris, M. Lane, and M. Malin</i>	12
Analysis of Potential MER Sites in the Southern Isidis Region <i>L. S. Crumpler, K. L. Tanaka, and T. M. Hare</i>	14
MER 2003 Landing Site Proposal: Amazonian Lacustrine Materials <i>R. A. De Hon</i>	16
A New Era in Geodesy and Cartography: Implications for Landing Site Operations <i>T. C. Duxbury</i>	17
MOLA-based Landing Site Characterization <i>T. C. Duxbury and A. B. Ivanov</i>	18
Mars 2003: Site Priorities for Astrobiology <i>J. Farmer, D. Nelson, R. Greeley, and R. Kuzmin</i>	20
Submarine Volcanic Landforms and Endolithic Microorganisms <i>M. R. Fisk</i>	22

Potential Noachian-aged Sites for MER-B <i>M. S. Gilmore and K. L. Tanaka</i>	23
Extreme Rock Distributions on Mars and Implications for Landing Safety <i>M. P. Golombek</i>	25
Thermal Inertia of Rocks and Rock Populations and Implications for Landing Hazards on Mars <i>M. P. Golombek, B. M. Jakosky, and M. T. Mellon</i>	27
Potential Mars Exploration Rover Landing Sites West and South of Apollinaris Patena <i>V. C. Gulick</i>	29
A Virtual Web Environment for Mars Landing Site Studies <i>V. C. Gulick, D. G. Deardorff, and G. A. Briggs</i>	31
Planetary GIS on the Web for the MER 2003 Landers <i>T. M. Hare, K. L. Tanaka, and J. A. Skinner</i>	33
Recent Results from Mars Global Surveyor Affecting Landing Site Selection and Habitats for Past or Present Biological Activity <i>W. K. Hartmann</i>	35
MER 2003 Operations Support and Landing Site Characterization by Mars Express HRSC/SRC Imaging Data <i>E. Hauber, G. Neukum, T. Behnke, R. Jaumann, R. Pischel, H. Hoffmann, J. Oberst, and the HRSC Science Team</i>	37
Terra Meridiani Hematite Deposit Landing Site Rationale <i>B. M. Hynek, R. E. Arvidson, R. J. Phillips, and F. P. Seelos</i>	39
Broad Perspectives on Mars Landing Site Selection: Geological Factors from Centimeter to Kilometer Scales <i>B. M. Jakosky and M. P. Golombek</i>	41
Physical Properties of Potential Mars Landing Sites from MGS TES-derived Thermal Inertia <i>B. M. Jakosky, M. T. Mellon, and S. M. Pelkey</i>	43
Atmospheric Constraints on Landing Site Selection <i>D. M. Kass and J. T. Schofield</i>	45
Eos Chasma as a Potential Site for the MER-A Landing <i>R. O. Kuzmin, R. Greeley, D. M. Nelson, J. D. Farmer, and H. P. Klein</i>	47

Melas Chasma: Major Scientific Opportunity for MER 2003 <i>N. Mangold, F. Costard, P. Masson, and J.-P. Peulvast</i>	49
Potential 2003 Landing Sites in the Cerberus Plains, SE Elysium Planitia <i>A. McEwen, P. Lanagan, R. Beyrer, L. Keszthelyi, and D. Burr</i>	51
Hubble Space Telescope Visible to Near-IR Imaging and Spectroscopy of Mars in Support of Future Landing Site Selection <i>R. V. Morris and J. F. Bell III</i>	53
Durius Valles Outflow Basin, Mars: Proposed Site for MER-A <i>D. M. Nelson, J. D. Farmer, R. Greeley, R. O. Kuzmin, and H. P. Klein</i>	55
Impact Crater Landing Sites for the 2003 Mars Explorer Rovers — Accessing Lacustrine and Hydrothermal Deposits <i>H. E. Newsom</i>	57
TES Hematite Landing Sites in Sinus Meridiani for 2003 Mars Exploration Rover <i>E. Noreen, K. L. Tanaka, and M. G. Chapman</i>	59
Ganges Chasma Landing Site: Access to Layered Mesa Material, Wall Rock, and Sand Sheet <i>J. W. Rice Jr.</i>	61
A Spectrally-based Global Dust Cover Index for Mars from Thermal Emission Spectrometer Data <i>S. W. Ruff and P. R. Christensen</i>	63
The Athena Science Payload for the 2003 Mars Exploration Rovers <i>S. W. Squyres and the Athena Science Team</i>	65
Scientific Rationale for Mars Exploration Rovers A and B Landing Sites: Our Biased View <i>K. L. Tanaka, L. S. Crumpler, M. S. Gilmore, E. Noreen, T. M. Hare, and J. A. Skinner</i>	67
Lander Detection and Identification of Hydrothermal Deposits <i>M. L. Urquhart and V. Gulick</i>	69
Potential MER Landing Site in Melas Chasma <i>C. M. Weitz, T. J. Parker, and F. S. Anderson</i>	71



EXO BIOLOGY AT SINUS MERIDIANI – 2003 AND BEYOND. Carlton C. Allen¹, Frances Westall², and Rachel T. Schelble³, ¹NASA Johnson Space Center, Houston TX 77058 (carlton.c.allen@jsc.nasa.gov), ²Lunar and Planetary Institute, Houston TX 77058 (westall@lpi.usra.edu), ³Department of Earth and Planetary Sciences, University of New Mexico, Albuquerque NM 87131 (rach@unm.edu).

Introduction: Science objectives for the 2003 Mars Exploration Rovers (MERs) relate to definition of the history of water and climate on Mars in locations where conditions may have been favorable for life. Specifically, the goal of each rover is to determine the aqueous, climatic, and geologic history of a site on Mars where conditions may have been favorable to the preservation of evidence of possible pre-biotic or biotic processes. Of the many potential landing sites permitted by engineering constraints, sites displaying what are believed to be significant concentrations of the mineral hematite ($\alpha\text{-Fe}_2\text{O}_3$) clearly have a high potential for satisfying the mission science objectives for the following reasons: 1) hematite is the only mineral yet identified on Mars that is generally associated with water; 2) hematite-rich sites are accessible to the 2003 mission; 3) the MER instruments are well suited to analyze the aqueous and geologic history of a hematite deposit; and 4) the MER instruments may be able to recognize macroscopic evidence of life potentially preserved in the geologic record. In addition, hematite is one of a limited number of minerals known to be associated with the preservation of microscopic evidence of life. A hematite-rich deposit with indications of potential biological activity would be a prime site for future sample return missions.

Hematite Deposits: Christensen et al. [1], using data from the Mars Global Surveyor Thermal Emission Spectrometer (TES), have identified gray crystalline hematite in a large region near the Martian equator. The spectral signature of hematite was identified in an area of apparently layered deposits approximately 350 km x 750 km centered near 2° S latitude between 0° and 5° W longitude, within Sinus Meridiani. Hematite has also been identified in the walls and interior layered deposits within Valles Marineris and in Aram Chaos and Margaritifer Chaos [2].

Hematite abundances derived from the TES spectra are dependent on particle size. For particles larger than 30 μm an abundance of ~10% is inferred, while abundances in the range of 25 to 60% are required if the particles are smaller than 10 μm . No other minerals have been detected in TES spectra of the hematite-rich areas. The TES detection limit for quartz, a mineral commonly associated with hematite in some terrestrial settings, is approximately 5% in a spectrum dominated by basalt [1].

Christensen et al. [1] discuss five possible origins for a Martian hematite deposit:

- Direct precipitation from standing, oxygenated, Fe-rich water
- Precipitation from Fe-rich hydrothermal fluids
- Low-temperature dissolution and precipitation through mobile groundwater leaching
- Surface weathering and coatings
- Thermal oxidation of magnetite-rich lavas

These authors “prefer precipitation from Fe-rich water, on the basis of the probable association with secondary materials, large geographic size, distance from a regional heat source, and lack of evidence for extensive groundwater processes elsewhere on Mars.” [1] Alternative scenarios infer a volcanic origin [2], or ferricrete formation.

Landing Sites: The initial list of potentially acceptable landing sites compiled by Golombek and Parker includes 35 locations within Terra Meridiani. Of these sites, five (including landing ellipses) lie completely within geomorphic unit *sm* (smooth surface) outlined by Christensen et al. [1], which generally corresponds to unit *Np12* (Noachian Plateau subdued crater unit). These sites and their locations are:

MER A

TM 9A	1.2° S	5.6° W
TM 10A	2.2° S	6.6° W

MER B

TM 19B	1.2° S	5.3° W
TM 20B	2.3° S	6.2° W
TM 21B	2.5° S	3.3° W

All of these sites, and by inference many other specific locations within Sinus Meridiani, meet the landing criteria established to date. Areas with particularly strong hematite spectral signatures can be mapped from additional TES data, with a nominal spatial resolution of 3 km [1].

MER Analyses – Aqueous and Geologic History: The Mars Exploration Rovers are designed to traverse distances of up to 100 meters per sol. Each rover will carry five major science instruments. Pancam, a stereo, multispectral imager, covers the visible and near-infrared (0.4 to 1.1 μm) spectra with an instantaneous field of view of 0.3 mrad/pixel (resolving 0.3 mm at a distance of 1 meter). This camera is bore-sighted to Mini-TES, an infrared (5 to 29 μm) spectrometer that will provide high resolution (20 or 8 mrad/pixel) spectra complementary to those from the orbiting TES. An alpha-proton x-ray spectrometer (APXS) will determine abundances of the major and minor rock-forming elements. The Moessbauer spectrometer will identify iron-bearing mineral species in rocks and soils. A Microscopic Imager will return sub-millimeter reflected light images of rock surfaces. The Rock Abrasion Tool (a.k.a. RAT) can expose interior surfaces of rocks by grinding away surface coatings.

The MER instrument suite, combined with the rovers’ kilometer-scale mobility, is extremely well suited to address the key questions of aqueous and geological history posed by the hematite deposits:

- Is the identification of hematite, based on orbital thermal emission spectra, in fact correct ? Combined Mini-TES, APXS, and Moessbauer data can confirm that identification and quantify hematite abundances.
- Is the layering observable from orbit within Sinus Meridiani of sedimentary or volcanic origin ? Pancam and Mini-TES images can distinguish layering on scales as fine as centimeters, which should aid in the identification of fine sedimentological textures as opposed to coarser volcanic layering.
- Is the hematite formed by a process involving water or by volcanism or other mechanisms ? Formation processes can be inferred from a combination of mineralogy (Mini-TES, APXS, Moessbauer) and texture (Pancam, Microscopic Imager).

MER Analyses – Macroscopic Evidence of Life:

Christensen et al. [1] list four possible origins for the Sinus Meridiani hematite deposit that involve water: direct precipitation from standing, oxygenated, Fe-rich water; precipitation from Fe-rich hydrothermal fluids; low-temperature dissolution and precipitation through mobile groundwater leaching; surface weathering and coatings. Each of these mechanisms is associated with the preserved remains of life in terrestrial environments. Some terrestrial hematite-rich deposits have macroscopic expressions, in particular microbial mat constructions such as stromatolites with undulating or hummocky topography (Figure 1). Even these, however, can be confused with inorganic mineral deposits, e.g. chalcidony or barite from hydrothermal precipitation.

The MER imaging suite (Pancam, Mini-TES, Microscopic Imager) has sufficient spatial and spectral resolution to recognize potential macroscopic evidence of life by morphology and spectra. However, it would be difficult to conclusively prove that the structures were produced by life processes.

Microscopic Evidence of Life: Single-cell organisms can be fossilized and preserved in the geologic record for billions of years [3]. Fossilization is strongly dependent on mineralogy, with silicon dioxide, iron oxides, and calcium carbonate minerals being the most likely to preserve microbes. Polymers are often secreted by microorganisms, and the intimate association of microbes and polymer known as biofilm can also be fossilized [4].

Terrestrial hematite deposits can contain fossil evidence of individual microorganisms. For example, the 2.0 Ga Gunflint banded iron formation contains many microbial fossils and biofilm layers, predominantly mineralized by hematite and silica [5], (Figure 2). Such features, on the micrometer scale, are significantly smaller than the resolution limit of the Microscopic Imager or any other MER instrument. Fossil microorganisms are only detectable by optical microscopic examination of thin sections and/or by electron microscopy. Thus, confirmation of ancient Martian

life by direct fossil evidence will require the return of samples to terrestrial laboratories. A key function of the 2003 Mars Exploration Rovers may be to discover and certify prime sites for the next decade's Mars Sample Return missions. The hematite deposits may well include one of those prime sites.

References: [1] Christensen P. R. et al (2000) *JGR*, 105, 9623-9642. [2] Noreen E. (2000) *GSA Annual Meeting*, A-303. [3] Schopf J. W. and Packer B. M. (1987) *Science*, 237, 70-73. [4] Westall et al. (2000) *JGR*, 105, 24,511-24,527. [5] Schelble R. T. (2000) *GSA Annual Meeting*, A-241.

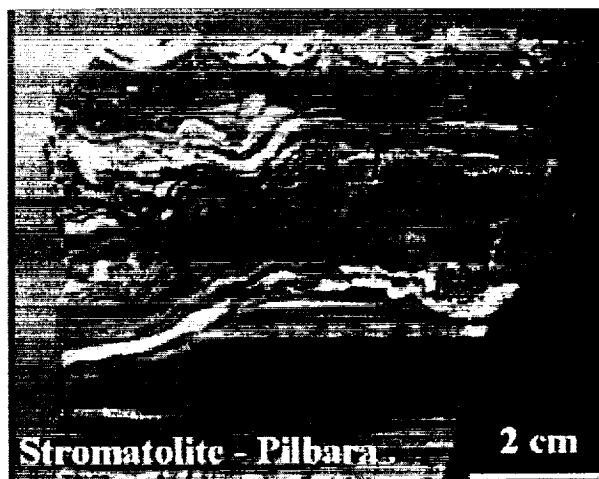


Figure 1. Stromatolitic structure; Warrawoona group, Australia



Figure 2. Fossilized filamentous organism; Gunflint banded iron formation, Canada (secondary electron scanning electron micrograph)

RESULTS FROM FIDO PROTOTYPE MARS ROVER FIELD TRIALS. R. E. Arvidson, Department of Earth and Planetary Sciences, McDonnell Center for the Space Sciences, Washington University, St. Louis, MO 63130, arvidson@wunder.wustl.edu, Tel: 314-935-5609, Fax: 314-935-4998.

The Field Integration and Design Operations (FIDO) prototype Mars rover was deployed in May 2000 in the Black Rock Summit area of Nevada and in the Arroyo Seco, JPL, in September 2000 in "blind" science operation tests to evaluate the most efficient ways of: (a) traversing across diverse terrains while conducting reconnaissance-level field science that allows site characterization, and (b) finding, approaching, and placing analytical instruments and a drilling system onto rock targets in ways that characterize in detail and sample materials that are representative of the sites traversed.

FIDO was equipped with instrumentation designed to simulate the Athena Payload for the 2003 Mars Exploration Rovers and the original 2003 and 2005 Mars Sample Return Rovers (Figure 1). Specifically, mast-based stereo cameras for navigation and false color infrared imaging were included, bore-sighted with an infrared (1.3 to 2.5 μm) point spectrometer. A deployable arm was equipped with a color microscopic imager for in-situ characterization of rocks and soils. A rock drill was included to evaluate approaches to drill deployment, core acquisition, and verification. Body-mounted belly cameras were used to fine-tune drill deployment, and front and rear hazard avoidance cameras were used for terrain hazard avoidance. The arm-based imager was used to confirm drill core presence.

FIDO was commanded by a science team unfamiliar with the site and sequestered at the Jet Propulsion Laboratory. The Web Interface for Telescience (WITS) was used for sequence generation and radiation. Simulated orbital hyperspectral (AVIRIS) and high spatial resolution image data (IKONOS and helicopter-borne) were analyzed for the Nevada site before and during the tests to define and update scientific objectives for rover operations. For the Nevada tests approximately 12 sols of Mars operations were simulated in which 2 gigabytes of data were collected. The rover drove approximately 30 m, approached a dozen targets, and deployed the arm and drill several times. For the Arroyo Seco tests the rover traversed more than 100 m in two earth days.

The primary lessons learned are that field science and sample collection can be accomplished very well using FIDO-class rovers on Mars, particularly if: (a) the landing and traverse sites expose materials that can be reached, observed, and sampled by the rover

within mission lifetimes and rover capabilities, (b) orbital and descent data over the traverse sites are available to place rover-based observations in a regional geologic context, (c) the science team focuses on important yet realistic objectives for traverse science, in-situ science, and sampling that are matched to rover capabilities and mission constraints, and (d) appropriate planning and visualization data sets and tools are in place to facilitate the fast-paced, non-deterministic nature of rover activities, data analysis, and sequence planning on a sol to sol basis.

A prime example supporting the lessons learned is the ability of the remote science team to identify and map basalts, dolostones and altered rhyolites in Nevada from AVIRIS, IKONOS, helicopter-borne, and rover-based data so that regional scale materials could be properly quantified and sampled at the local scale using FIDO systems. That is, they were able to characterize regional scale materials, develop hypotheses, and test the ideas through local observations from FIDO.

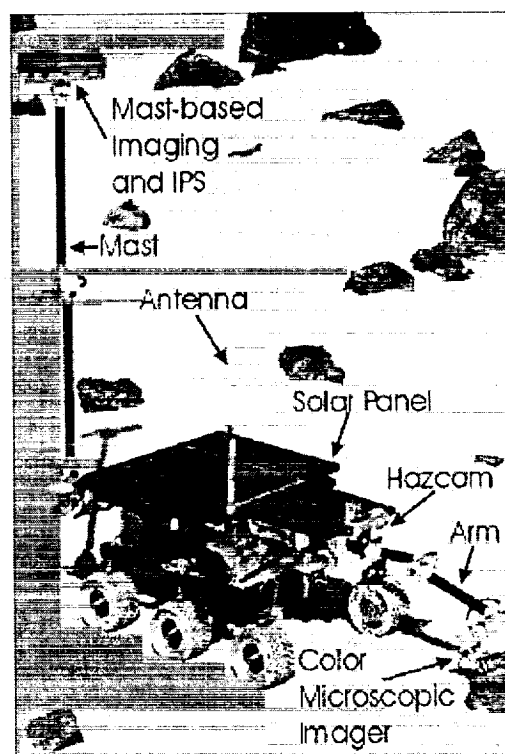


Figure 1. FIDO and its instrumentation.

POTENTIAL MER LANDING SITES IN THE TERRA MERIDIANI AND VALLES MARINERIS REGIONS OF MARS. N. G. Barlow, Department of Physics, University of Central Florida, Orlando, FL. 32816. ngb@physics.ucf.edu

Introduction: The 2003 Mars Exploration Rovers (MER) are tasked with exploring a region of Mars where conditions may be favorable for preserving evidence of pre-biotic or biotic processes. In particular, the landing sites are expected to possess clear evidence for surface processes involving ancient water. Three sites have been identified which satisfy the engineering requirements for these missions. Two of the sites are in the Terra Meridiana area of Mars while the third is on the floor of Eos Chasma in the Valles Marineris canyon system. Two of the three sites are close to areas previously recommended by others for the MS01 landing site.

Site 1. Hematite Deposit, Terra Meridiana. The proposed landing site is located near 2.3°S 3.1°W near the southern boundary of Terra Meridiana hematite deposit identified by [1] (Fig. 1). The region is at a MOLA-derived elevation of between -1.2 and -1.4 km. Thermal inertia values are about $200 \text{ J m}^{-2} \text{ K}^{-1} \text{ s}^{-1/2}$ [2] and MOLA derived roughness values indicate slopes of less than 0.2° [3]. Rock abundances are less than 10% [4]. The terrain is mapped as unit Npl₂, a Noachian-aged subdued crater unit. [5] have previously proposed landing sites for the MS01 mission in this general area. The scientific rationale for selecting this site include the location of the site on the proposed hematite deposit, which is believed to have precipitated from iron-rich water. This deposit may have been precipitated from a standing body of water, from hydrothermal fluids, or through mobile ground water leaching [1]. The presence of the hematite strongly indicate that water was available in this location during the time of the deposit's emplacement in the Noachian period. If hydrothermal activity was involved, the warm and wet conditions in this region would have been favorable for the development of pre-biotic or biotic chemistry. Although this deposit may have been modified by subsequent geologic processes (primarily aeolian), small craters in the region could have recently exposed more pristine material which could be sampled by the rovers.

Site 2. Crater floor, Terra Meridiana. The second proposed landing site is located near 8.3°S 7.1°W on the floor of a 144 km diameter impact crater (Fig. 2). The rim of this crater is dissected by numerous small gullies. The floor appears to be covered by a smooth deposit which has covered the lower portions of the crater's central peak. Small craters on the crater

floor have likely excavated less altered portions of this deposit from greater depths. The crater is in the same region as several of the recently reported sedimentary deposits [6]. Therefore several lines of evidence suggest that the smooth floor deposits of this crater may be ancient lakebed sediments. The MOLA-derived elevation of the proposed landing site is -1.9 km and the thermal inertia is $\sim 330 \text{ J m}^{-2} \text{ K}^{-1} \text{ s}^{-1/2}$ [2]. Rock abundances are less than 10% [4]. The terrain is listed as smooth crater floor deposits and the crater is superposed on the Npld (Noachian aged dissected plains) unit. Roughness values derived by MOLA indicate slopes of about 1-2° in the middle of the landing ellipse. The outer edges of the landing ellipse encounter rougher terrain associated with the crater rim. The southern boundary of the ellipse abuts the crater's central uplift. This site has not previously been proposed for landing site consideration.

Site 3. Floor of Eos Chasma, Valles Marineris. The third proposed landing site is located on the floor of Eos Chasma in the Valles Marineris canyon system (Fig. 3). This site is located near 11.1°S 38.0°W, close to an MS01 landing site proposed by [7]. The site is located about 30 km from the canyon's south-east wall, which would provide an extremely impressive skyline from a public relations standpoint. In addition, stratigraphic layering may be visible from the landing site, allowing a better view of this layering than is possible from orbit. The plains capping the wall are dissected by small channels which connect the wall to another area of chaotic terrain to the east. This indicates that ground water systems were likely active in this region in the past and that these channels may have transported water and other materials onto the floor of the canyon in the location of the landing site. To the north of the landing site is an area of jumbled chaotic terrain. This area is near the confluence of Gangis, Capri, and Eos Chasmata, which [7] has argued to be a topographic trap for water and debris. This could provide a location for standing bodies of water to exist at least episodically over much of the history of Valles Marineris. These locations may have existed long enough for pre-biotic or biotic processes to occur, the remains of which may be retained within the sediments at the landing site. The elevation of the proposed site is -4.0, rock abundances is <10% [4], and thermal inertia is estimated at $\sim 330 \text{ J m}^{-2} \text{ K}^{-1} \text{ s}^{-1/2}$ [2]. Slopes within the

landing ellipse are approximately 1-2°. The terrain is mapped as Hch, Hesperian aged channel material.

Summary. The three landing sites proposed here all meet the engineering requirements for the MER rovers. In addition, geologic analysis suggests that water has existed in all three areas, perhaps as long-lasting standing bodies of water in which pre-biotic or biotic chemistry could have arisen. The sediments located in these locations could still retain evidence of these chemical processes. In any event, all three sites provide the rovers with access to materials which likely have been emplaced within an aqueous environment. All three sites are Hesperian to Noachian in age, indicating that materials can be sampled which can provide information about the ancient aqueous and climatic conditions on Mars. Analysis of surface materials will provide important new constraints on the geologic history of Mars at the selected site.

References: [1] Christensen P. R. et. al. (2000) *JGR*, 105, 9623-9642. [2] Mellon M. T. et. al. (2000), *Icarus*, in press. [3] Aharonson O. et. al. (2000), *JGR*, submitted. [4] Christensen P. R. (1986), *Icarus*, 68, 217-238. [5] Christensen P. R. et. al. (1999), *Second Mars Surveyor Landing Site Workshop*, 17-18. [6] Malin M. C. and Edgett K. S. (2000), *Science*, 290. [7] Clifford S. M. and George J. A. (1999), *Second Mars Surveyor Landing Site Workshop*, 19-20.

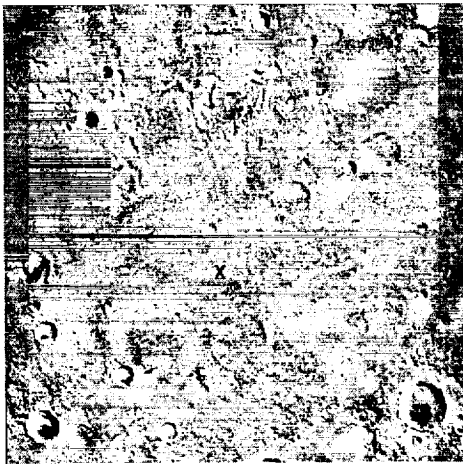


Figure 1. Proposed landing site 1: Hematite deposit in Terra Meridiani. The proposed landing site is located near the southern boundary of the hematite deposit in Terra Meridiani. The landing site is located near 2.3°S 3.1°W.



Figure 2. Proposed landing site 2: Crater floor, Terra Meridiani. The proposed landing site is located on the smooth deposits blanketing the floor of this 144-km-diameter crater. The landing site is located near 8.3°S 7.1°W.

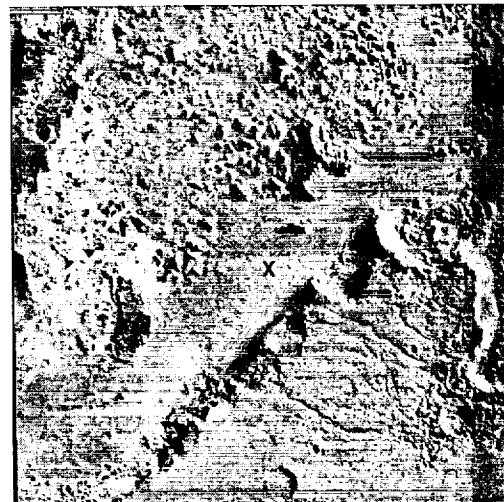


Figure 3. Proposed landing site 3: Floor of Eos Chasma, Valles Marineris. The proposed landing site is located on the floor of Eos Chasma northwest of the canyon wall. The top of the wall is dissected by small channels while to the northeast is the confluence area of Gangis, Candor, and Eos Chasmata where water may have ponded. The landing site is located near 11.1°S 38.0°W.

MINERALOGY CONSIDERATIONS FOR 2003 MER SITE SELECTION AND THE IMPORTANCE FOR ASTROBIOLOGY. J. L. Bishop, SETI Institute/NASA-ARC, MS 239-4, Moffett Field, CA 94035 (jbishop@mail.arc.nasa.gov).

Much of the discussion of site selection on Mars is based on interesting images of the surface combined with safety issues. I argue that the two rovers should be sent to mineralogically distinct regions. Compositional information is still poorly constrained on Mars; however, the instruments on the 2003 MERs will provide a unique opportunity for detailed characterization including mineral identification. There is strong motivation for sending one rover to a "typical" region on Mars to be used as a ground truth for the Thermal Emission Spectrometer (TES), while the other rover should be sent to a site where water and chemical alteration are likely to have occurred. Determining the mineralogy of the Martian surface material provides information about the past and present environments on Mars which are an integral aspect of whether or not Mars was suitable for the origin of life. Understanding the mineralogy of terrestrial samples from potentially Mars-like environments is essential to this effort.

Introduction: Chemical and mineralogical analyses were performed on a variety of terrestrial samples including altered volcanic tephra, hydrothermal springs material and Antarctic sediments in order to interpret data expected from Mars. Comparison of the spectral and chemical properties for different size separates and related samples provides information about the crystalline minerals in these samples and how they may have formed. Identification of secondary minerals on Mars may indicate the presence of water, hydrothermal processed, chemical alteration and sites of interest to Astrobiology. As a result of the recent evidence for water [1] and sedimentary deposits [2] on Mars the importance of chemical alteration has become more apparent.

Chemistry and mineralogy of altered volcanic material: Volcanic material has been studied by numerous groups in an effort to understand the surface material on Mars. Altered volcanic samples from the Hawaiian islands, and elsewhere, in recent studies [3,4] exhibited a range of chemical and mineralogical compositions, where the primary minerals typically included plagioclase, pyroxene, olivine, hematite, and magnetite. The kind and abundance of weathering products varied substantially due to the environmental conditions. The alteration of the volcanic material was evaluated through changes in specific elements, and through detection of phyllosilicates and iron oxides.

Chemical analyses of altered tephra/ash samples from the Halcakala crater basin on Maui indicate that the brightly colored material near cinder cones is higher in Fe and lower in Ti than the surrounding material [3,4]. This supports the formation of secondary iron oxides as opposed to high temperature minerals.

Reflectance spectra of selected altered tephra samples are shown in Figs. 1-2. These samples exhibit a range of minerals from the weak iron oxide/oxyhydroxide (FeOx) band near 0.9 μm in samples 391 and 392, to the strong FeOx $\sim 0.9 \mu\text{m}$ band observed for samples 250 and 394. Additional features due to phyllosilicates, jarosite and alunite are observed in Figs. 2,3. The FeOx minerals hematite and

maghemite also exhibit mid-IR bands which are observed for samples 250 and 394 (Fig. 2).

Figure 1 VIS/NIR Reflectance Spectra of Tephra.

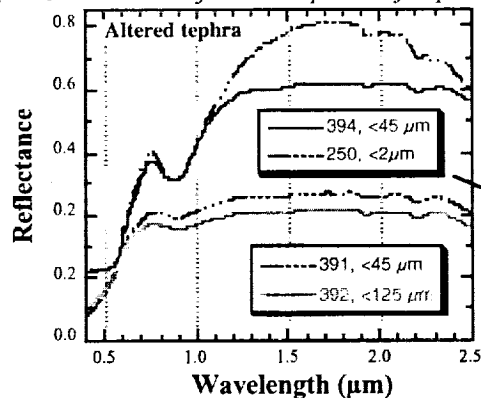


Figure 2 Mid-IR Reflectance Spectra of Tephra.

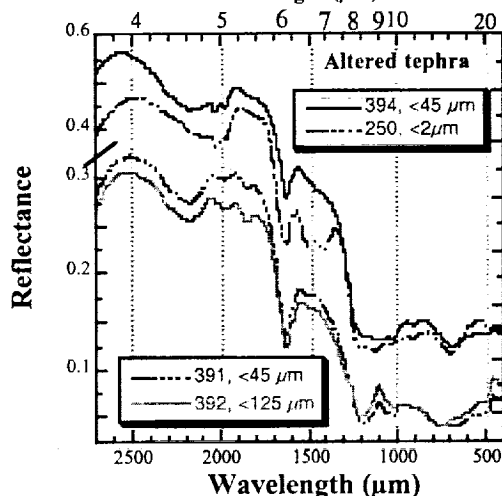
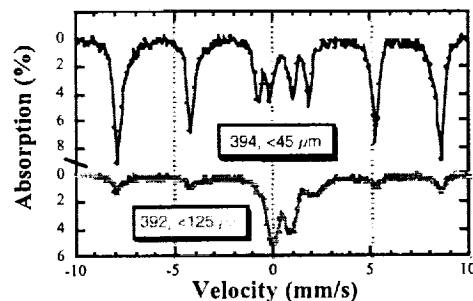


Figure 3 Mössbauer Spectra (295 K).

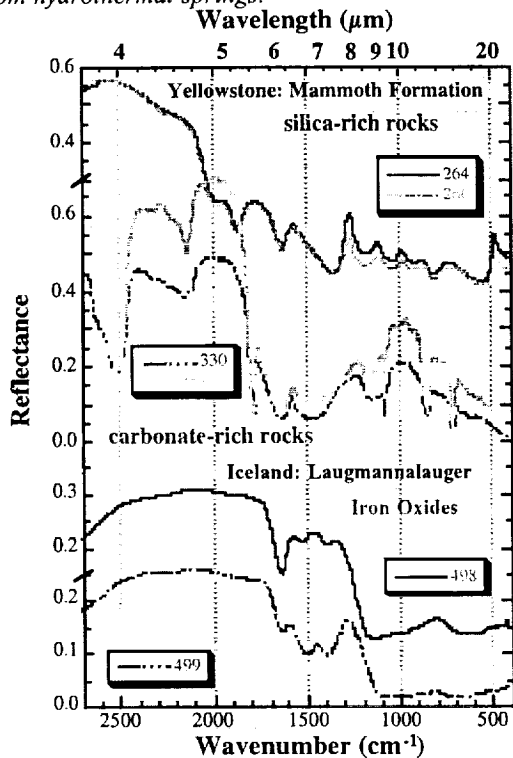


Mössbauer spectra measured at 295K of the altered tephra readily discriminate between Fe(II) and Fe(III) minerals [4]. A comparison of samples 392 and 394 shows a much stronger FeOx sextet for 394 which is consistent with the strong FeOx bands in the VIS-IR

spectra. Sample 392 exhibits a weak FeOx component and a stronger Fe(II) doublet assigned to olivine and pyroxene. Low temperature Mössbauer spectra show evidence of hematite, jarosite and olivine in 394 [4].

Chemistry and mineralogy of hydrothermal deposits: Carbonate and silica-rich rocks have been collected and analyzed from the hydrothermal springs at Yellowstone [5]. These samples typically contain a combination of biogenic and inorganic products. Material has also been collected from hydrothermal springs in Iceland, which is dominated by np/fine-grained FeOx and contains small amounts of silica, carbonate and phosphate. If one of the MERs is sent to a region where hydrothermal processes were likely, mini-TES should be able to identify features due to silica, carbonates and iron oxides as in Fig. 4.

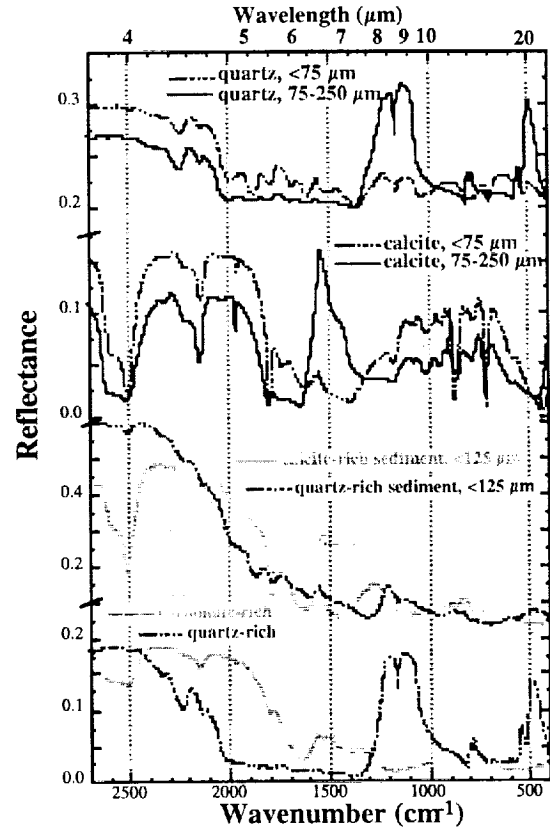
Figure 4 Mid-IR Reflectance Spectra of material from hydrothermal springs.



Chemistry and mineralogy of Antarctic sediments: Lakebottom sediments from the Dry Valleys region of Antarctica were analyzed in order to study the influence of water chemistry on the mineralogy and geochemistry of these sediments, as well as to evaluate techniques for remote spectral identification of potential biomarker minerals in possible sedimentary deposits on Mars. Lakes from the Dry Valleys region of Antarctica have been investigated as possible analogs for extinct lake environments on early Mars [6]. In recent studies, sediments from the perennially ice-covered Lake Hoare in the Taylor Valley indicated changes in chemistry and mineralogy for the oxic and anoxic regions of the lake due to biological activity [7]. If one of the MERs is sent to a sedimentary deposit, mini-TES should be able to identify sedimentary minerals, such

as the quartz and calcite in Fig. 5, if they are present.

Figure 5 Mid-IR Reflectance Spectra of minerals [8] and sediments from Lake Hoare, Antarctica.



The exciting discoveries of water seepage [1], sedimentary layers [2] and a gray hematite deposit [9] on Mars open many new questions about surface water and the possibility of other crystalline minerals. TES is capable of identifying most crystalline minerals that occur in large regions on Mars, spanning tens of km or more. Smaller, 1-2 km, regions along boundaries of flow channels, volcanic rims or basins, or impact craters might also contain crystalline minerals that would be more difficult to identify remotely on Mars. This would be an ideal location for one of the 2003 MERs to explore. Mineral identification of fresh and altered rock surfaces by mini-TES will provide important ground truth data for TES and other orbital spectrometers. We should take advantage of this opportunity to place the MERs in mineralogically distinct regions.

References: [1] Malin M. & K. Edgett (2000) *Science*, 288, 2330. [2] Malin M. & K. Edgett (2000) *Science*, 290, 1927. [3] Bishop J. et al. (1998) *JGR*, 103, 31457. [4] Bishop J. et al. (2000) *LPSC #1874*. [5] Bishop J. et al. (1999) *Mars 2001: Integrated Sci.*, LPI, 6. [6] Doran et al. (1998) *JGR*, 103, 28. [7] Bishop J. et al. (1996) *GCA*, 60, 765; Bishop J. et al. (2000) *GCA*, sub. [8] Christensen P. et al. (2000) *JGR*, 105, 9623. [9] Salisbury J. et al. (1991) *Mineral Spectroscopy*.

Acknowledgements: The spectra were measured at RELAB, a multi-user, NASA-supported facility (NAG5-3871) and assistance from T. Hiroi is much appreciated.

ASSESSING LAYERED MATERIALS IN GALE CRATER

N.T. Bridges, Jet Propulsion Laboratory, MS 183-501 4800 Oak Grove Dr., Pasadena, CA 91109; nathan.bridges@jpl.nasa.gov.

Introduction: The recent analysis of high resolution MOC images of layered outcrops in equatorial regions [1] reinforces two important ideas, which will probably eventually become paradigms, about Mars: 1) It has had a long, complex geologic history marked by change, as manifested in the different layers observed, and 2) Standing bodies of water existed for substantial lengths of time, indicating clement conditions possibly conducive to life.

Although observations of layering and evidence for lakes and oceans has been reported for years based on Mariner 9 and Viking data [2-6], the MOC data show that this layering is much more pervasive and complex than previously thought. These layered sites are ideal for studying the geologic, and possibly biologic, history of Mars. Here, a layered site within Gale Crater is advocated as a MER target. This is one of the few layered areas within closed depressions (e.g., other craters and Vallis Marineris) that meets the landing site constraints and is accessible to both MER A and B.

General Geology: Gale is a 150 km diameter crater at the margin of the planetary dichotomy in Elysium Planitia. Its ejecta superposes Noachian subdued crater material (Npl₂) and dissected material (Npld) [7]. The contact between the ejecta and Npld is truncated by Hesperian smooth material (Hpl₃). These relationships thereby constrain the crater age as close to the Noachian/Hesperian boundary (~3.5-3.8 Ga).

Recent MOC images show layered mounds and other landforms in the northern part of Gale (Figures 1 and 2). The following interpretations come largely from those of Malin Edgett (it is my approach to advocate this landing site; full credit to the discovery and initial interpretation of the layers goes to Malin and Edgett). The number of layers is in the 100s. The stratigraphic relationships of the layers indicate periods of layer formation, erosion, impact cratering, and further layer formation. The fact that the layers are found on isolated mounds indicates that some process has eroded an originally more extensive, layered material into the topography seen today. A channel, presumably formed by water, cuts the layers. It appears to have been filled in places, with some of this fill subsequently stripped away. Dark sand dunes are also observed in some areas.

Rationale For a MER Landing Site

Gale Crater offers a geologic bonanza for a potential MER mission. The sequence of layers will enable the investigation of local geologic, and possibly biologic, history. Visible/near IR and thermal IR images and spectra from Pancam and TES will be able to assess the oxidation state, composition, and mineralogy of layers. *In situ* investigation of individual layers with APXS and Mossbauer will allow detailed assessment of elemental abundances and iron mineralogy. The microscopic imager will be able to study details of the layers (presence of cross bedding, conglomerates, breccias, etc.). In addition to the layers, the channels and dunes within Gale crater also offer investigation sites for understanding fluvial and aeolian processes.

Landing Site Engineering Constraints

The landing ellipses for both MER A and B can fit within Gale crater (Figure 1). This site also meets all of the engineering criteria defined by the project. The layered materials as revealed in the MOC image are rough and would make a poor landing site. However, MOC wide angle and Viking images show that this layered material may extend into the mid-regions of the crater. Ellipses can be fit within the smooth, southern half of Gale, with interesting layered deposits to the north. In order for Gale to be further considered for a landing site, more MOC images throughout the crater interior are advocated. This will enable identification of a safe landing zone within interesting terrain that can be fully accessed by the rovers.

References:

- [1] Malin M.C. and Edgett, K.S. (2000) *Science*, 290, 1927. [2] McCauley, J. F. (1978) *U.S. Geol. Surv. Misc. Inv. Ser. Map I-897* [3] Nedell, S. S. (1987) et al., *Icarus* 70, 409 (1987) [4] Squyres, S. W., (1989) *Icarus* 79, 229. [5] Komatsu, G. et al. (1983), *J. Geophys. Res.* 98, 11105. [6] N. A. Cabrol and E. A. Grin, (1999), *Icarus* 142, 160. [7] Greeley, R. and Guest, J.E. (1987) *U.S. Geol. Surv. Misc. Inv. Ser. Map. I-1802-B*.

GALE CRATER MER SITE N.T. Bridges

<u>Site</u>	<u>Lat. (°)</u>	<u>Lon.(°W)</u>	<u>MOC Image</u>	<u>Elev. (km)</u>	<u>FCI</u>	<u>Rocks</u>	<u>Albedo</u>	<u>Unit</u>
Gale	-4.88	222.88	M0301521 M00-01602	-3.6	6.4	8	0.264	s, c



Figure 1: Gale Crater as seen in MOC Wide Angle images M01-00352 and M03-00740. MER A ellipse shown in red, MER B ellipse shown in green.



Figure 2: MOC narrow angle image of layered material within Gale Crater. See: http://www.msss.com/mars_images/moc/dec00_seds/gale/Channel_M03-01521sub1a.jpg

EXPLORING IMPACT CRATER PALEOLAKES IN 2003. N. A. Cabrol and E. A. Grin, SETI Institute/NASA Ames Research Center. Space Science Division. MS 245-3, Moffett Field, CA 94035-1000. Email: ncabrol@mail.arc.nasa.gov. Fax: 650-604-6779. Phone: 650-604-0312.

Introduction: Paleolakes in impact craters have been surveyed for the past 20 years and have raised considerable interest because of their potential to document many of the questions that are at the heart of the Mars exploration program, especially Astrobiology and search for life [1-46]. Recent high-resolution MOC images seem to provide another support to their existence [47] and are giving new data to explore these past lakes that Viking had helped us unravel [1-46]. They also show the importance of a continuing exploration program at increasing resolution. It is now possible to fully investigate the broad spectrum of martian crater lakes from Noachian to Amazonian, up to very recent times, since fresh gullies have been also observed in impact craters [40]. Before the confirmation by MOC, several studies on the subject [1-46] had pointed out the importance of martian limnology as a method to understand the past climate, hydrogeology, and possibly biology of Mars. Considering the questions raised both by the Viking and MGS mission about these crater lakes and their extraordinary potential for astrobiological investigations, the next logical step is to explore them *in situ*, and it is possible with MER-A and MER-B in 2003.

Scientific rationale: As we explore Mars in the search of water and possibly traces of life, impact crater paleolakes present strong scientific and engineering arguments that designate them as sites to be explored by the 2003 missions.

Water and Climate

Lake sediments are the record of the dynamics of depositional environments, and provide information about the climate under which they were formed. These bottom sediments consist of mineral grains produced by various erosional processes which took place in the surrounding drainage area. Therefore, these sediments have directly or indirectly experienced various climatic, hydrologic and hydraulic conditions and reflect paleo-environmental conditions. The stratigraphic distribution of sediments reflects these changes through time, while their horizontal distribution represents the present state of lake sedimentation. A critical parameter in the classification of terrestrial lakes is *climate*, which strongly controls the characteristics of lake deposits. On Earth, climate controls the amount of precipitation and evaporation, the nature of the weathering, and the nature of the soil in the catchment area. Further, the amount of clastic sediments depends upon the seasons and water discharges. Exploring martian lake varves will help us to better understand the climate and hydrological cyclicity on Mars, while we are discovering its complexity through the intense layering of the planet [47-52].

Geology

The information stored in martian lakes will bring more knowledge about the planet's history. During both their active (wet) and dormant (dry) cycles, lakes accumulate sediments or experience erosional phases that exhume older sediments. When hydrologically active, lakes are collecting both aqueous sediments from their catchment areas and aerial material originating from volcanic activity, glaciation, and dust storms of

unusual magnitude. When dry, lakebeds accumulate aeolian material and any other aerial deposits. In impact crater basins, this record is confined in topographically well defined environments. In that respect, martian impact crater paleolakes could become the Rosetta Stone of Mars by helping us decipher the history of the planet, as considerable amount of information is stored in a reduced environment, with the possibility to put our observations into their original time context by comparing surveyed rocks with local outcrops.

Biology

Impact crater paleolakes are among the most promising sites for the search for life, and/or precursors of life, on Mars [1-47]. Lacustrine deposits are well-known to be favorable environments for the preservation of life (extant and/or extinct). Lakes provide the best conditions for fossilization processes [8, 11, 28, 33, 41, 54]. Impact crater lakes also provide diversified environments, from warm thermally-driven when a lake is formed just after the crater formation to cold-ice-covered waters. It is unknown if any potential life on Mars existed on a continuous time scale or was terminated and restarted at multiple events [55-56]. Despite this uncertainty, we expect that evolutionary trends would have allowed organisms to establish new ecological niches in response to a changing climate and environment. In the case of some of the crater paleolakes sites already suggested for 2003 [53] like Gale, Gusev and Schiaparelli, a series of ecological niches could have been present from the time following impact until Mars lost its hydrosphere and the potential to sustain life on the surface. For some time following impact, these basins may have had the ability to sustain life in a thermally driven subaerial or subsea environment. Such terrestrial analog environments have been discussed [54, 57-58]. The preservation of biological information in thermal spring deposits on Mars, as well as related sampling strategies were discussed by Walter and Des Marais [59]. Various microorganisms in crater lakes may have adapted to physical and chemical changes induced by the modification of the climate (i.e., temperature, pH, salinity). Such changes would in turn have had direct implications on species abundance, diversity, and dominance. As they dried up, resulting playas may have favored the existence of halophiles. Any microbial life that existed in these types settings are likely to have been preserved in mineral deposits, such as carbonates [60, 61], and evaporites [62] and in the scenario of a volcanic setting, possibly in silica. Each of these fossilization agents have different preservation potentials in the fossil record. In terms of identification, different deposits may be identified through characteristic spectral signatures. As the temperature became progressively cooler, microbes may have retreated from the lake water to subareal habitats, and in turn migrated to protected niches in or under rocks on the surface. These types of environments have been identified in some of the Earth's deserts, such as the Dry Valleys of Antarctica [63-65]. There are also potential martian analogs represented by the perennially ice-covered lakes in Antarctica. These lakes are hosts of microbial mats composed primarily of bacteria, cyanobacteria, and algae, that exist without sunlight most of the year [66].

The different environments listed above could all have sustained life that may be still present in the fossil record. The absence of crustal recycling on Mars open up for the possibility that fossilized life forms from the various ecological niches described could be present right at the surface today if freshly exposed in outcrops, when potential extent life should be searched for underground. The mineral deposits in which life may be preserved would have a good likelihood of being detected with spectral data.

Engineering rationale:

Impact crater paleolakes are sites where representative rock and sedimentary units of diverse geological origins and ages will be collected. As there are two missions sent to Mars, we suggest that one MER be targeted to explore for diversity in an impact crater paleolake, while the other could explore a typical unit representative of one critical geological period or transition period on Mars. Some of the arguments developed in the previous paragraphs show that a mission in an impact crater paleolakes will provide a critical scientific pay-off, and increase tremendously our knowledge of Mars' history in one mission.

Time Machine

How far we can go back in time and how much of the martian history we can unravel during the 2003 mission will depend on how old is the explored crater basin, how much its record has been eroded, and how long we can explore the site. In our previous survey of martian impact crater lakes at Viking resolution [32, 26, 41] we have shown that many lacustrine episodes were Hesperian in age, several were Amazonian. We also pointed out that the number of crater lakes we had observed (180) would probably increase significantly as the MOC high-resolution would allow to reach sediments of the Noachian record. To collect as much information as possible, a sound strategy could be then to explore a crater basin formed during the Noachian that has accumulated a significant and accessible sedimentary record, including lacustrine deposits, since its formation. Several such crater basins are already suggested in the Memorandum of candidate-sites for 2003 [53], including Schiaparelli, Gusev and Gale crater [29, 47]. Other crater paleolakes listed in our catalog [32] exist in the required landing zones for MER-A and MER-B. We will present the various science and engineering arguments (pros and cons) for those representing the best chances of mission success considering the science objectives, onboard instrumentation, and engineering constraints of the 2003 missions.

References^(a):

[1] Brakenridge, G. R., et al. 1985 *Geol.* 13, 859-862; [2] McKay et al., 1985. 313, 561-562. [3] Goldspiel, J. M. and S. W. Squyres 1991. *Icarus* 89, 392-410; [4] Scott et al., 1991. *Orig. Life, Ev. Biosp.*, 21, 189-198; [5] Cabrol, N. A. 1991. *Ph-D Thesis*; [6] De Hon, R. A. 1992, *Earth, Moon, and Planets*, 56, 95-122; [7] Rice, J. W., Jr, 1992 LPI Tech. Rept. 92-08, Part I, 23-24; [8] Farmer, J. D., and D. J. Des Marais 1993, In *Case for Mars V*, 34-35; [9] Cabrol, N.A., and E.A. Grin 1995, *Plan. Space. Sci.* 43, 1/2, 179-188; [1-] Scott et al., 1995. *U. S. Geol. Surv. Misc. Inv. Series*, Map I-2561; [11] Wharton et al. 1995. *J. Paleolimnology* 13, 267-283; [12] Landheim, R. 1995. Master Thesis, ASU; [13] Forsythe, R. D.,

and J. R. Zimbelman 1995, *JGR*, 100, 5553-5563; [14] Cabrol, N. A., and E. A. Grin 1996, *Origins of Life*, 26, 3-5.; [15] Newsom et al., 1996. *JGR* 101, 14951-14955; [16] Grin, E. A., and N. A. Cabrol 1997, *Icarus* 130, 461- 474; [17] Kempe, S., and J. Kazmierczak 1997, *Plan. Space. Sci.* 45, No.11, 1493-1499; [18] Cabrol, N.A. 1997. In: *ESA Report*; [19] Cabrol, N.A. 1997. 28th LPSC; [20] Gulick, V. C. 1998, *JGR* 103, p. 19,365-19388; [21] Barlow, N. G. 1998. *Mars Surveyor 2001 Landing Site Workshop*. NASA ARC; [22] Nelson et al., 1998a,b. *Mars Surveyor 2001 Landing Site Workshop*. NASA ARC; [23] Greeley, R., and R.O. Kuzmin 1998, *Mars Surveyor 2001 Landing Site Workshop*; [24] Cabrol et al., 1998. *Icarus* 133, 98-108; [25] Zimbelman, J. R. 1998. *Mars Surveyor 2001 Landing Site Workshop*; [26] Cabrol, N. A. 1998, 29th LPSC, 1009. [27] Cabrol, N. A. 1999, 30th LPSC, 1024; [28] Farmer, J. D., and D. J. DesMarais 1999, *JGR.*, 104: (E11) 26,977-26,995. [29] Cabrol et al., 1999. *Icarus* 139, 235-245; [30] Rice et al., 1999. LPI Contribution No. 972, 6241 (abstract); [31] Zimbelman, J. R., and J. W. Rice, Jr., 1999. *Mars Surveyor 2001 Landing Site*; [32] Cabrol, N. A., and E. A. Grin 1999. *Icarus*, 142, 160-172; [33] Farmer, J. D. 2000, LPI Cont. 1062, 110-112; [34] Haberle et al., 2000. *31th Lun. Plan. Sci. Conf.* 1509; [35] Ori et al., *JGR* 105, E7, 17,629-17,643; [36] Cabrol, N. A. 2000. In: *GSA special book*, in press. [37] Moore, J. M., and D. Wilhems 2000 *Personal Communication*; [38] Cabrol, N. A., and E. A. Grin 2000, *Icarus* 149, in press; [39] Ruff, S. W. 2000. *First Astrobiology Science Conference*, NASA Ames Research Center, April 3-5, 2000, 7; [40] Malin, M. C. and K. S. Edgett 2000., *Science* 288, 2330-2335; [41] Cabrol et al., 2000, *Icarus* (submitted); [42] Grin, E. A. 2000, In: *GSA Special Book on subglacial lakes* (submitted); [43] Grin, E. A., and N. A. Cabrol 2000, *Icarus*, submitted; [44] Haberle et al., 2000 *JGR* (submitted); [45] Kuzmin et al., 2000, USGS Map I-2666; Newsom et al., *JGR*, submitted; [47] Malin and Edgett 2000. *Science*, 290, 1927-1937; [48] McCauley, 1978, USGS Map I-897; [49] Lucchitta 1982. NASA TM-85127, 233-234; [50] Lucchitta 1985. NASA TM-87563, 506-508; [51] Lucchitta et al., 1986. *JGR* 91, E166-E174; [52] Nedell et al., 1987. *Icarus* 70, 409-441; [53] Golombek, M., and T. J. Parker 2000. Mars exploration rover landing sites Memorandum; [54] Wynn-Williams et al., 2000, *PNAS* (submitted); [55] Maher, K.A. and D.J. Stevenson 1988, *Nature* 331, 612-614; [56] Sleep et al. 1989. *Nature* 342, 139-142; [57] Brock 1967. *Science* 158, 1012-1019; [58] Barns et al., 1994, *PNAS* 91, 1609-1613; [59] Walter and Des Marais 1993. *Icarus* 101, 129; [60] Schopf 1983 *the Earth's earliest biosphere*; [61] McKay and Nedell 1988. *Icarus* 73, 142-148; [62] Rotschild 1990. *Icarus* 88, 246-260; [63] Friedman 1982. *Science* 215, 1045-1053; [64] Friedman 1986. *Adv. Space. Res.* 6(12), 265-268; [65] Friedman and Koeriem 1989. *Adv. Space. Res.* 9(6), 167-172; [66] Wharton 1984. *Phanerozoic Stromatolites II*, 53-70.

^(a)From [1-47] the references listed try to be as representative as possible of the research done in the past 15 years on the subject of impact crater paleolakes. It is by no mean an exhaustive list. Considering the limited space allotted for the abstract, we were forced to reduce the number of references related to abstracts of communications.

THE TES HEMATITE-RICH REGION IN SINUS MERIDIANI; A PROPOSED LANDING SITE FOR THE 2003 ROVER. Philip R. Christensen, Joshua Bandfield, Victoria Hamilton, and Steven Ruff, Arizona State University, Tempe AZ 85284, Richard Morris and Melissa Lane, Johnson Space Center, Houston TX, Michael Malin, Malin Space Science Systems, San Diego CA, and the TES Science Team.

The Thermal Emission Spectrometer (TES) instrument on the Mars Global Surveyor (MGS) mission has identified an accumulation of crystalline hematite ($\alpha\text{-Fe}_2\text{O}_3$) that covers an area with very sharp boundaries approximately 350 by 750 km in size centered near 2°S latitude between 0 and 8° W longitude (Sinus Meridiani) [Christensen *et al.*, 2000; Christensen *et al.*, submitted]. The depth and shape of the hematite fundamental bands in the TES spectra show that the hematite is relatively coarse grained ($>5\text{-}10\ \mu\text{m}$). The spectrally-derived areal abundance of hematite varies with particle size from ~10% for particles $>30\ \mu\text{m}$ in diameter to 40-60% for unpacked $10\ \mu\text{m}$ powders [Christensen *et al.*, 2000]. The hematite in Sinus Meridiani is thus distinct from the fine-grained (diameter $<5\text{-}10\ \mu\text{m}$), red, crystalline hematite considered, on the basis of visible and near-IR data, to be a minor spectral component in Martian bright regions.

A global map of the hematite abundance has been constructed using TES data from the MGS mapping mission. The boundaries of the hematite-rich region are sharp at spatial scales of ~10 km. Within this region there are spatial variations in spectral band depth of a factor of two to three. This unit has outliers to the north that appear to have formed by stripping and removal. We have interpreted the Sinus Meridiani material to be an in-place, rock-stratigraphic sedimentary unit characterized by smooth, friable layers composed primarily of basaltic sediments with ~10-15% crystalline gray hematite [Christensen *et al.*, 2000; Christensen *et al.*, submitted].

The hematite-rich surface discovered by TES closely corresponds with smooth-surfaced unit ('sm') that appears to be the surface of a layered sequence [Christensen *et al.*, 2000; Christensen *et al.*, submitted]. The presence of small mesas superposed on 'sm' and the degraded nature of the small impact craters suggests that material has been removed from this unit. These layered materials do not appear to be primary volcanic products (i.e., lava flows) because there are no associated lava flow lobes, fronts or pressure ridges; there are no fissures or calderae, nor any other features that can be interpreted as volcanic within 'sm' [Christensen *et al.*, 2000; Christensen *et al.*, submitted]. Bowl-shaped depressions in 'sm' and the remnant mesas on top of a por-

tion of this unit suggest that deflation has removed material that was once above the present surface of 'sm'. The most likely cause of the deflation is wind, which suggests that the layered materials are relatively friable.

We conclude that the hematite-rich material in Sinus Meridiani is a rock stratigraphic sedimentary formation, which we have proposed to name the Meridiani Formation [Christensen *et al.*, 2000; Christensen *et al.*, submitted]. It is the first rock formation identified by mineralogical composition on Mars, and its location differs, especially along the northern boundary, from the smooth unit ('sm') mapped by Christensen *et al.* [Christensen *et al.*, 2000] on the basis of morphology. The Meridiani Formation is interpreted to be sedimentary in origin and is characterized by friable layers composed primarily of basaltic sediments with ~10-15% crystalline hematite, has no large ($> 7\ \text{km}$), fresh craters, and is mappable over $>175,000\ \text{km}^2$.

We have grouped the proposed formation modes for gray hematite detected by TES into two classes: (1) chemical precipitation and (2) thermal oxidation of magnetite-rich lavas. Chemical precipitation models include (1a) low-temperature precipitation of Fe oxides/oxyhydroxides from standing, oxygenated, Fe-rich water, followed by subsequent alteration to gray hematite, (1b) low-temperature leaching of iron-bearing silicates and other materials to leave a Fe-rich residue (laterite-style weathering) which is subsequently altered to gray hematite, (1c) direct precipitation of gray hematite from Fe-rich circulating fluids of hydrothermal or other origin, and (1d) formation of gray hematitic surface coatings during weathering [Christensen *et al.*, 2000; Christensen *et al.*, submitted].

Although we exclude none of the above models, the geologic setting of the martian hematite deposits and terrestrial analogue samples, lead us to preferred models that the deposits of gray hematite formed by chemical precipitation from Fe-rich aqueous fluids, under either ambient or hydrothermal conditions (models 1a and 1c). [Christensen *et al.*, submitted].

The thermal inertia in the region of high hematite signature (latitude 3°S to 2°N; longitude 0° to 7°W) measured using high resolution, pre-dawn Viking Infrared Thermal Mapper

(IRTM) data [Christensen and Moore, 1992] varies from 5.3 to 10.1 (units of $10^{-3} \text{ cal cm}^{-2} \text{ sec}^{-1/2} \text{ K}^{-1}$; 221 to 423 in units of $\text{J m}^{-2} \text{ sec}^{-1/2} \text{ K}^{-1}$), with an average value of 7.4. These values are only slightly higher than the Martian average value of ~ 6.5 [Palluconi and Kieffer, 1981], and indicate an average particle size of the surface materials of 800-900 μm [Presley and Christensen, 1997]. The rock abundance for this area varies from 1 to 13%, with an average value of 7% areal rock cover [Christensen, 1986]. These values are typical for much of Mars [Christensen and Moore, 1992], but are lower than the values observed at the Viking Lander and Pathfinder sites [Golombek et al., 1999]. Based on these results, the physical characteristics of this site satisfy all of the engineering requirements for the Rover mission currently planned.

References

- Christensen, P.R., The spatial distribution of rocks on Mars, *Icarus*, 68, 217-238, 1986.
- Christensen, P.R., R.L. Clark, H.H. Kieffer, M.C. Malin, J.C. Pearl, J.L. Bandfield, K.S. Edgett, V.E. Hamilton, T. Hoefen, M.D. Lane, R.V. Morris, R. Pearson, T. Roush, S.W. Ruff, and M.D. Smith, Detection of crystalline hematite mineralization on Mars by the Thermal Emission Spectrometer: Evidence for near-surface water, *J. Geophys. Res.*, 105, 9623-9642, 2000.
- Christensen, P.R., M.C. Malin, R.V. Morris, J.L. Bandfield, and M.D. Lane, Martian hematite mineral deposits: Remnants of water-driven processes on early Mars, *Nature*, submitted.
- Christensen, P.R., and H.J. Moore, The martian surface layer, in *Mars*, edited by H.H. Kieffer, B.M. Jakosky, C.W. Snyder, and M.S. Matthews, pp. 686-729, University of Arizona Press, Tucson, AZ, 1992.
- Golombek, M.P., H.J. Moore, A.F.C. Haldermann, T.J. Parker, and J.T. Schofield, Assessment of Mars Pathfinder landing site predictions, *J. Geophys. Res.*, 104, 8585-8594, 1999.
- Palluconi, F.D., and H.H. Kieffer, Thermal inertia mapping of Mars from 60°S to 60°N, *Icarus*, 45, 415-426, 1981.
- Presley, M.A., and P.R. Christensen, Thermal conductivity measurements of particulate materials, Part II: Results, *J. Geophys. Res.*, 102, 6651-6566, 1997.

ANALYSIS OF POTENTIAL MER SITES IN THE SOUTHERN ISIDIS REGION;

L. S. Crumpler¹, K. L. Tanaka², and T. M. Hare². ¹New Mexico Museum of Natural History and Science, 1801 Mountain Road NW, Albuquerque, NM 87104; ²U. S. Geological Survey, Flagstaff, AZ 86001; lcrumpler@nmmnh.state.nm.us.

Introduction. The southern Isidis basin rim is an area with spectacular massifs (Libya Montes), one of the highest valley-network densities on Mars, including restricted paleolake basins, and a demonstrable long-lived fluvial history. A reassessment of the potential landing sites available for the southern Isidis rim region, using the new engineering constraints for MER landers, does not significantly degrade the access to desirable geologic materials in Isidis rim targets relative to that outlined in previous ('01) targeting exercises, but does degrade access to desirable geologic map units. Opportunities remain strong for addressing the goals of the Mars exploration and MER programs as currently defined. The geologic environments within accessible target areas preserve likely sedimentary materials associated with the long fluvial history of southern Isidis and Libya Montes. Thus sites in this region support the mission goal of documenting the history of climate and water on Mars. In this study we evaluate the results of our detailed geologic mapping and its correlation with remote sensing properties to define the best sites for accomplishing MER science goals.

Geologic Characteristics of Sites. Sites in southern Isidis that meet the MER A and B engineering constraints and the basic science goals occur mostly within the slopes adjoining fluvially modified highlands where valley-networks descend and terminate in the Isidis basin. These slopes have been mapped previously [1-5] as "terminal plains materials". Terminal plains material is featureless at typical Viking resolutions and DIMs, but is characterized in 10-m to 50-m resolution images (MOC and Viking) as rolling moderate albedo plains interrupted at 100 meter distances by small secondary impact craters and, at 0.5 to 1 km distances, by small dune fields. Although terminal plains are typically streaked in Viking image mosaics, suggesting abundant aeolian fines in the surface, neither high-resolution image data nor TI data support the existence of an excessive fines component. Terminal plains are sites of high ferric iron, consistent with possible aqueous alteration of fundamentally mafic highland materials.

Mapping and Analysis Status. Given that the terminal valley-network deposits in Isidis Planitia where it transitions to the highlands can accommodate the current large (~180-km by 30-km) targeting ellipses, whereas central Libya Montes may not, we are expanding detailed geologic mapping from Libya Montes into the proximal portions of the Isidis plains. The object will be to resolve what geologic characteristics are present that are relevant to the MER mission. Several questions being addressed include: To what extent (how far from the mappable highlands) do valley-network sediments contribute to surface in the rim plains? What

is the areal extent of surficial materials, including aeolian deposits and do they obscure the relevant geologic target materials? Are enigmatic pitted mound lines available together with otherwise desirable target materials and what are their possible origins? [6-8]

Conclusions. Most of the valley-networks and intermontane plains in the Isidis rim are excluded currently from direct targeting and sampling because they either lie above the minimum altitude or may be too mountainous to enable fitting viable targeting ellipses. However, several factors enable viable sites occur within the lower elevation reaches of this very desirable fluvial terrain along the rim that enable the principal mission goals while also attaining a reduction in landing hazards. All safe sites along the Isidis rim plains are not geologically equal from the perspective of MER mission objectives. Sites that take advantage of deposits likely to have accumulated at the termini of valley-networks draining western Libya Montes are more desirable because they sample a greater number of paleo lake basins and larger drainage areas.

First, many of the valley-networks converge to major trunk lines that in turn exit out onto the plains along the rim. These sites are restricted to a few accessible areas and are thus sites where valley-network sediments are accessible. This is largely the case in the western part of the southern Isidis rim plains. Second, several large impact craters in the plains along the rim have excavated samples of a potentially wide variety of geologic materials across a large vertical sedimentary section in the areas over which valley-network sediments have accumulated. In many ways this enhances, relative to sites within the valley-networks themselves, the likelihood that sediments, and not pre-existing terrains excavated by the valley-network channels, will be available for study. Third, several landing ellipses lie within the theoretical and observed ballistic, discontinuous ejecta limits of young, large impact craters that have sampled nearby Syrtis Major Planum lavas, increasing the probability of sampling materials from middle martian geologic history. Fourth, the hydrologic characteristics of the basin rim insure that any water that made its way into the plains along the terminus of valley-network trunk lines has flowed down the hydrologic gradient and interacted with sediments in the near surface along the basin rim. Fifth, new opportunities for opportunistic surface investigations within the Isidis plains not previously considered may be considered for several possible ellipse areas, including pitted mounds typical of the inner Isidis rim plains. Both volcanic and hydrologic origins have been proposed for these.

A tabulated list of the primary targets in the Isidis region together with relevant remote sensing

SITES IN SOUTHERN ISIDIS: Crumpler, Tanaka, and Hare

properties for MER A and MER B within the Isidis rim region are submitted with this report.

References. [1] Crumpler, L. S., abstract, *Second Mars Surveyor Landing Site Workshop*, 22-24, LPI, Buffalo, June 22-23, 1999; [2] Crumpler, L. S., in *Lunar Planet Sci. XXVIII*, 1999; [3] Crumpler, L. S., in *Lunar Planet. Sci. XXIX*, Abstract #1946, LPI, Houston, (CD-ROM), 1998; [4] Crumpler, L. S., in *Mars Surveyor 2001 Landing Site Workshop*, NASA-

Ames, Moffett Field, CA, January 26-27, 1998; [5] Crumpler, L. S., in *Lunar Planet. Sci.*, XXVII, 273-274, 1997; [6] Grizzaffi P. and Schultz P.H. *Icarus* 77, 358-391, 1989. [7] Davis P.A. and Tanaka K.L., in *Lunar Planet Sci. XXVI*, 321-322, 1995. [8] Tanaka, K. L., in *Lunar Planet. Sci. XXXI*, Abstract #2023, LPI, Houston, (CD-ROM), 2000.

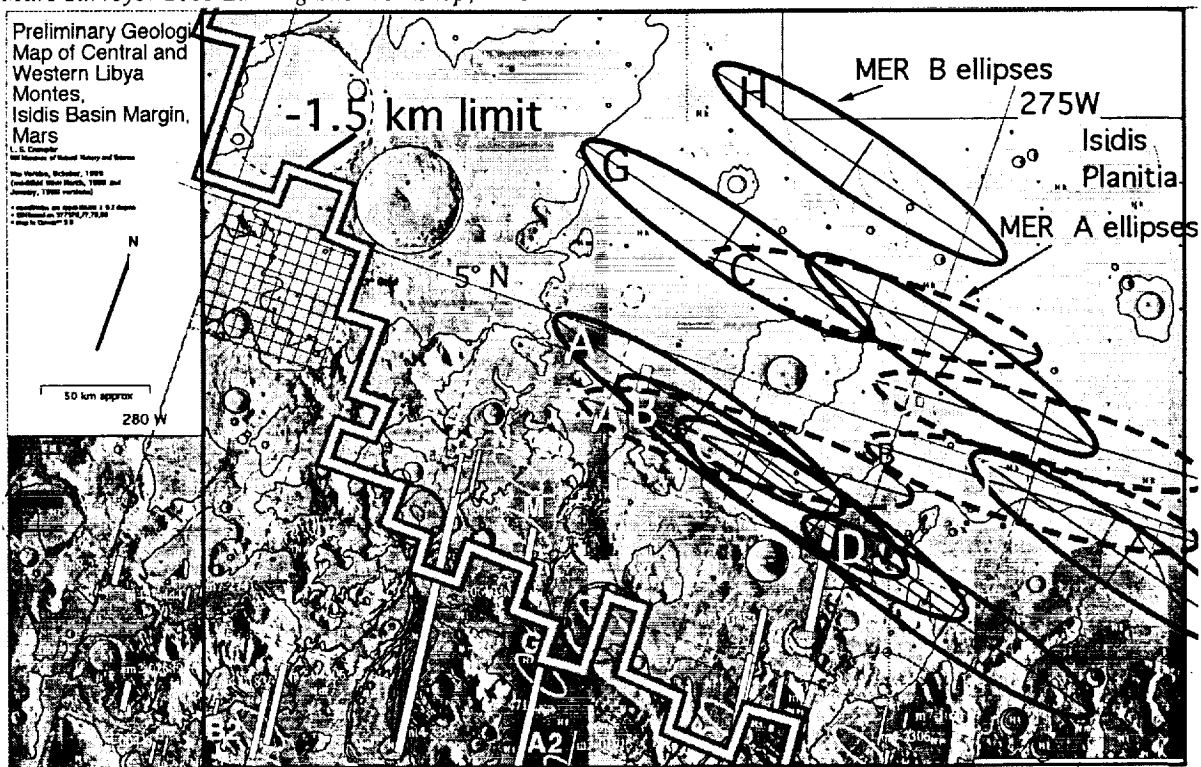


Figure 1. Northern segment of the line geologic map of the southern Isidis rim region overlain on the regional DIM. For discussion of geologic units see [3, 4, 5]. Large ellipses represent approximate 180 x 30 km landing targeting ellipses typical of MER A and B at a latitude of about 5°N. Smaller ellipses, originally proposed for MS Landers '01. Also shown are foot prints for narrow angle MOC data and corresponding image numbers.

Table 1. Coordinates and ranking of Isidis basin margin sites as of 12/00.

Site	Latitude	Longitude	Principal Geologic Unit
MER B			
(1) A	4.6	276.5	sediment fans, discontinuous ejecta
(2) B	4.2	275.6	sediment fans, discontinuous ejecta
(3) C	4.1	275.3	sediment fans, discontinuous ejecta
B alternates			
D	3.8	274.2	sediment fans, highland material
E	5.6	274.9	knobby plains
F	4.6	273.2	sediment fans
G	5.8	276.7	knobby plains
H	6.7	276.0	knobby plains
MER A			
(4) A	4.5	276.0	sediment fans, discontinuous ejecta
(5) B	4.8	274.0	sediment fans, discontinuous ejecta

MER 2003 LANDING SITE PROPOSAL: AMAZONIAN LACUSTRINE MATERIALS. R. A. De Hon, Department of Geosciences, University of Louisiana at Monroe, Monroe, LA 71209.

Introduction: A generalized target region is proposed for a possible landing target for the Mars Exploration Rover in 2003. The proposed site is along the southern boundary of the Elysium Basin.

Mission: MER 2003 A or B

Proposed Site: Within the region 5°N to 5°S and 190°W to 205°W on the southern boundary of Elysium Planitia

Primary Goal: Investigate young sediments (Elysium Basin bright material, unit Aebb) presumably lacustrine sediments, possibly evaporites (1)

Secondary Goals: Investigate crater ejecta sampling materials subjacent to sedimentary cover. Materials that may be sampled include knobby material (unit Aebk), etched material (unit Aebe), and eolian or volcanic material (unit Aml).

Site Characteristics

Elevation: -1.5 to 2.5 km

Rock abundance: Low

Thermal Inertia: Marginal

Advantages:

Engineering: Region is at low elevation, near equator, and smooth

Science: Terrestrial analogs provide evidence of abundant biotic activity.

Existing MOC Imaging: SP2350/04 at 0.6°N, 186.4° and AB1113/03 at 2.2°N, 183.3° provide some indication of possible surface morphology.

Problems and Pitfalls:

Engineering: Surface materials may provide poor radar return which would hamper landing.

Science: Possible eolian cover may mask primary target material.

Discussion: Current mission objectives limit potential sites to those with a presumed or an identifiable aqueous history in the anticipation of finding evidence of prebiotic or biotic activity. Engineering constraints limit the landing sites to low elevation and low latitude. A candidate landing zone is chosen in southern Elysium Planitia. Within this zone several landing ellipses are possible. Additional MOC images are desirable.

The southern Elysium Planitia zone corresponds to a potential shoreline of a large lacustrine basin (Scott and Chapman, 1995). The site offers the advantages a relatively smooth surface and low slopes for landing and rover operation. If the southern Elysium basin is a paleolake, then the near shore environment offers a high potential for developing biotic communities while the lake was in existence.

Terrestrial analogs ranging from Antarctic ice covered lakes to Pleistocene paleolakes abound (2, 3). The near shore environment in these basins includes algal mats, tufa towers, tracks and trails as well as shells and other hard parts of former residents. The biggest problem of a robotic search for life is designing a set of experiments that will be able to investigate evidence that is incorporated within existing sediments or rocks. Terrestrial searches often require microscopic observation and extensive sample "picking".

References: (1) Scott and Chapman, 1995; (2) Eugster and Hardie, 1978; (3) Gierlowski-Kordesch and Kelts, 1994

A NEW ERA IN GEODESY & CARTOGRAPHY: IMPLICATIONS FOR LANDING SITE OPERATIONS.

T. C. Duxbury, Jet Propulsion Laboratory, California Institute of Technology, Pasadena, CA, 91109, tduxbury@jpl.nasa.gov

The Mars Global Surveyor (MGS) Mars Orbiter Laser Altimeter (MOLA) global dataset has ushered in a new era for Mars local and global geodesy and cartography. These data include the global digital terrain model (DTM – radii), the global digital elevation model (DEM – elevation with respect to the geoid), and the higher spatial resolution individual MOLA ground tracks.

Currently there are about 500,000,000 MOLA points and this number continues to grow as MOLA continues successful operations in orbit about Mars. The combined processing of radiometric X-band Doppler and ranging tracking of MGS together with millions of MOLA orbital crossover points has produced global geodetic and cartographic control having a spatial (latitude / longitude) accuracy of a few meters and a topographic accuracy of less than 1 meter [1].

This means that the position of an individual MOLA point with respect to the center-of-mass of Mars is known to an absolute accuracy of a few meters. The positional accuracy of this point in inertial space over time is controlled by the spin rate uncertainty of Mars which is less than 1 km over 10 years that will be improved significantly with the next landed mission.

MOLA observed features or areas on Mars are subject to these same levels of inherent accuracy but are limited at a larger uncertainty because of the 160 m MOLA spot size and 300 m spacing between points along track. This spatial sampling or resolution of MOLA degrades the accuracy at the 100 m level when interpolating a feature location because of the limited spatial resolution. Relating these features to earth, as is needed for targeting a lander, becomes additionally corrupted at the few hundred meter level due to Mars ephemeris uncertainties. Continued orbiter and landed missions will reduce this error.

Techniques for registering other dataset to MOLA are becoming more common, allowing the registration and map projection of higher resolution datasets such as Viking Orbiter and MOC NA imaging to the MOLA reference surface and latitude / longitude coordinate grid. These registered higher spatial resolution datasets will share the positional uncertainties due to MOLA spatial resolution and Mars ephemeris uncertainties at the few hundred meter level.

Prior to MGS / MOLA, the positional uncertainties of features relative to the Mars center-of-mass, inertial space and relative to earth were at the 10 km level. The MOLA dataset is now reducing this uncertainty by

2 orders of magnitude, ushering in a new era for Mars geodesy and cartography.

This level of accuracy now reduces the cartographic map error contribution to the MER landing ellipses to a negligible number. Also, the global radii and elevation data will play a major role in downsizing potential landing sites when applying entry engineering constraints.

Such accuracies also support the evolving Entry, Descent and Landing (EDL) technologies by providing absolute inertial ties that could also be used by approach optical navigation for landing targeting



MOLA Global DEM using only 1/5th of the existing dataset

References: [1] Neumann G. A., Rowlands D.D., Lemoine F. G., Smith D. E., and Zuber M. T., submitted to *JGR*, September 11, 2000.

Acknowledgements: This work would not be possible without the MGS MOLA instrument under Dr. David E. Smith, Goddard Space Flight Center, and the MOLA team. This research was carried out at the Jet Propulsion Laboratory, California Institute of Technology, under contract to the National Aeronautics and Space Administration, Mars Data Analysis Program.

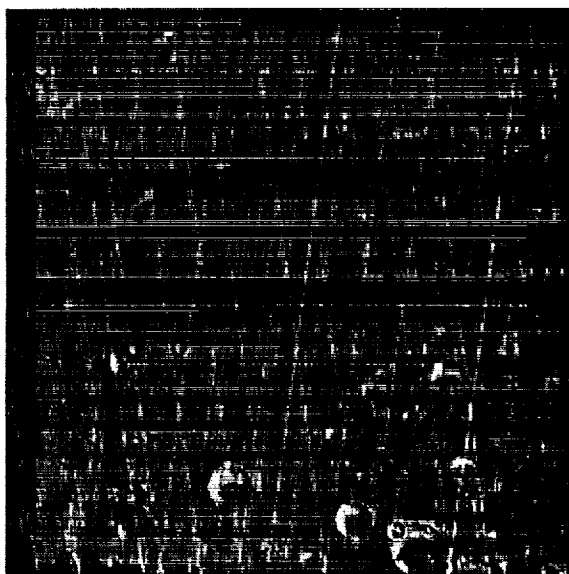
MOLA-BASED LANDING SITE CHARACTERIZATION. T. C. Duxbury and A. B. Ivanov, Jet Propulsion Laboratory, California Institute of Technology, Pasadena, CA, 91109, tduxbury@jpl.nasa.gov and Anton.B.Ivanov@jpl.nasa.gov,

The Mars Global Surveyor (MGS) Mars Orbiter Laser Altimeter (MOLA) data provide the basis for site characterization and selection never before possible. The basic MOLA information includes absolute radii, elevation and 1 μm albedo with derived datasets including digital image models (DIMs – illuminated elevation data), slopes maps and slope statistics and small scale surface roughness maps and statistics. These quantities are useful in downsizing potential sites from descent engineering constraints and landing / roving hazard and mobility assessments. Slope baselines at the few hundred meter level and surface roughness at the 10 meter level are possible.

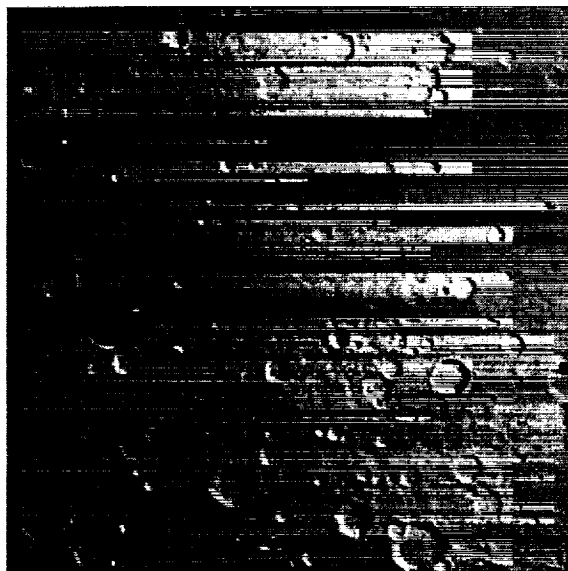
Additionally, the MOLA-derived Mars surface offers the possibility to precisely register and map project other instrument datasets (images, ultraviolet, infrared, radar, etc.) taken at different resolution, viewing and lighting geometry, building multiple layers of an information cube for site characterization and selection. Examples of direct MOLA data, data derived from MOLA and other instruments data registered to MOLA are given for the Hematite area.



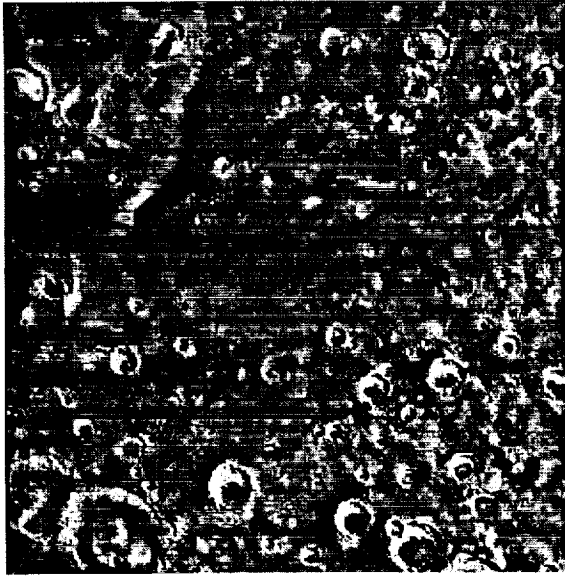
MOLA digital elevation model (DEM) in the Hematite area (~1.3 M MOLA points)



MOLA coverage in the Hematite area (~750 orbits)

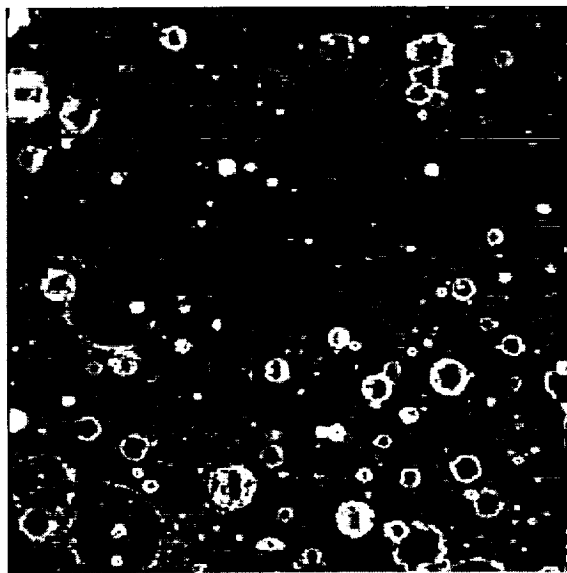


Derived digital image model (DIM) in the Hematite area produced by illuminating the MOLA DEM

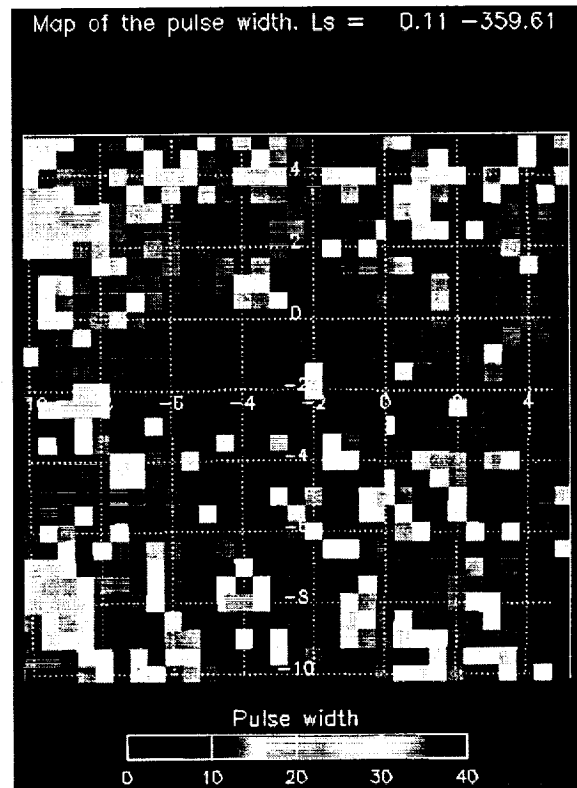


Acknowledgement: this work would not be possible without the success of the MGS MOLA instrument provided by Dr. David Smith, Goddard Space Flight Center and the MOLA team. This work was conducted at the Jet Propulsion Laboratory, California Institute of Technology, under contract to the National Aeronautics and Space Administration, Mars Data Analysis Program.

Map-projected and gridded Viking Orbiter imaging data registered to the MOLA reference surface and coordinates



MOLA-derived Hematite area slope map



Such pulse width maps combined with the slope map information on the left can be used to compute surface roughness

MARS 2003: SITE PRIORITIES FOR ASTROBIOLOGY. Jack Farmer¹, David Nelson¹, Ron Greeley¹ and Ruslan Kusmin², ¹Arizona State University, Dept. of Geology, P.O. Box 871404, Tempe AZ 85287-1404, jfarmer@asu.edu; ²Vernadsky Institute, Russian Academy of Sciences, Kosygin St. 19, Moscow, 117975, GSP-1 Russia.

Introduction: The exploration for past or present Martian life remains the primary goal of the Mars exploration program (1). In implementing this goal, the Astrobiology community has consistently recommended an approach that will create the proper environmental context for exploration through a synergistic use of orbital reconnaissance and landed *in situ* science (2-3). These broadly-based investigations are regarded to be an essential prelude for targeting sites for *in situ* life detection experiments and sample return(s) (4).

"Follow the Water"

In exploring for Martian life, two independent investigation pathways were recently identified by the Astrobiology community as co-priorities in missions preceding the 2007 opportunity. These include: 1) determining the locations of sedimentary deposits formed by past surface and subsurface hydrological processes (this will enable the exploration for a record of past life) and 2) mapping the three-dimensional distribution of water in all its forms (as a prelude to exploring potential habitats of subsurface liquid water that could sustain extant life).

The mantra, "follow the water", has been an organizing theme in constructing the new Mars exploration program. It appears that over the next few opportunities (through 2007) implementation of this goal will be achieved through a combination of orbital mapping (infrared spectral mapping of mineralogy to identify ancient surface and subsurface water systems and radar sounding from orbit to locate reservoirs of modern subsurface water) and landed rover missions. Orbital missions in 2001 and 2005 will be interleaved with surface investigations in 2003 that will

place twin rovers (MER A and B) at two sites to gather information about surface mineralogy and petrology. This data will provide the basis for assessing ancient depositional environments at each site, while providing ground truth mineralogy to assist the interpretation of previously acquired orbital data.

Astrobiology Goals for 2003

It is clear that the 2003 mission will play a pivotal role in implementing the present strategy for Astrobiology. But to effectively "follow the water", this mission must be targeted to the sites that have the best chance of providing access to aqueously-deposited sedimentary rocks. Of course, in order to ensure overall mission success, this must be accomplished within well-defined engineering safety guidelines. The challenge to the community will be to find the best compromises between the often conflicting demands of mission science and safety.

To provide a forum for engaging the broader Astrobiology community in scientific discussions about landing site priorities for the 2003 mission, we reviewed a number of high priority sites (see Table 1) for members and invited guests of the NASA Astrobiology Institute (NAI), Mars Focus Group (MFG). This group was originally chartered to enhance opportunities for the involvement of astrobiologists in Mars program planning and to identify new directions in astrobiological research that could support upcoming missions. Landing site discussions were organized around the virtual institute model, with background information for site reviews being provided over the web, prior to "face to face" videoconference presentations and discussions. The format for discussion was organized around the two lines of evidence that

can be used to identify regions on Mars where hydrological processes were once active: geomorphic evidence and mineralogical evidence. The overall goal was to identify compelling science objectives that could be pursued at each of the sites given in Table 1, and to develop consensus recommendations regarding landing site priorities. These discussions (ongoing at the time this abstract was submitted) have continued via email and teleconference, up until the time of this workshop. The purpose of this presentation is to review science and site recommendations of the NAI Mars Focus Group and to expand the forum for follow-on discussions to include the broader planetary science community.

References: [1] Ed Weiler, personal communication, October, 2000; [2] NASA Special Publication #530 (January, 1995) "An Exobiological Strategy for the Exploration of Mars" (http://exobiology.arc.nasa.gov/ExobiologyProgram/Mars_Exo_Strategy_Doc.html); [3] NASA Astrobiology Institute, Mars Focus Group Science Recommendations for a Revised Mars Program Architecture January 10, 2000 (Jack Farmer, Chair; [4] NASA Mars Exploration Payload Advisory Group (MEPAG), Life Subgroup Report, Nov. 2000 (Ronald Greeley, Chair).

TABLE 1. ASTROBIOLOGY SITES FOR MARS 2003

ENVIRON	LAT/LONG	MER SITE
Cryo-Magmatic (Hydrothermal)		
Apollonaris Chaos	10-13°S/186-190°W	A
Aram Chaos	0-5°N/17-24°W	B
Lacustrine Basin		
Gusev Crater	14.2°S/184.8°W	EP 55A-A
Gale Crater	6.8°S/222.4°W	EP 82A-A
Sinus Meridiani	0-5°S/0-10°W	A or B
Candor Chasma	6-9°S/169-173°W	A or B
Fluvial Channel/Alluvial Plain		
Mangala Vallis	4.5°S/148°W	B
Durius Valles	14.6°S/187.6°W	EP 56A

SUBMARINE VOLCANIC LANDFORMS AND ENDOLITHIC MICROORGANISMS M. R. Fisk, College of Oceanic and Atmospheric Science, 104 Ocean Admin Bldg, Oregon State University, Corvallis, OR 97331-5503 USA, Phone 541-737-5208, (mfisk@oce.orst.edu).

Subaqueous volcanic eruptions produce characteristic landforms and lava flow morphologies that are distinct from subaerial eruptions. Eruptions from fissures on the sea floor produce hummocks rather than flat lava flows. Hummocky lava flows typically have dimensions of 500 m wide, 5000 m long, and 50 m high. The hummocks are made of piles of bulbous pillows that are about 1 m in diameter. Because of the high specific heat of water and the large temperature difference between magma and liquid water (about 1100°C) the exteriors of lava flows are quenched to glass. Cooling of lava flows in air does not have this effect.

The quenched volcanic glass in aqueous environments contains microorganisms that dissolve the glass and leave secondary minerals such as clay, iron oxides, and sulfides in the voids. The microbial excavation of the glass produces a wide variety shapes and sizes. These microbially produced excavations may be 100 μm long by 3 μm diameter tubes, starbursts of radiating tubes, branching 1 μm diameter tubes, or other shapes. These tubes and excavations are distinctive, they are associated with bacteria, and they are preserved along with the glass

In surveys of volcanic glass from subaqueous lava flows we have found this evidence of microbial activity in rocks at ocean subbottom depths of a few meters to 1500 m. These rocks range in age from about 1 million years to 170 millions years. Where submarine volcanic rocks have been uplifted to dry land, the glass may also preserve microbial patterns of glass alteration.

Comparisons of terrestrial and Martian landforms could reveal the locations of subaqueous volcanic activity on Mars. Given the similarity of compositions of igneous rocks on the two planets, subaqueous eruptions on Mars will have quenched glass exteriors. Evidence of microbial colonization of the glass will be preserved as long as the glass is preserved. Also, the microbial activity that produces the characteristic microbial tubes appears to be extremely slow and is unlikely to occur after the rocks are collected. Hummocky regions built from successive eruptions of lavas into water could produce unequivocal evidence of past life on Mars.

POTENTIAL NOACHIAN-AGED SITES FOR MER-B. M. S. Gilmore¹ and K. L. Tanaka², ¹Dept. of Earth and Environmental Sciences, Wesleyan University, 265 Church St. Middletown, CT 06459, mgilmore@wesleyan.edu, ²U.S. Geological Survey, 2255 N. Gemini Dr., Flagstaff, AZ 86001.

Introduction: Two Mars Exploration Rovers (MER) are slated for launch in 2003 and will land in the equatorial region of Mars. These rovers are more formidable in both size and instrument complement than the Sojourner rover, potentially allowing greater range. For landing, they will be housed in an airbag system nearly identical to Pathfinder allowing them to land in an area with elevation below 1.3 km, RMS slopes <6°, rock abundance <20%, and fine component thermal inertia >3-4 cgs units. MER-A may land between 15°S to 5°N and MER-B between 10°S and 10°N.

Numerous sites have been identified by the JPL team as meeting the above engineering requirements for the landing of the rovers [1]. Here we focus on a subset of these that lie in Noachian-aged terrain, as defined by Viking-era geologic mapping [2]. This subset is further reduced by the first author's support of the selection (if possible) of a site in the Valles Marineris which can only be reached by MER-A, this study therefore focuses on those Noachian-aged sites that can be reached by MER-B.

Scientific Rationale: A primary goal for the Mars exploration program is to search for evidence of ancient or extant water on Mars as water is essential for past and future (human) life on Mars. Valley networks are recorded in Noachian-aged surfaces and interpreted to require warmer conditions in the martian past [3]. The only martian meteorite we have from this era, ALH84001, includes carbonates precipitated from water; such minerals are effective on the Earth at preserving life [4] and may (with high uncertainty) have done so in this meteorite [5]. As life gained a foothold on Earth within 1 Ga of its formation, it is possible, that life also appeared on Mars. Noachian terrains are most likely to contain rocks from an era that had abundant liquid water and perhaps signs of life. Additionally, each of the three successful landings on Mars was in the northern plains where rocks consistent with basalt were measured. Although basaltic components have been identified spectroscopically in the southern hemisphere [6], this crust is still a candidate for primary crust that, like the Moon, could be the result of a magma ocean. Measurement of the composition of the highlands crust would constrain models for the bulk composition of the planet and place the martian meteorites in better context.

Methods: Available (as of Dec 2000) MOC images were examined for several defined ellipses in the

Terra Meridiani region and the Xanthe Terra region. The images include examples of Noachian plateau sequence (unit Npl₁), Noachian subdued crater unit (unit Npl₂) and Hesperian Ridged plains material (unit Hr) as defined by [2]. We examined the morphological characteristics of the images and assessed the terrains for safety and accessibility to outcrops.

Results: *Sinus Meridiani.* Several sites in Terra Meridiani intersect the hematite deposit identified by TES aboard MGS [7]. One of the landing ellipses (TM23B; 3.4°S, 3.1°W) has particularly good MOC coverage as a consequence. The images reveal a low-albedo smooth surface in Sinus Meridiani as has been observed by other researchers [e.g., 8]. Round, subtle depressions are interpreted to be filled craters; most craters on the surface are shallow, filled with dark material, and have bright rims. This has been interpreted by [7] to indicate the dark material covers bright material exposed in the crater rims. This is consistent with observations in ellipse TM20B (2.3°S, 6.2°W), the eastern half of which lies within the mapped hematite region. MOC image M10-01349 (centered 2.77°S, 5.43°W) is dominated by dark material interrupted by occasional outcrops of brighter terrain. An 8km crater intersecting the frame exposes bright material at its rim. This bright material is covered in some places by dark material that fills topographic lows. Although the dark material appears as a veneer perhaps meters thick here and throughout the area, it is abundant enough to have covered the crater walls and floor. Bright materials from the rim have subsequently shed down the crater wall resulting in bright streaks and may be contributing to bright dunes on the floor.

Ellipse TM22B (3.2°S, 7.1°W) also contains some smooth and dark deposits punctuated by mesas and knobs and bright dune fields. The portions of the MOC images within the ellipse appear relatively free of large hazards, but are not within the mapped hematite area proper.

Western Arabia/Terra Meridiani. Several ellipses in the region intersect two or more geologic units. In particular wA3B (9.2°N, 6°W), TM10B (5.6°N, 8.3°W) and TM11B (4.2°N, 7.8°W) include a contact between Npl₁ and the overlying Npl₂. Although the likelihood of landing on the contact is small, mechanical processes (cratering, weathering) may have resulted in the exposure of both rock units throughout the area. No MOC images were available within these ellipses

and these areas should perhaps be considered for future targeting.

Ellipses TM15B (0.3°N, 9.7°W) and TM17B (0.5°S, 9°W) may include units Npl₁, Npl₂ and Hr. Examination of MOC images within these ellipses reveal a very rough surface that likely corresponds to unit Hr. This surface is extensively layered with knobs and appears unsafe for landing of the rovers. Nearby MOC images of Hr confirm a rough morphology in this region covered by extensive dark dunes deposits, however exposures of unit Hr to the northwest in western Arabia (e.g., within TM12B) are smoother at the ~2m scale. Further imaging and investigation is required for those who advocate landing in unit Hr.

Xanthe Terra. Several ellipses can be defined in Xanthe Terra in Noachian unit Npl₂ amidst the chaos northeast of the Valles Marineris. Only one of these ellipses, XT34B (6.2°N, 40.6°W) contained a MOC image displaying a cratered surface at ~10m/pixel. Examination of other MOC images in the region reveals a surface of moderate albedo and relatively smooth at ~2m/pixel. The Npl₂ unit here has more craters than Sinus Meridiani, particularly <1 km in diameter, although most craters are subdued and shallow, with indiscernable ejecta and duneforms on their floors. Of the examined images, dunes were not ubiquitous, but confined to crater floors and regions adjacent to larger craters. This may indicate a surface with better access to rocks than surfaces with numerous dunes.

Potential Sites: Ellipses TM20B, TM22B and TM23B each contain dark, smooth deposits coincident

with the mapped hematite that appear relatively free of large hazards. The smooth terrain north of the large crater in the region of ellipse TM20B is particularly smooth with outcrops of underlying material on the surface (not just in craters). This may be an ideal situation where both the surface materials, which are unusual on Mars and may be well characterized by the instruments (particularly the Mössbauer spectrometer) on board the rovers, and underlying, presumably Noachian materials may be accessible by the rover. Landing in this unit may thus achieve the goals of determining the composition of the martian highlands, measuring the composition of the hematite region, and sampling rocks from an era that had water and may have had life. The 1st and 3rd of these goals may be satisfied at the other Noachian sites mentioned here, but more imaging and research is required to assess the safety of these sites within the proposed landing ellipses. For such sites, an ellipse that includes a contact between the two major Noachian units is preferred.

References: [1] Golombek, M. and Parker, T. (2000) *MER Engineering Constraints and Potential Landing Sites Memo*. [2] Scott D.H. and Tanaka K. L.. (1986) *USGS Maps I-1802-A*; Greeley R., and Guest J. E. (1987) *USGS Map I-1802-B*. [3] Carr M. H., (1996) *Water on Mars*, Oxford. [4] Walter M. R. and DesMarais D. J. (1993) *Icarus* 101, 129-143. [5] McKay D. S., et al., (1996) *Science* 273, 924-930. [6] Bandfield et al. (2000) *Science* 287, 1626-1630. [7] Christensen P.R. et al., (2000) *JGR* 105, 9623-9642. [8] Edgett K.S. and Parker T.J. (1997) *GRL* 24, 2897-2900.

EXTREME ROCK DISTRIBUTIONS ON MARS AND IMPLICATIONS FOR LANDING SAFETY. M. P. Golombek, Jet Propulsion Laboratory, Caltech, Pasadena, CA 91109, mgolombek@jpl.nasa.gov.

Introduction: Prior to the landing of Mars Pathfinder, the size-frequency distribution of rocks from the two Viking landing sites and Earth analog surfaces was used to derive a size-frequency model for nominal rock distributions on Mars [1]. This work, coupled with extensive testing of the Pathfinder airbag landing system [2], allowed an estimate of what total rock abundances derived from thermal differencing techniques [3] could be considered safe for landing. Predictions based on this model proved largely correct at predicting the size-frequency distribution of rocks at the Mars Pathfinder site and the fraction of potentially hazardous rocks. In this abstract, extreme rock distributions observed in Mars Orbiter Camera (MOC) images are compared with those observed at the three landing sites and model distributions as an additional constraint on potentially hazardous surfaces on Mars.

Mars Rock Distributions: The Viking landing sites and the Mars Pathfinder landing site show rock size-frequency distributions that largely follow an exponential when expressed in cumulative fractional area covered by rocks of a given diameter or larger versus diameter plots. The distributions can be fit by equations of the form: $F_k(D) = k \exp[-q(k)D]$, where $F_k(D)$ is the cumulative fractional area covered by rocks of diameter D or larger, k is the total area covered by all rocks, and an exponential $q(k)$, which governs how abruptly the area covered by rocks decreases with increasing diameter [1]. Similar rock distributions were also measured at a wide variety of rocky locations on the Earth. These similar distributions and the Viking distributions specifically, were used to develop a model size-frequency distribution for Mars in which k is equal to the total rock abundance [3] and the exponential, which from the Viking sites was approximated by $q(k) = 1.79 + 0.152/k$. These distributions form a family of non-crossing curves (Figure 1) that flatten out at small rock diameter at a total rock abundance of 5-40% [3].

The distribution of rocks measured at the Mars Pathfinder landing site [4] follows the model distribution for total rock abundance of 16% (Figure 1). The large size fraction in the measurement of the annulus 3-6 m from the lander is slightly skewed due to the presence of one large rock, Yogi, in a small counting area. For large rocks (before the resolution drop off at <1 m diameter) in the far field [5], the area covered is consistent with the model results for 16% rock abundance.

Extreme Rock Distributions: As a further test of these model rock distributions and the distribution of very large rocks on Mars in general, a survey of 25,000 released high-resolution MOC images revealed roughly 25 (~0.1% of the total) with fields of hundreds to thousands of boulders. These large and dense boulder fields were typically at the base of scarps or around fresh craters. Two 400 m and 500 m diameter fresh impact craters, 3 relatively fresh grabens, and the caldera scarps of Olympus Mons were counted.

Boulders were fairly easy to identify as pairs of light and dark pixels (bright and shaded sides) on the images. The diameter was simply the number of pixels across, scaled for the image resolution, and emission angle. In practice, boulders down to one pixel diameter could be measured as a light and dark pixel pair. Although there was some uncertainty in the identification, it was generally repeatable, with two different observers yielding similar results [6]. Measured boulder diameter is probably within ± 1 pixel. The smallest diameter boulder measured was about 1.6 m and the largest was just over 20 m.

Of the six images with boulder fields counted, the maximum subareas are shown in Figure 1, which include the crater rims, the graben floors, and the Olympus Mons caldera scarps. In general, the average and minimum rock distributions in the boulder fields are a factor of 2-5 and 10 smaller, respectively, than the maxima, so that those shown here can be considered representative of the maximum boulder distributions on Mars.

All of the fields have boulders 10 m in diameter or larger, with 0.1-3% area covered by boulders >5 m in diameter, 0.01-3% area covered by boulders >10 m in diameter, and <0.01% area covered by boulders ≥ 20 m diameter. Even though these distributions are up to an order of magnitude greater than the model rock distributions, the shape of the distributions are generally parallel to the model distributions showing the sharp decrease in area with increasing diameter. The flattening of the distributions at small diameter is probably a resolution effect, but even so, it is not clear what happens to these extreme distributions at smaller diameter. It is possible that the number of small rocks continues parallel to the model distributions, which would represent surfaces covered by 100% rocks. Although such large distributions are not observed in thermal differencing measurements at larger spatial scales observed from orbit (down to 3 km pixels [3]), they could exist on smaller spatial scales. Alternatively, the distribu-

tions could flatten out at larger diameters or even be composed of multiple branches or segments [e.g., 7]. For reference, the maximum distribution of large rocks seen from a lander, on the rim of a crater in the far field of Viking 1, is elevated above that found in the near field [1], but the trend is parallel to the 30-40% model distributions at these diameters.

Not shown are the plots of cumulative number of rocks per square meter versus diameter for the three landing sites and the boulder fields. These distributions can also be fit with exponential functions with noticeable curvature to the distributions at large and small diameters (on a log-log plot), but with more linear distributions at intermediate diameters. For the 3 landing sites, less than $0.01/\text{m}^2$ rocks ≥ 1 m diameter are present. For the boulder fields, 0.00004 - $0.0004/\text{m}^2$ rocks ≥ 5 meters diameter are present, and 10^{-6} - $10^{-3}/\text{m}^2$ rocks ≥ 10 meters diameter.

Implications for Nominal Rock Hazards: These extreme rock distributions must be compared with those observed at the 3 landing sites to be placed in perspective. All three landing sites fall within the rockiest 15% of the planet [3]. In thermal measurements and surface rock counts [1, 3, 4], the three landing sites have total rock abundances of 15-20%, yet have $<1\%$ of their surfaces covered by rocks >1 m diameter. Furthermore, the highest resolution MOC images of the landing sites show at most one or two rocks in the entire imaged areas [8], which cover tens of square kilometers. This suggests 10^{-6} - $10^{-7}/\text{m}^2$ rocks greater than a few meters diameter, which is consistent with extrapolations to these diameters from the measured populations at the landing sites and areas covered by these large rocks of thousandths of a percent.

For reference, the Mars Pathfinder airbag system was successfully tested against surfaces with $\geq 10\%$ area covered by rocks 1 m in diameter [2]. The airbag stroke was around 1 m and they withstood repeated impacts against 0.5 m high rocks during testing. As a result, rocks greater than 1 m diameter were considered potentially hazardous, for typical height to diameter ratios of 0.5. The landing site constraint for Pathfinder and the preliminary constraint for the MER mission is $\leq 1\%$ of the area be covered by rocks >0.5 m high. Note that the reconstruction of the Pathfinder landing indicates the lander bounced 10-20 times traversing about 1-2 km distance [9]. Airbag testing against a tilted platform showed the total impact area to be about 13 m^2 . If the lander bounced 10-20 times, a total area of 130 - 260 m^2 was sampled. For cumulative number $0.01/\text{m}^2$ rocks ≥ 1 m diameter measured at Pathfinder, 1-3 rocks of this size were likely encountered without damage during landing.

Summary: Comparison of MOC images with rare fields of hundreds to thousands of boulders 2-20 m in diameter with the three landing sites, where such boulders are virtually absent, suggests that most of Mars where boulders cannot be seen is relatively free of large rocks and thus safe for Pathfinder airbag landing.

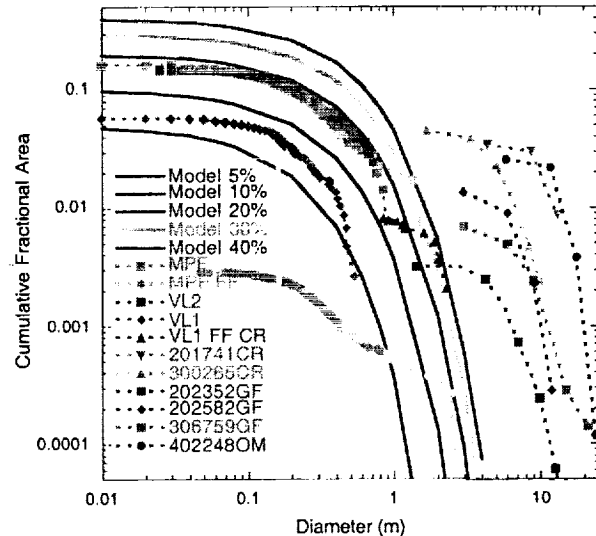


Figure 1. Cumulative fractional area covered by rocks of diameter D and larger versus diameter plot of the 3 landing sites, model rock distributions for Mars, and rare boulder fields measured in MOC images. The model rock distributions for 5, 10, 20, 30 and 40% [1] are shown as solid lines. Rock distributions measured from the near field of Viking 1 (VL1), 2 (VL2), and Pathfinder (MPF) are shown as a symbol for each rock or rock diameter. Rock distributions estimated from the far fields of Pathfinder (MPF FF) and the crater rim near Viking 1 (VL1 FF CR), which is the rockiest area visible from a lander, are shown as symbols for each rock or rock diameter. Extreme rock distributions for each MOC image number shown, represent the maximum rock distributions for all the rocky areas measured in these images (6-10 per image), with a symbol for each rock diameter and dashed connecting lines. Areas at crater rims are marked CR, areas in the floors of graben are marked GF, and the Olympus Mons caldera scarps are marked OM.

References: [1] Golombek M. & Rapp D. (1997) *JGR*, 102, 4117-4129. [2] Golombek M.P. et al. (1997) *JGR*, 102, 3967-3988. [3] Christensen P.R. (1986) *Icarus*, 68, 217-238 and pers. comm. [4] Golombek M.P. et al. (1997) *Science*, 278, 1743-1748. [5] Haldermann A.F.C. et al. (2000) *LPS XXXI*, Abs. #1846. [6] Rock survey and measurements were made by W. Koeppen and S. Patel. [7] Malin M.C. (1988) NASA TM 4041, 502-504, (1989) NASA TM 4130, 363-365. [8] T. Parker, pers. comm. [9] Golombek M.P. et al. (1999) *JGR*, 104, 8523-8553.

THERMAL INERTIA OF ROCKS AND ROCK POPULATIONS AND IMPLICATIONS FOR LANDING HAZARDS ON MARS. M. P. Golombek¹, B. M. Jakosky², and M. T. Mellon², ¹Jet Propulsion Laboratory, Caltech, Pasadena, CA 91109, mgolombek@jpl.nasa.gov, ²Laboratory for Atmospheric and Space Physics, University of Colorado, Boulder, CO 80309-0392.

Introduction: Rocks represent an obvious potential hazard to a landing spacecraft. They also represent an impediment to rover travel and objects of prime scientific interest. Although MOC images are of high enough resolution to distinguish the largest rocks (an extremely small population several meters diameter or larger), traditionally the abundance and distribution of rocks on Mars have been inferred from thermal inertia and radar measurements [1], our meager ground truth sampling of landing sites [1, 2], and terrestrial rock populations [3]. In this abstract, we explore the effective thermal inertia of rocks and rock populations, interpret the results in terms of abundances and populations of potentially hazardous rocks, and conclude with interpretations of rock hazards on the Martian surface and in extremely high thermal inertia areas.

Effective Thermal Inertia of Rocks: Spectral differencing of thermal measurements of Mars have been used to derive the rock component of a two component surface for an assumed effective thermal inertia of rocks [4]. These estimates typically assume an effective thermal inertia of about 1250 (SI units or $\text{J m}^{-2} \text{s}^{-0.5} \text{K}^{-1}$) for rocks of diameter 0.1-0.15 m [5]. In a review of thermal inertia data versus particle size, Jakosky [6], found that rocks greater than 0.2 m in diameter should have an effective thermal inertia approaching 2500, whereas particles of 0.001 to 0.03 m size should have effective thermal inertias of about 400. To derive the effective inertia of a rock population we applied a simple empirical model of effective inertia versus rock diameter that is consistent with these estimates. This model, assumes that rocks with diameters greater than 0.26 m have inertias of 2100, rocks with diameters 0.01-0.03 m have inertias of 400 and rocks in between have inertias that vary as the 0.75 power of their diameter [2]. The effective inertia for the entire rock population is calculated by summing the products of the thermal inertias and areas for each rock and dividing by the total area covered by all the rocks. This calculation is thus most sensitive to the shape of the cumulative fractional area versus diameter distribution of rocks and not the total area covered (which is normalized out). For the cumulative fractional area of rock versus diameter distributions reported in Golombek and Rapp [3], this parameter is the exponential factor, $q(k)$ in the equation: $F_k(D) = k \exp[-q(k)D]$, where $F_k(D)$ is the cumulative fractional area covered by rocks of diameter D or larger, k is the total area covered by all rocks, and $q(k)$, which governs how abruptly the area covered by rocks drops off at large diameter.

Effective Thermal Inertia of Rock Populations: Applying this equation to rock distributions on Mars and Earth analog sites shows that the total effective rock inertia typically covers a narrow range of 1700-2100. For measured rock distributions at the three landing sites, the total effective thermal inertia of the rock populations are 1700 for Pathfinder and 1900 for the Viking sites (without outcrops Viking 1 yields 1700). Most Earth analog sites reported in Golombek and Rapp [3] show a similar total effective thermal inertia of 1700-2100 for the measured rock distributions. The cumulative fractional effective rock inertia versus diameter plots generally mimic the cumulative fractional area versus diameter plots and are consistent with simple exponential functions in which the pre-exponential factor is the effective inertia of the entire rock population, and the exponential factor controls the decrease with large diameter.

Rock size-frequency distributions with gradual drop off in cumulative area with large diameter (such as the Ephrata Fan distributions), similarly show relatively flat cumulative fractional effective inertia versus diameter plots in which the cumulative fractional inertia of rocks greater than 0.26 m in diameter is 90% of the total. The other extreme is found in rock distributions with abrupt decrease in cumulative fractional area with increasing diameter such as Mars Hill in Death Valley or the Goldstone basalt surfaces in the Mojave Desert [3], in which less than half the cumulative fractional effective inertia is produced by rocks of diameter greater than 0.26 m. If $q(k)$ is less than about 4, the total effective inertia of the rock population will be ≥ 1700 . For example, the 5% model rock distribution in Golombek & Rapp [3] has a total effective rock inertia of about 1250 for a $q(k)$ of almost 5.

Potentially Hazardous Rocks: The effective inertia of rocks versus diameter equation shows that only rocks with effective inertias of 2100-2500 can be considered potentially hazardous as they correspond to rocks with diameters 0.26 m in diameter or greater. Rocks potentially hazardous to the MER landers are those greater than 0.5 m high [2] or those with diameters of 1 m or greater [3]. Note that the size-frequency distributions of rocks measured at the three landing sites have <1% area covered by rocks greater than 1 m diameter [2, 3], even though these sites are among the rockiest on the planet [4]. For a rock populations with a total effective inertia of 1700-2500, as opposed to the 1250 assumed in [4], less area would be covered by rocks [5] for a given bulk inertia. Conversely, any surface materials whose effec-

tive thermal inertia is less than 2500, should not be considered potentially hazardous.

Rock Abundance for Different Effective Rock Inertias: To address the change in inferred rock abundance (total area covered by a population of rocks) for different effective rock thermal inertias, a simple thermal model of the bulk inertia of the surface was solved for different rock inertia, rock abundance, and fine component inertia. Rock component thermal inertias of 1300, 1700, 2100, and 2500 were evaluated with a suite of fine component thermal inertias from 77 to 542. For each combination of rock and fine component thermal inertias, we calculated the surface temperature at 5AM local Mars time for the two materials (rock and fines) using a standard thermal model [7] and determined the corresponding black-body spectral emission at these temperatures. For a range of rock abundances (0-50%), we then mixed the corresponding spectral emissions and calculated the resulting 20 μm temperature (using an IRTM equivalent response function). Finally we derived the bulk thermal inertia from the 20 μm temperature using the algorithm of Mellon et al. [7]. (Throughout these calculations we assumed a surface albedo of 0.25, a infrared dust opacity of 0.1, and an atmospheric pressure of 6 mb). This yields a plot of bulk thermal inertia versus rock abundance for different effective rock inertias along lines of constant fine component thermal inertia (Figure 1).

Figure 1 shows that for changes in effective rock inertia from 1300 (lower solid lines) to 2500 (upper dashed lines) for any given fine component thermal inertia, the total change in rock abundance for any given bulk inertia is about 20%, which is the uncertainty typically reported for these estimates [1, 4]. The difference in rock abundance for rocks with effective inertias of 1300 versus 2500, should roughly correspond to the difference in relative area covered by rocks with diameters of 0.15 m versus 0.26 m, respectively. As a check for consistency, the difference in area covered by rocks of diameter 0.15 m and 0.26 m for the three landing sites is similarly between 10% and 20% of the total rock abundance.

Thermal Inertia and Landing Hazards on Mars: Figure 1 also encompasses most of the trade space possible for surfaces on Mars for different combinations of bulk and fine component thermal inertias for different rock abundances and effective rock inertias. For reference, all three of the landing sites fall in a zone of 260-440 bulk inertia, 15-20% rock abundance, and resulting fine component thermal inertia of roughly 200 to 340 (with Pathfinder the highest and Viking 2 the lowest). All of these surfaces are considered safe for the Pathfinder landing system [2, 3]. Given our present state of knowledge, we can infer that most areas with <20% rock abundance (among the rockiest 90% of the planet [4])

and fine component thermal inertia greater than 1300 to 1700 should be acceptable for the Pathfinder landing system [3].

Figure 1 and the discussion herein also allow us to evaluate the potential hazards of extremely high thermal inertia areas on Mars. Mellon et al. [7] report surfaces with Thermal Emission Spectrometer derived bulk thermal inertias that exceed 800 SI units. Landing sites being considered for the MERs in Valles Marineris have bulk inertias this high. These surfaces must have high fine component thermal inertias of 650-800, given that rock abundance does not exceed ~30-35%. Surfaces with fine component thermal inertias this high have generally been interpreted as being duricrust or some other cemented or cohesive surface [1, 7]. Given our previous discussion that argues only materials with effective inertias greater than about 2500 SI units be considered hazardous, none of these surfaces should be considered especially hazardous a priori, without other information.

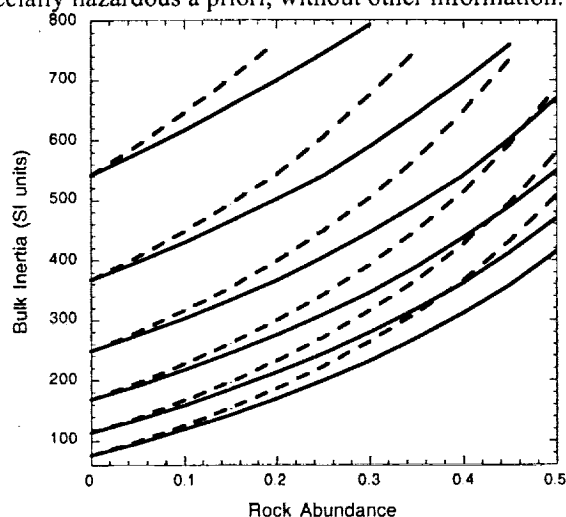


Figure 1. Plot of rock abundance versus bulk thermal inertia for various lines of constant fine component inertia. Solid lines are for an effective rock inertia of 1300; dashed lines are for effective rock inertias of 2500. Intermediate values of effective rock inertia (e.g., 1700, and 2100 SI units) fall in between these two for each group of fine component thermal inertia values. Fine component thermal inertia values of 77, 114, 168, 249, 367, and 542 are shown and can be distinguished by where these curves intersect the ordinate or the line of zero rock abundance.

References: [1] Christensen P.R. & Moore H.J. (1992) Mars Book, UA, 686-727. [2] Golombek M.P. et al. (1997) *Science*, 278, 1743-1748; *JGR*, 102, 3967-3988. [3] Golombek M. & Rapp D. (1997) *JGR*, 102, 4117-4129. [4] Christensen P.R. (1986) *Icarus*, 68, 217-238. [5] Kieffer H.H. et al. (1973) *JGR*, 78, 4291-4312; (1977) *JGR*, 82, 4249-4291; Christensen P.R. (1982) *JGR*, 87, 9985-9998; (1986) *JGR*, 91, 3533-3545. [6] Jakosky B.M. (1986) *Icarus*, 66, 117-124. [7] Mellon M.T. et al. (2000) *Icarus*, in press.

POTENTIAL MARS EXPLORATION ROVER LANDING SITES WEST & SOUTH OF APOLLINARIS PATERA. Virginia C. Gulick, NASA/Ames Research Center; MS 239-20; Moffett Field, California 94035; vgulick@mail.arc.nasa.gov

The region to the south and west of Apollinaris Patera offers several potential landing sites for the 2003 rovers. The region provides a unique opportunity to sample outcrop lithologies ranging from highland Noachian basement rocks, to Hesperian aged lava flows, channel and flood plain materials, to Amazonian volcanic, ash flow, and channel deposits. Pristine impact craters exhibiting lobate ejecta blankets are found both on the volcano itself and on the surrounding terrain implying a ground water rich environment well into the Amazonian. Indeed there is evidence for past volcano-ice interaction.

Apollinaris is located on the highland/lowland boundary at 8.5°S and 186°W. The volcano itself has been mapped [1] as Hesperian in age, the highlands immediately to the south are Noachian. Ma'adim Valles lies the south and water from the valley apparently flowed around the volcano before emptying into the Elysium basin to the north. A large fan structure emanates from the southern flank of the volcano. The fan is dissected by numerous valleys, which likely have been modified by fluvial processes [2].

This area is of particular scientific interest for a rover mission. The region contains a wide variety of rocks of different origins and ages. Erosional processes associated with fluvial, volcanic, and aeolian activity have shaped the surrounding terrain. In addition, the volcano is surrounded by extensive, relatively smooth areas at low elevations (-2 to -3 km) which permit good access and rover mobility [1].

There is extensive evidence of ground water in the region. A 23 km diameter impact crater lies on the northwest flank of the volcano and exhibits a fresh lobate ejecta blanket. Ground water outflow resulted in chaos zones to the west of the volcano. The remaining isolated mesas likely reveal the pre-erosion stratigraphy. These mesas may expose either sediment from an ancient sea or highlands material. A narrow Amazonian channel emanates from the Medusae Fossae formation on the volcano's NE flank and broadens rapidly toward the north.

Volcanic hydrothermal processes have likely had a pervasive influence on shaping the surrounding regions as evidenced by the chaotic terrains on the volcano's western boundary and

fluvial erosion of materials on its southern flank. The presence of impact craters with pristine lobate ejecta blankets, not only in the surrounding plains but also at the summit of the volcano, argues for the continued water-rich nature of the region until well into the Amazonian.

Using stereo photogrammetric methods, Robinson *et al.* [3] estimated a volume of 10^5 km³ for the volcano. The main caldera is 85 km in diameter and 0.8 to 1.5 km deep. This implies a magma chamber volume during the late stages of eruption of 4,000 to 6,000 km³. Given the unmistakable evidence for persistent ground water in the region, it is inescapable that volcanic intrusions associated with the construction of Apollinaris would have been associated with long-lived hydrothermal systems. Gulick [4,5] and Gulick *et al.* [6] modeled hydrothermal systems associated with magmatic intrusions. They found that the lifetime of hydrothermal systems associated with 5,000 km³ intrusions was 10^7 years. Assuming multiple intrusions over the lifetime of the volcano, it is likely that the hydrothermal activity associated with the growth of Apollinaris lasted in excess of 10^8 years. Hydrothermal fluids were likely discharged along the flanks of the volcano, particularly the western flank where a 500 m high basal escarpment defines the edge of the construct. Long-lived thermal springs would likely have been pervasive along these scarps as well as on other low-lying regions west of the volcano's flanks.

The basal scarp of Apollinaris may suggest that the volcano began forming in a water or ice rich environment. The small, pristine impact craters with lobate ejecta blankets that formed on the volcano may suggest that water may have remained in the subsurface until relatively recent times.

Three of the preliminary MER landing sites (EP57-59A) lie along the western edge of this region. However another site, centered within the Apollinaris Chaos at 11.1 S, 188.5 W (previously identified by Nelson *et al.* [7]) better samples the region of likely volcano-ground water interaction. MOC images of this region reveal relatively flat topography with a few 200 m high mesas. TES thermal inertias are low,

but within the acceptable range. The MOC images do indicate some dune fields, however, which may be problematic. Additional MOC data of the region is needed to more fully characterize the surface and define a specific landing site.

Table 1.

Engineering parameter	Constraint	Apollinaris Patera region
Thermal Inertia	5-10 cgs	5.9 cgs
Rock Coverage	< 20%	5-9%
Fine Comp. TI	>4 cgs	4.5-4.8 cgs
Slopes	<10deg.	No info. Avail.
Albedo	low	0.25-0.26
Elevation	<-1 km	-2 to -3 km

In conclusion Apollinaris provides an exceptional site for astrobiological, geological,

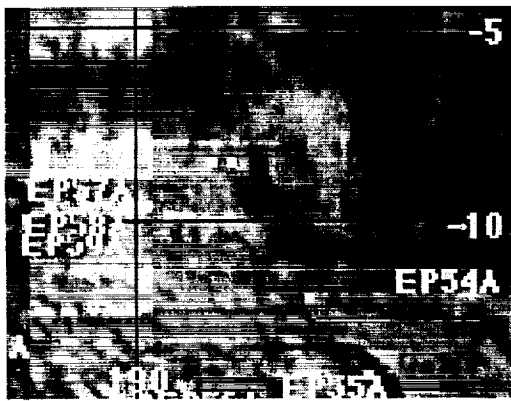


FIGURE 1: TES thermal inertia data of region surrounding Apollinaris Patera (center). Dark blue regions do not meet engineering constraints.

and climatological purposes. Fluvial (including ground water sapping) and associated processes were likely pervasive from the late Noachian, through the Hesperian, and into the Amazonian. Long-lived and large scale hydrothermal systems were certainly present throughout much if not all of this period. Thermal springs likely persisted for long periods. Water from the highlands via Ma'adim Valles and other smaller valley networks deposited highland-derived material in the area. In short, Apollinaris provides an excellent variety of rock types and ages and may preserve evidence of biologic or pre-biologic processes in associated thermal spring deposits.

REFERENCES [1] Scott *et al.* 1993. U.S.G.S. Map I-2351. [2] Gulick V.C. and Baker V.R. 1990. JGR 95, 14325-14344. [3] Robinson M.S. *et al.* 1993. Icarus 104, 301-323. [4] Gulick, V.C. 1993. Ph.D. thesis. Univ. of Ariz. [5] Gulick, V.C. JGR, 1998. [6] Gulick, V.C. *et al.* 1998 LPSC. [7] Nelson *et al.* (1999) Buffalo NY landing site workshop.

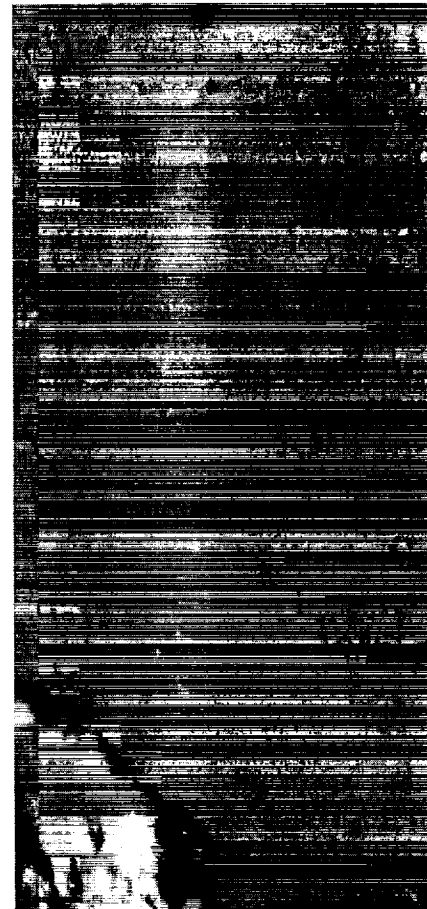


Figure 2. Portion of MOC image ab103804 of region near 11 S, 189 W. Resolution is 4.8 m/px.

A VIRTUAL WEB ENVIRONMENT FOR MARS LANDING SITE STUDIES. V.C. Gulick^{1,2}, D. G. Dardorff³, G. A. Briggs². ¹Space Science Division, MS 245-3, ²Center for Mars Exploration, MS 239-20, ³NAS Data Analysis Group, MS T27A-1, All are at NASA Ames Research Center, Moffett Field, CA 94035. *Email:* vgulick@mail.arc.nasa.gov.

INTRODUCTION: A collection of web tools is available for both the landing site and broader Mars science communities to better utilize, visualize, and analyze Mars Global Surveyor data. These tools have grown out of a two year effort between the Center for Mars Exploration (CMEX), and the NAS data visualization group at NASA Ames Research Center (ARC), to promote interactions among the planetary community and to coordinate landing site activities. The web site will continue to evolve over the next several years as new tools and features are added to support the ongoing Mars missions.

WEB SITE TOOLS: The tools described below as well as some others are accessible at the NASA Ames Mars Landing Site Studies web page <http://marsoweb.nas.nasa.gov/landingsites/>.

A Clickable, Zoomable Map Interface. We have implemented a map interface (Fig. 1) from which a variety of data sets can be overlain and visualized. MOLA topography, TES thermal inertia and mineralogical maps can be overlain upon MDIM base maps. Both past and presently proposed landing sites can also be displayed. Clicking on an individual site brings up its own web page which provides links to workshop abstracts, the PDS image atlas for Viking images, 3D VRML terrain environments (see below), and landing site evaluations.

MOLA data visualization. We have developed a web tool (Fig. 2) that allows the user to quickly locate MOLA H-product tracks over any specified area and to visualize the data. Individual ground tracks are overlain on the appropriate MDIM base map with elevations denoted by both a color mapping and a simultaneously displayed profile. When running the mouse over the profile a line is shown that connects the profile to the base map while also displaying the point-by-point location and altitude. A number of additional data display options are available.

MOC images with annotated Viking context images. We continue to collect high-resolution MOC images and to generate annotated Viking context images containing the footprint location of each MOC image. In most cases, the Viking context images are of high enough resolution to show how the terrain in the MOC images fits into the surrounding landscape. Annotated Viking context images of some pre-mapping phase MOC data were provided by Alfred McEwen (University of Arizona). We are continuing this effort to make all MOC data available at this site in a similar format.

3D terrain models of any area on Mars. VRML (*Virtual Reality Markup Language*) models allow a

perspective image of any object to be rotated by a user and viewed from any angle. Previously we constructed three-dimensional perspective models for all proposed landing sites and these are still available at the web site. We have now added the capability for users to construct their own VRML model of any region on Mars. Regions of interest can be selected either graphically or by numeric input. The resulting VRML is immediately generated. Users can choose to add MOLA profiles (Fig. 3) and MOC images to the perspective views as well. There is also an option to view geologic map overlays in this 3D format. Viewing the images with a web browser requires a VRML browser plug-in. Information on how to obtain and use the free plug-ins (Windows, Unix, and Mac operating systems) is posted on our web site. We recommend that only the newest browser and plug-in versions be used.

Web-based image processing of MOC images. When browsing MOC images on-line it is often difficult to determine if a given image is of interest without doing additional elementary image processing, such as adjusting the contrast. To fill this need we have developed a Java-based image-processing tool that allows users browsing MOC images to view histograms, adjust contrast and brightness as well as other tasks.

Importing MOC images into NIH Image. Currently MOC images can not be directly opened into the shareware program NIH Image. We have developed and placed on our web site a macro that allows the user to directly import MOC images (in the new PDS format) into Image. This macro also allows the user to obtain latitudes and longitudes of any points of interest on the image, distances between points in an image, as well as a variety of other useful image parameters. The macro can also be used for the Windows shareware version of NIH Image developed by Scion Image Corporation.

A Postdoc Mars Landing Site Studies group. Postdoc (for Post document) is a collaborative, web-based environment that allows individuals to post and retrieve documents in virtually any format, including image, text, slide, spreadsheet, audio and video files. Users can employ Postdoc to propose a landing site, submit both science and engineering evaluations, post supporting image, graphics or word documents of their proposed landing site(s), or create their own email subgroup list for their respective landing sites. Others in the landing site community may request membership to those subgroups from the "owner" of that subgroup. Postdoc creates a common meeting place where the landing site community can post their work on candidate landing sites both to inform and to facilitate

collaborations within the community and with the Project.

PLANNED ENHANCEMENTS. Planned future enhancements include the use of Concept Maps as a user interface for links to relevant site data (e.g. abstracts, science evaluations, images, maps, and online reference materials). The goal is to allow users and peer reviewers to create and edit Concept Maps in a collaborative fashion. Additional Java-based application tools for analyzing and visualizing MGS data are also planned. Such tools will allow Macintosh users, for example, to be able to read and work with MGS TES data, since a Mac application program is currently unavailable.

Collaborative tools will be enhanced to include collaborative whiteboards, collaborative image viewing and annotation, and support for possible Usenet news groups, chat rooms, and/or list-serve mailing lists. Some of these capabilities are already provided on Postdoc, which allows user-uploadable and retrievable materials and threaded mail archives.

We also plan to improve the integration of all MOLA, MOC, and TES archives so that all three of these data types can be viewed in one image.

CONCLUSION. This web site is intended to be a general repository for the latest Mars mission images, data, and data products that pertain to landing site selection. We encourage the community to make use of this resource not only for landing site studies but also for general Mars studies as well. We welcome submissions of data sets as well as suggestions for enhancing and improving this site.

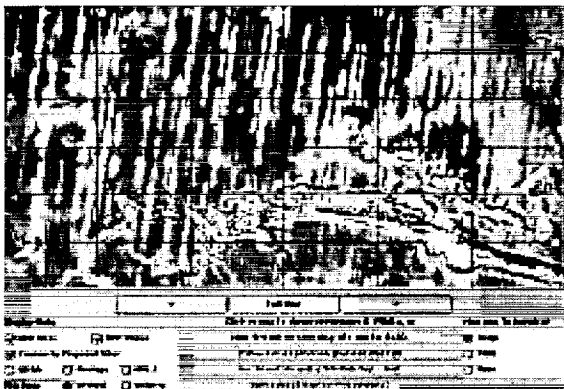


Figure 1: View of map-interface tool showing TES thermal inertia data overlain on MDIM base. Potential MER A and B landing sites are marked.



Figure 2: Sample view of MOLA data visualization tool. Profile on right is keyed to selected ground track. Orbit track, latitude, longitude, and altitude of selected point is shown at bottom.



Figure 3: 3D VRML terrain model of Valles Marineris with overlain MOLA track. User can zoom and rotate terrain model to view site from different perspectives. Vertical exaggeration is user-adjustable.

PLANETARY GIS ON THE WEB FOR THE MER 2003 LANDERS. T. M. Hare, K. L. Tanaka, J.A. Skinner, 2255 N. Gemini Dr., U.S. Geological Survey, Flagstaff, AZ, 86001; thare@usgs.gov

Introduction. PIGWAD or "Planetary Interactive GIS-on-the-Web Analyzable Database," has been operational since May of 1999. It currently provides GIS database support for the research and academic planetary science communities. We are now focused on creating a Mars Exploration Rover (MER) web-based landing-site analysis page. Along with the NASA Ames Research Center's web site [1], the PIGWAD web server also contains mission information including engineering constraints. The marriage of these two web sites gives scientists a great resource of information to analyze for landing-site selection.

Background. The use of Geographic Information Systems (GIS) [2] has continued to boom in the planetary sciences [3-11]. Not only does it bring together post-mission datasets to address science issues, but now it plays an important roll in pre-mission phases to assess feasibility and safety and to formulate objectives. GIS was used in the selection of landing sites for the Mars Polar Lander and the Mars Surveyor 2001 Lander and is being used for camera targeting for Titan. NASA's Planetary Geology and Geophysics Program, which enabled PIGWAD to evolve from the drawing board to a useable system on the internet, as well as NASA's Mars Data Analysis Program, offer support and guidance as this product develops.

Approach. Our current choices for web mapping applications are based on Environmental Systems Research Institute's (ESRI) ArcView Internet Map Server and Arc Internet Map Server [12]. We rely heavily on the ArcView application for our MER landing-site analysis page, because ArcView supports high-level customizations through its programming language called Avenue. For example, to help with Mars landing-site selection, we can offer planetary scientists a landing-site ellipse generator (Fig. 1), which gathers statistical information about a site's rock abundance, elevation, slope, morphological descriptions and other data needed to choose an optimally safe and scientifically interesting landing site (Table 1).

Currently, users have access to the Viking digital image mosaic versions (MDIM) 1 and 2 [13], Viking image- and stereo-resolution maps, geologic maps, Mars Orbiter Laser Altimeter

(MOLA) tracks, MOLA topography, MOLA shaded relief, Mars Orbiter Camera (MOC) footprints and image centers, and Viking Infrared Thermal Mapper Data (IRTM). Slight misalignments among these datasets will be present until they have been registered to a new, common spheroid definition.

Schedule. PIGWAD's MER 2003 website is currently on-line at <http://webgis.wr.usgs.gov> (Fig. 1). We will update our site as needed, which means that some of our pages occasionally will be down for brief periods. We will add more Mars Global Surveyor datasets including MOC context and narrow-angle imagery, MOLA topographic-point data and datasets derived from the Thermal Emission Spectrometer.

Summary. GIS provides the tools (1) to view and reference diverse sets of image, vector, textual, and numerical data together, and (2) to perform various spatial/statistical analyses, including advanced spatial intersections, unions, and robust conditionals. By incorporating this functionality into a user-friendly web environment, investigators can easily implement the analytical power of PIGWAD to assist with MER landing-site selection.

References. [1] NASA/Ames MER web site: <http://marsoweb.nas.nasa.gov/landingsites/> (webmaster G. Gulick) [2] Environmental Systems Research Institute (1995) *Understanding GIS: The ARC/INFO Method*, GeoInformation International, United Kingdom, i, 1-10. [3] Carr, M.H. (1995) *JGR* 100, 7,479. [4] Zimbelman, J.R. (1996) *GSA Abs.* 28, A-128. [5] Lucchitta, B.K. and Rosanova, C.E. (1997), *LPSC XXVIII*, 839-840. [6] Dohm, J.M., et al. (in press) *USGS Map I-2650*. [7] Tanaka et al. (1998) *JGR* 103, 31,407-31,419. [8] Hare, T.M. et al. (1997) *LPSC XXVIII*, 515. [9] Gaddis, L. et al. (1998) *LPSC XXIX*, 1807-1808. [10] Rosanova, C. E. et al. (1999) *LPSC XXX*, #1287. [11] Lias, J. H. et al., (1999) *LPSC XXX*, #1074. [12] Hare, T.M and Tanaka, K.L. (2000) *LPSC* #1889. [13] Kirk, R.L. et al, (2000) *LPSC XXXI*, #2011.



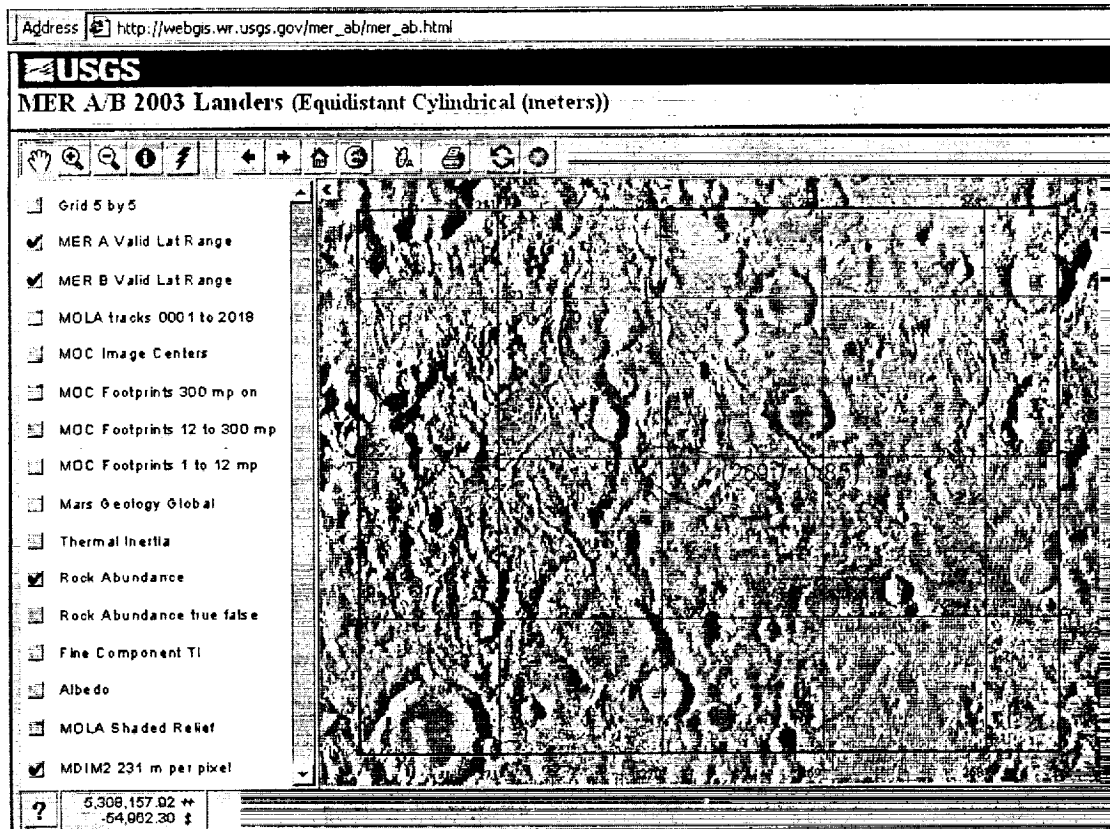


Figure 1. The MER 2003 ArcView IMS interface showing the Mars Digital Image Mosaic version 2 (gray scale), Viking-derived rock abundance (color squares), and user-generated ellipse (intersected data shown in Table 1). This example does not use the ellipse definitions for either MER lander.

Table 1. Data table generated from the ellipse shown in Fig. 1. Other statistical data including elevation, slope, and geologic units will be generated in future versions of the program.

Ellipse Generated for Lon = 269.7 Lat = 0.85 - Landing Diameter: 28km - Map Scale: 1:2000000
Theme: Thermal Inertia / Count: 2 / Mean: 77 / Range: (74,80) / Standard Deviation: 4
Theme: Rock Abundance / Count: 3 / Mean: 9 / Range: (7,11) / Standard Deviation: 2
Theme: Fine Component TI / Count: 4 / Mean: 72 / Range: (68,79) / Standard Deviation: 5

RECENT RESULTS FROM MARS GLOBAL SURVEYOR AFFECTING LANDING SITE SELECTION AND HABITATS FOR PAST OR PRESENT BIOLOGICAL ACTIVITY. W. K. Hartmann, Planetary Science Institute, 620 N. 6th Avenue, Tucson, Arizona 85705; hartmann@psi.edu .

Mars Global Surveyor (MGS) has been contributing a number of new results that change our picture of Mars. They raise the prospect of a more active planet than had been suspected by some workers, and include a wide range of landing site ages, exhumed ancient terrains, and ongoing geothermal activity creating sporadic underground aquifers that might offer habitats for microbial life, either in the present or past. Recent reports in *Nature*¹ enhance the possibility that microbes could survive long dormant states in such environments.

This paper lists some such results and their influence on landing site selection.

1. Impact gardening: Viking investigators concluded that no craters smaller than 50 m across existed on Mars because of atmospheric filtering of bolides – leading to a rarely-voiced but “subliminal” assumption that impact gardening is not important on Mars. MGS has shown full populations of craters, with no apparent atmospheric losses, down to diameter $D = 10$ m or less on Mars. Lunar mare populations of such craters saturate the surface at sizes of $D \sim 200$ m and pulverize surface materials to create about 5-10 m of regolith in 3500 Myr. Scaling to Mars suggests similar or larger depths of regolith on Noachian surfaces, and gardening to depths of order 1 m on surfaces a few hundred Myr old on Mars. This means that Noachian deposits from lakebeds or other fluvial features cannot survive in pristine form if exposed continuously on Mars. The details of this work are presented by Hartmann².

2. Volcanism has extended into recent geologic time on Mars: This is shown by igneous Mars meteorites with ages as young as 170 and 300 Myr, and independently by crater count data^{3,4}. Non-negligible parts of Mars are covered by young lavas with rough textures, including low latitude regions such as Elysium Planitia. This raises the opportunity of visiting well preserved lavas, but it is not clear what useful Mars science could come from this unless we could do in situ dating to calibrate the system of crater retention ages.

3. Mars meteorites confirm exposure of Martian rocks as recently as 670 Myr ago^{5,6}. This means that even non-Noachian deposits may show water alteration effects, which could be sought by chemical analyzers on rovers.

4. As shown in Figure 1, the first hematite area found on Mars by TES shows unusual geomorphology and crater populations. There is a very ancient population of very degraded, shallow, 200-m scale craterforms virtually at saturation, which I call “fossil craters.” Saturation is present on Phobos in this size range, but is

extremely rare on the surface of Mars because the oldest craters of this size have been eroded away. In addition, this area shows a population of very young, sharp rimmed small craters suggesting a crater retention age of the order 10 Myr. These data suggest that this area may mark an extremely old Noachian surface, where hematite was concentrated by fluvial activity, which was then exhumed. The old surface may even be a lakebed.

5. The Malin/Edgett⁷ gullies confirm existence of recent aquifers on Mars. I suggest that the reason they are concentrated in high latitudes is that this is where Martian ground ice is near the surface, and they form by geothermal melting of the underside of permafrost ice layers. Combined with above new results on young volcanism, this suggests that underground water activity has been common and sporadic throughout Mars history. Some of these gullies have deltaic deposits that spread on top of Martian dunes. These could be easily reached by rovers and might allow sampling of recent fluvial deposits. These would allow tests for modern biological material in recent aquifers. Unfortunately most of these lie outside of latitude constraints for near-term missions.

6. The recently announced Edgett/Malin⁸ stratified deposits have two implications. (a) They confirm massive sedimentary deposits, some of which may be fluvial. (b) Because some have low crater densities, they are probably in a process of exhumation and deflation, which might offer the best opportunities on Mars to sample ancient sediments that have been protected from impact gardening. Some of these are within equatorial latitude constraints for near-term missions.

7. Recent work in *Nature*¹ suggests the observation of microbes revived after dormancy of 250 Myr in a salt crystal. If verified, this greatly strengthens the possibility that sporadic Martian aquifers could contain living microbial material.

In the short term, these new results offer many opportunities for rovers to reach materials of different age that reflect fluvial processes. In the longer term, if even in situ dating techniques become available, these would be of the highest priority to tie down the ages of late Hesperian or early Amazonian lavas and thus calibrate the overall crater-dating system.

References: [1] Vreeland R. H., Rosenzweig W. D. and Powers D. W. (2000) *Nature*, 407, 897-900. [2] Hartmann W. K. (2000) in press, *Icarus*. [3] Hartmann W. K. and Berman D. C. (2000) *JGR*, 105, 15011-15025. [4] Hartmann W. K. and Neukum G. (2000) in press, Mars Chronology volume, ISSI (Bern). [5] Shih C.Y. et al. (1998) *LPSC XXIX*, #1145. [6] Swindle T.

et al. 2000 *Meteoritics & Planet. Sci.*, 35, 107-115. [7]
 Malin M. and Edgett K. (2000) *Science*, 288, 2330-2335.
 [8] Malin M. and Edgett K.. (2000) *Science*, 290, 1927-1937.



Figure 1a. The area of hematite deposits discovered in Terra Meridiani by the MGS/TES instrument, from MGS/MOC frame M00-01661. The area appears to be nearly saturated with extremely ancient, "fossil craters" revealed by shallow rings. Also present is an extremely sparse population of fresh, sharp-rimmed craters. Bright areas are dune fields in "fossil crater" floors.

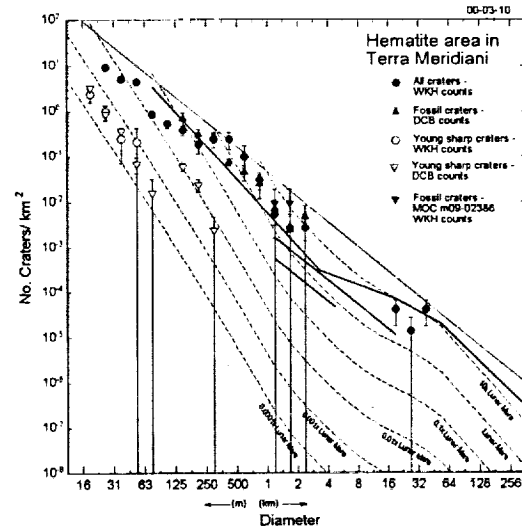


Figure 1b. Crater counts for the hematite area. The old "fossil crater" population lies above the normal Martian steady state curve (solid bent line), and approaches saturation density. The population of young, sharp-rimmed craters suggests the area was exhumed only a few million years ago. Exposure of ancient, preserved lakebeds and other "pristine" Noachian deposits may require a combination of burial (to protect from gardening) and recent exhumation (to expose the ancient deposits in intact condition).

MER 2003 OPERATIONS SUPPORT AND LANDING SITE CHARACTERIZATION BY MARS EXPRESS HRSC/SRC IMAGING DATA. E. Hauber, G. Neukum, T. Behnke, R. Jaumann, R. Pischel, H. Hoffmann, J. Oberst¹, and the HRSC Science Team, ¹DLR-Institute of Space Sensor Technology and Planetary Exploration, Rutherfordstr. 2, D-12489 Berlin, Germany (email: Ernst.Hauber@dlr.de).

Introduction: The High Resolution Stereo Camera (HRSC) imaging experiment onboard the Mars Express (MEX) mission to be launched in 2003 will provide unique high-resolution multispectral stereo images [1]. A Super-Resolution Channel (SRC) will obtain very high-resolution images (2.3 m/pixel) within the context of the HRSC nadir swath. Here, we present the instrument characteristics and imaging modes of the SRC, and we outline the capabilities of HRSC/SRC to support rover operations of the MER 2003 mission, to characterize the landing site properties, and to provide information on the wider geological context of the landing sites. At the workshop, we will also give an overview of the current activities of the HRSC Science Team to select target sites to be imaged during the nominal operational lifetime of the mission of 1 Martian year.

Instrument: The HRSC is a multiple line pushbroom instrument. Nine superimposed image tracks are acquired nearly simultaneously (along-track) by 9 CCD line sensors (each with >5000 pixels) mounted in parallel and behind one single optics. At a periapsis height of 250 km, the swath width is about 52 km and the resolution is ~10 m/pixel. The HRSC will cover $\geq 50\%$ of the Martian surface at a spatial resolution of ≤ 15 m/pixel, in stereo, four colors, and at five phase angles. More than 70% of the surface can be observed at a spatial resolution of ≤ 30 m/pixel [2], assuming an average HRSC data transfer capacity of 1 Gbit/day. Thus, the HRSC will close the existing gap between medium to low-resolution coverage on the one hand and the very high resolution images of the Mars Observer Camera (MOC) on the Mars Global Surveyor (MGS) mission as well as the in-situ observations and measurements by landers on the other hand. The goals of the HRSC will not be met by any other planned mission or experiment. It will also make a significant contribution to the scientific objectives of the MEX lander module Beagle II by providing information on the geological context of the landing site.

The scientific output of the HRSC experiment is significantly extended by using an additional external Super Resolution Channel (SRC). The SRC is based on an ongoing instrument development for the Rosetta Lander and will be mounted on the MEX spacecraft below the HRSC stereo scanner in a common honeycomb structure in order to minimize interfaces with the spacecraft (Fig. 1). It is a framing device and uses an interline CCD detector to cope with the very short exposure times. The 1 m focal length telescope provides

a spatial resolution of 2.3 m/pixel at an altitude of 250 km. The design is characterized by

- CCD area array detector with 1024 x 1032 pixels.
- Highly miniaturized and low-power detector and control electronics.
- Compact 3D multi-chip module technology using thinfilm multilayer metallization, dycostrate, plasma-etching and chip-on-wire technology.
- Selectable dynamic range of 8 and 14 bit per pixel.
- Internal data buffer.
- Light-weight Maksutov-Cassegrain telescope with a focal length of 1 m and an f-number of 9.



Figure 1: SRC optics and HRSC/SRC instrument.

Imaging Operations: The channel is operated in parallel with the HRSC stereo scanner yielding nested-in super-resolution images in order to avoid any location problems and to obtain the contextual information. One SRC image covers only 4% of the nominal HRSC sensor swath (one HRSC pixel is covered by 25 SRC pixels). Approximately 230 HRSC lines are required to image an SRC frame. Near pericenter it takes less than 1 s to scan an SRC frame with HRSC lines. Both single spot observations and overlapping image strips can be acquired. SRC imaging can be specifically commanded in order to obtain adjacent and overlapping single images for assembling larger image mosaics (Figs. 2-4). Theoretically, it is even possible to obtain SRC stereo images of limited areas by taking – during one orbit – a forward-looking mosaic and a backward-looking mosaic. However, the instrument is not mounted on a steering platform. Therefore, the spacecraft has to be slewed in order to acquire SRC image mosaics. Currently, the possibilities to obtain SRC image mosaics are under study, particularly with respect to spacecraft pointing.

Objectives: The major task to be fulfilled by the SRC within the framework of the HRSC/SRC experiment is to support the HRSC science objectives by obtaining very high-resolution panchromatic imagery for photo-

geologic purposes (e.g. investigating gullies possibly eroded by recent water release [3] and layered deposits which might indicate a different climate in the early martian history [4]), and to decipher morphological details which remain ambiguous or cannot be resolved by nominal HRSC data. *This is especially important for landing site characterization.* MOC images clearly show that many areas which appear to be quite flat and featureless at medium resolution exhibit a remarkable surface roughness at a spatial resolution in the meter range. Detailed information on the surface characteristics of possible landing sites is a prerequisite for planning future lander missions and surface operations in detail and to address questions like mission safety or environmental conditions.

MER 2003 Landing Site Imaging: The MEX spacecraft will arrive at Mars at the end of December, 2003. The first mapping orbit will be reached on January 4th, 2004, and the first periapsis pass will take place on January 4th, 2004, at 08:52 a.m. (UTC). The geographic position of the first periapsis will be located at 14.77°S and 114.8°E, and the elevation of the Sun above the equator will be ~50°. The location of the periapsis will drift towards South during the following orbits, and good imaging conditions of the latitudinal belt of the MER 2003 landing sites (15°S to 10°N) will be restricted to the period before the end of January, 2004. The MEX spacecraft is in its commissioning phase during the first two months after arrival at Mars. Thus, negotiations with ESA will be required to take images *immediately after arrival at Mars.*

References: [1] Neukum G. et al. (1996) *Act. Astron.*, 38, 713-720. [2] Neukum, G. et al. (2000) *LPS XXXI*, abstract 1906. [3] Malin, M.C. and Edgett, K.S. (2000) *Science*, 288, 2330-2335. [4] Malin, M.C. and Edgett, K.S. (2000) *Science*, 290, 1927-1937.

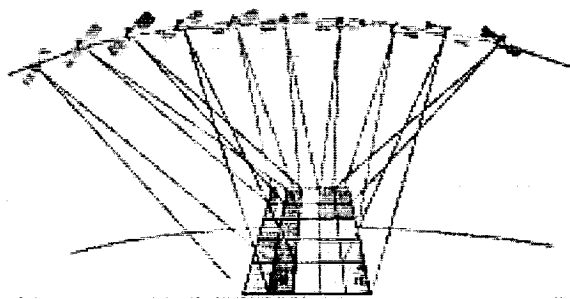


Figure 2: Geometry of images obtained during one orbit for assembling contiguous SRC image mosaics.

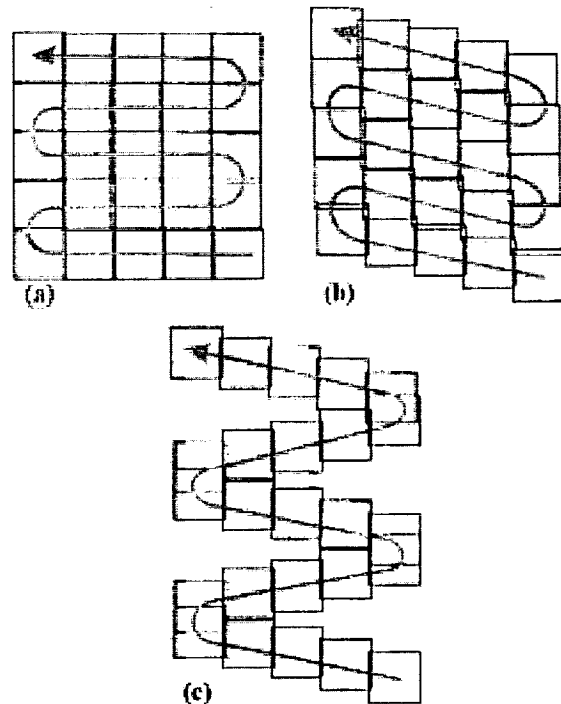


Figure 3: Different modes of spacecraft slewing and corresponding footprints of SRC image mosaics.

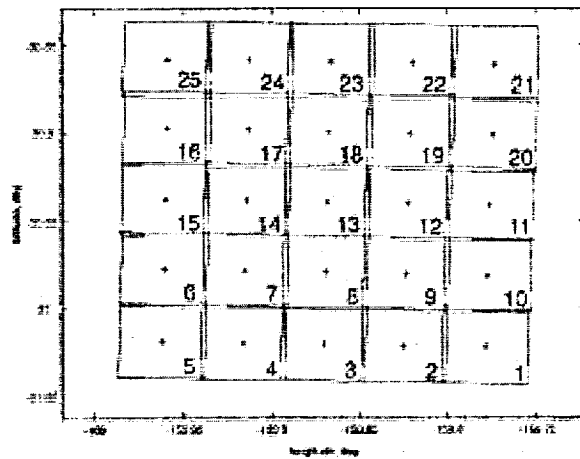


Figure 4: Example of projected SRC footprints assembled into an image mosaic (cf. Fig. 2).

TERRA MERIDIANI HEMATITE DEPOSIT LANDING SITE RATIONALE. B. M. Hynek, R. E. Arvidson, R. J. Phillips and F. P. Seelos, Department of Earth and Planetary Sciences, Washington University, One Brookings Drive, St. Louis MO 63130 (hynek@levee.wustl.edu).

Introduction: The primary hematite deposit in Terra Meridiani lies in a unique region of Mars that has undergone regional-scale tilting toward the Chryse Trough due to tectonic activity associated with formation of the Tharsis rise. This tilting and perhaps accompanying climate change led to large-scale denudation of the Martian highlands, followed by widespread deposition. Stripping of the deposits has exposed a number of layered systems, including the hematite unit. Landing a rover on the hematite deposit would enable the testing of multiple working hypotheses regarding the deposition of these layered materials. Most of these hypotheses require surface or near-surface water at the time of formation (Late Noachian-Early Hesperian), raising the possibility of finding prebiotic or biotic materials.

Regional Setting: The formation of the Tharsis rise has profoundly affected the global shape of the planet. Recent modeling of Mars Global Surveyor data indicate that the long-wavelength topography and gravity field of Mars are explained by the oblateness and the Tharsis load. Global deformation of the lithosphere (elastic outer spherical shell) resulted from the Tharsis loading [1]. The majority of the Tharsis igneous complex was emplaced by the end of the Noachian [2], and resulted in both topography and gravity lows circumferential to the Tharsis rise (Chryse Trough), and topography and gravity highs nearly antipodal to Tharsis (the "Arabia Dome") [1].

The entire western flank of the Arabia Dome has likely undergone extensive fluvial denudation [3] in response to the emplacement of Tharsis. This loading created a regional tilting, resulting in erosion and incision of the martian uplands, and transport to and deposition of sediment in the Chryse Trough. The system was likely governed by the overall potential energy associated with the gradient across the aeropotential and the ability of the system to erode and transport. Using fine-scale topographic grids we estimated that $\sim 4.5 \times 10^6 \text{ km}^3$ of material has been eroded from the cratered uplands and transported to local and distal sinks [3]. The morphology, rate of denudation and extensive nature of upland degradation indicate that precipitation-fed surface runoff is the most likely geomorphic agent capable of such a process, indicative of a warmer and wetter Mars during the Late Noachian interval.

The primary hematite deposit lies within the denuded zone between the Chryse Trough and the up-

lifted Arabia Dome. Superposition relations and crater counts reveal that the hematite deposit formed coeval or immediately after the denudation event [3], indicating that surface and/or near-surface water may still have existed at the time of formation.

Characterization and Formation Mechanisms of Martian Hematite: The 350 by 350-750 km-sized deposit located in Terra Meridiani is interpreted to be composed of coarse-grained, gray crystalline hematite [4]. Data from the Mars Orbiter Laser Altimeter (MOLA) and the Mars Orbiter Camera (MOC) indicate that the deposit is smooth, superposed on surrounding materials, and buries valley networks (Figure 1). MOC images show that the hematite deposit has been stripped by wind erosion to reveal layering and underlying cratered surfaces in places. The images also reveal an abundance of layered materials in and around the Terra Meridiani region, which Malin and Edgett [5] interpret as sedimentary deposits.

A number of formation mechanisms have been proposed for the martian hematite deposit, many of which require liquid water. Christensen et al. [4] advocated precipitation from a standing body of Fe-rich water based on the association with nearby layered deposits, large areographic extent, and distance from a regional heat source. Lane et al. [6] proposed subaqueous deposition, burial, and metamorphism, with subsequent exhumation. Alternatively, the hematite may be a result of an igneous intrusion or an altered ignimbrite deposit without aqueous activity [7].

Ability to Test Multiple Working Hypotheses: The Athena payload on MER is well suited to test mechanisms of hematite formation. The Pancam and MINOTES have the ability to determine both geologic setting and mineralogical compositions [8]. Thus mineralogy within nearby layering (or at minimum the surface layer) could be determined before a traverse is even attempted. In-situ analysis of the nearby terrain, including detailed compositional information provided by the Alpha Particle-X-Ray-Spectrometer, iron-bearing mineralogy determined by the Mossbauer Spectrometer, as well as fine-scale textural properties using the Microscope Imager, would allow the deciphering of the complex geologic history in this unique region of Mars [8]. A lacustrine origin of the hematite could be confirmed by finding features such as wave-cut terraces, shoreline deposits, cross-bedding within layers, fluvio-lacustrine sequences and imbricated pebbles, most of which should be evident if this hypothesis

is correct. Conversely, an igneous origin could be confirmed by detection of welded tuffs. Spectral information provided by Pancam and Mini-TES could distinguish volcanic from aqueous cementation, including mineralogic differences and temperature of formation. Results from field tests of the Athena payload indicate that most, if not all, of these geologic, mineralogic, and compositional indicators are easily detectable [9].

References: [1] Phillips R.J., Zuber M.T. et al., (2000) *Science*, (submitted), [2] Banerdt W.B., Golombek M.P (2000) *LPS XXXI*, abs. no. 2038, [3] Hynek B.M. and Phillips R.J. (2000) *Geology*, (submitted). [4] Christensen J.L., Bandfield, J.L., et al. (2000) *JGR*, 105, no. 4, 9623-9642, [5] Malin M.C. and Edgett K.S., *Science*, 290, 1927-1937, [6] Lane M.D., Morris R.V., et al. (2000) *LPS XXXI*, abs. no. 1140, [7] Tanaka K.L. Chapman, M., et al. (2000) *GSA Abs. with Programs*, 32, no. 7, abs. no. 52142, [8] Squyres S.W., Arvidson R.E., et al., this conference, [9] Arvidson, R.E., this conference.

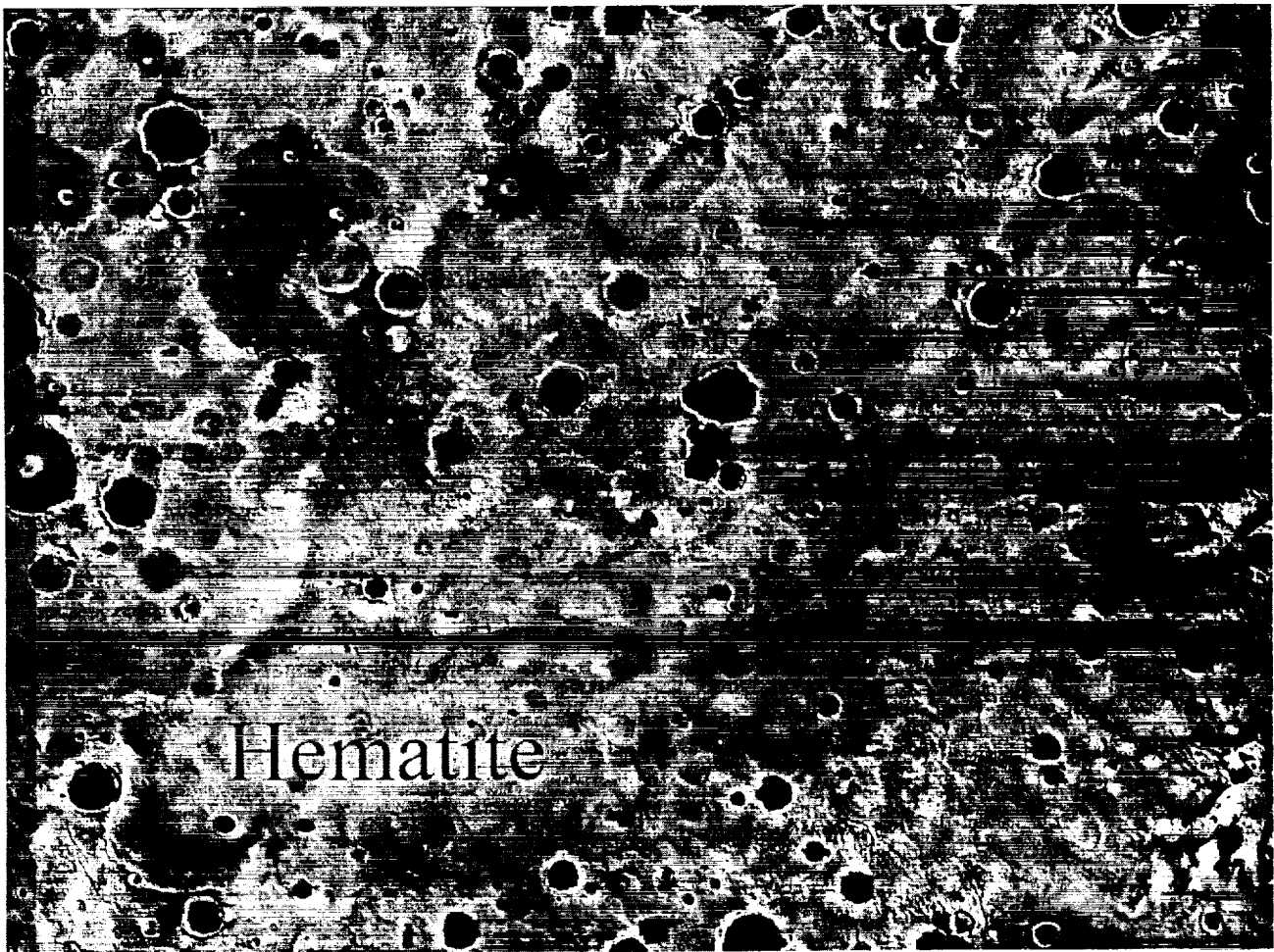


Figure 1. MDIM overlain with MOLA elevations coded in color. Blues = low, reds = high, with relief of 2.7 km. Regional tilt has been removed. Covers 5°S to 10°N and $\pm 10^\circ$ about prime meridian. Hematite deposit is labeled. High areas correspond to erosional inliers that preserve layered stratigraphy.

BROAD PERSPECTIVES ON MARS LANDING SITE SELECTION: GEOLOGICAL FACTORS FROM CENTIMETER TO KILOMETER SCALES. B. M. Jakosky¹ and M. P. Golombek². ¹Laboratory for Atmospheric and Space Physics, University of Colorado, Boulder, CO 80309 (email bruce.jakosky@lasp.colorado.edu); ²Jet Propulsion Laboratory, Caltech, Pasadena, CA 91109 (email mgolombek@jpl.nasa.gov).

Introduction: Selection of a landing site for the '03 and later Mars surface missions represents a balance between potential science results and landing site safety. Although safety has to be the prime consideration, it is the melding together of spacecraft hazard analysis with science analysis that provides the key to understanding the nature of the surface for determining both its safety for landing and its scientific potential. Our goal here is to discuss the geological factors that go into a determination of site safety, at scales from centimeters up to kilometers, and to understand the implications for the resulting scientific return that can be expected.

In particular, we wish to focus on integrating together the following issues:

- The nature of the bedrock geology at scales greater than 100 m.
- The scientific desire to sample the major terrains (such as the ancient highlands, which have not been seen yet from the surface).
- The structure of the surface at centimeter-to-meter scales as derived from remote-sensing observations.
- The scientific desire to sample surfaces representing the different types and range of surficial properties and processes.
- Our ability to understand the information at different scales (e.g., Viking 100-m imaging, MOC 2-m imaging, remote sensing decimeter-scale properties) as a means of determining surface characteristics.
- The potential to use science as a driver in site selection.
- The trade-off between safety and science.

Each of these topics is discussed in more detail below.

Bedrock geology. The major goals of the Mars program over the next decade follow the "water" theme, with the highest-priority goal being to understand the potential for life to exist or have existed on Mars. Thus, sites that have high potential for liquid water and, therefore, for life, would be highest priority for in situ exploration with spacecraft that carry instruments suitable for characterizing these environments. Numerous sites have been identified as prom-

ising based on 100-m-scale imaging. These include chaos regions and outflow channels that have had liquid water flowing through them, possible hydrothermal and aqueous sites associated with both volcanism and liquid water or with chemical alteration of surface minerals, the ancient highlands that existed at a time when liquid water was more abundant at the surface than it is today (and, of course, the valley networks and river tributaries that exist there), ancient crater lakes that appear to have had standing bodies of water within them in the past, periglacial sites where ground ice has been present, and the troughs of Valles Marineris that may represent both standing bodies of water and the ability to sample units that had previously been up to kilometers below the surface. Clearly, it will be the geological content of the sites at this scale that determines what the missions ultimately will learn at these locations. For reference, the MER mission goals are to determine aqueous, climatic and geologic history of sites that may have been favorable to the preservation of evidence of biotic or prebiotic processes.

Decimeter-scale structure. Remote-sensing observations provide information on the properties and structure of the surface at the decimeter-to-meter scale. Different techniques are sensitive to the abundance and distribution of fine materials (such as dust), crusted materials (duricrust), and rocks (including the size, shape, and distribution). Approaches include determination of thermal inertia (and its relationship to abundances of fines, crusts, and rocks) and radar reflectivity (bulk density and rock distribution). In addition, rock abundance can be determined from thermal-emission measurements at multiple wavelengths. The surface properties inferred from these observations provide information on the extent to which various surficial processes have acted.

The processes responsible for the decimeter-scale structure are not necessarily the same ones responsible for the 100-m-scale structure as seen from orbiter images. For example, the two Viking landing sites do not show obvious evidence at the ground for the same processes identified as having acted from orbit. The Mars Pathfinder site, though, does show evidence for the same processes having acted.

Intermediate-scale structure. MGS MOC images provide information at a scale intermediate between the bedrock geology and the decimeter-scale remote-sensing observations. Thus, they provide a geological

tie point in understanding the nature of the processes that have acted. This tie point has provided evidence for processes not previously identified at either the larger or finer scales (such as the gullies and seeps described by Malin and Edgett, as well as large-scale blanketing of the surface by aeolian sediments). In addition, it sometimes complicates the interpretation. For example, MOC imaging of the Mars Pathfinder site does not connect up compellingly either with the orbiter imaging or with the lander imaging; while lander imaging shows evidence for the same flood processes as seen from orbit, such evidence is lacking at the intermediate MOC resolution, which appears to identify predominantly aeolian processes.

Major terrain types—geology and remote sensing. The two Viking landers and the MPF lander all sampled the northern-hemisphere lowlands. VL-1 and MPF were in regions that had sustained past flooding, and VL-2 was in an area that showed evidence for ground ice and permafrost activity. No lander observations are available to provide guidance as to the characteristics of the southern-hemisphere ancient highlands. Thus, our view of the nature of the martian surface is extremely biased, without observations of the representative terrains. In fact, it is arguable that the ancient terrain represents the single most important unit on the planet as it records the first-order processes relating to Mars' history.

Furthermore, the remote-sensing observations indicate that the three landing sites have properties that do not appear to be representative of the global distribution. In particular, the combination of thermal inertia, albedo, and radar properties suggest that we have not sampled the end-members in the population of surface properties. Although these same remote-sensing observations allow us to effectively extrapolate surface properties to other locations, the degree of confidence that we have in such an extrapolation depends strongly on understanding the range of properties and processes that can occur.

Science, safety and trafficability of the surface. Many of the extremes in surface properties are likely to be either unsafe for landing or difficult for a rover to traverse. Regions of low thermal inertia are likely to consist of at least centimeters-thick deposits of very fine dust less than about 30 μm in size. Such deposits would likely be safe for landing but would be difficult to traverse. In addition, they would be less interesting from the science perspective, in that they likely formed out of dust deposited from the atmosphere rather than from materials derived locally, and they would contain fewer exposures of unweathered rock.

Regions with the greatest abundance of rocks at the surface would be difficult to land on and traverse, but would be stronger sites for science. They likely would be unblanketed, with dust being not deposited or continually stripped, and would have abundant exposures of unweathered rocks. These regions likely have the highest thermal inertias on the planet.

Regions of moderate or intermediate thermal inertia contain abundant exposures of duricrust, fine materials that have been cemented together by, for example, salts. Again, these would represent weathered materials that have been substantially altered.

It is not clear what the ideal site is—a safe but uninteresting one, or a the scientifically exciting site on which it may be difficult for a rover to get around.

Science as a driver. A very large number of preliminary landing ellipses have been mapped out, based on available Viking images and remote-sensing data and representing those sites that meet first-order safety criteria. While it is clear that safety has to be the major driver, it will not be possible to obtain exhaustive MOC images or do detailed investigations of all of these sites in order to down-select to a smaller number of viable sites. The down-select will have to be done early in the process, and the scientific value of the sites can and should be a major input into the down-select. Given the large number of ellipses being considered for the MER missions, the most exciting and promising sites from the science perspective should be targeted for detailed MOC imaging and other analyses. The down-select will take place whether science input is used or not; therefore, now is the right time to push the scientific content of the various sites in the process.

So what's the bottom line? Landing site selection for the '03 MER missions as well as the follow-on missions in later years (and eventually sample return) depends on a complex interplay of a large number of parameters. These include the desire to land safely and be able to traverse over the surface successfully, the desire to understand the different types of geologic processes that have occurred and their distribution over the planet, and the desire to sample (with landers, rovers, or return missions) from among a range of specific types of sites. It is imperative that we use the early missions to understand not only specific sites but also the types of sites that are available and the range of surface properties and processes that can occur. Certainly, science has to be the primary driver behind site selection, to the extent that the scientific choices do not compromise lander/rover safety and lifetime.

PHYSICAL PROPERTIES OF POTENTIAL MARS LANDING SITES FROM MGS TES-DERIVED THERMAL INERTIA. B.M. Jakosky, M.T. Mellon, and S.M. Pelkey, Laboratory for Atmospheric and Space Physics, University of Colorado, Boulder, CO 80309 (emails: bruce.jakosky@lasp.colorado.edu; michael.mellon@lasp.colorado.edu; pelkey@argyre.colorado.edu).

Introduction: We are mapping thermal inertia at ~3-km spatial resolution for selected regions of Mars that are of potential biological relevance, using observations made by the Mars Global Surveyor Thermal Emission Spectrometer. The sites that we examined include potential landing sites as well as other locations that can help us to understand the nature and distribution of surface properties. Thermal inertia is a direct indicator of physical properties of the surface at the same decimeter-to-meter scale to which a lander or rover is sensitive. Our goal here is to understand landing site safety and science potential for upcoming lander, rover, and sample-return spacecraft missions.

Thermal inertia: The thermal inertia (I) of the surface is derived from the diurnal variation of surface temperature, as determined from orbiter thermal emission measurements. Thermal inertia depends formally on the thermal conductivity, density, and specific heat of the surface, and is a direct indicator of the physical structure of the surface. In particular, the dependence of conductivity on the nature of the surface materials allows one to use remote determinations of I to derive information on the physical properties of the surface.

Low-inertia surfaces can be produced only by a covering of low-thermal-conductivity material such as unconsolidated fine dust. On Mars, the lowest thermal inertia values require the surface to be predominantly covered by at least a centimeters-thick layer of dust with average particle size less than about 30 μm . Surfaces with higher thermal inertia are more complicated. Based on geological analogs and *in situ* observations at the Viking and Pathfinder landing sites, thermal inertia can be increased by increasing the average particle size of the surface (for example, from dust to sand), adding rocks onto the surface, or increasing the degree of cementation of a crust.

The Viking and Pathfinder landing sites provide ground truth that helps us understand how to interpret thermal inertia. Clearly, however, these three sites have complex surficial geology. Each site contains a number of different components, including deposits of fine material, crusts that consist of fines bonded together, and rocks of various sizes, shapes, and textures. Each site has been acted on by a number of geological processes, possibly including flood, volcanism, impact, and aeolian processes. Thus, using a single number such as thermal inertia to describe the surface is difficult at best; combined with the inherent ambiguity in

the interpretation of high thermal inertias, this will limit the results that can be obtained.

However, it is clear despite this that thermal inertia provides important information on the nature of the surface at decimeter scales, especially when combined with other remote-sensing observations. Previous analyses indicate that there are large regions containing deposits of fine dust and other large regions dominated by the degree of cementation of duricrust.

Analysis of specific regions. We have mapped thermal inertia for a region 10° across in latitude and longitude and centered on each of 35 sites that include potential landing sites and other regions. In each case, problematic observations were eliminated, and the maps of thermal inertia were superimposed on the Viking-based MDIM for geological context.

In addition to examining the detailed relationship between the geomorphology and the thermal inertia at each site, we noted for each feature whether there was a correlation between the thermal inertia and the geomorphology and a qualitative assessment of the degree to which they correlated, the range in I within the particular feature of interest, and the range in I in the surrounding terrain.

We examined sites that included regions of possible hydrothermal or aqueous activity, lacustrine or fluvial sites, and periglacial sites. In addition, we examined areas that have been mentioned as possible landing sites in previous discussions for the '01 and '03 missions (such as the "hematite" region).

The general trend that is followed is that those sites that are in regions of lower thermal inertia also have lower thermal inertia themselves, and their thermal pattern does not correlate well with the geomorphology (i.e., the thermal inertia of the feature does not stand out markedly from that of the surrounding terrain). For sites that are in regions of intermediate thermal inertia, their thermal inertia is substantially higher than the regional values and correlates much more strongly with the morphology (i.e., it does stand out). Where the thermal inertia is already moderate to high, thermal inertia in channels and other aqueous features tend to be among the highest measured on the planet.

Discussion: The distribution of thermal inertia over the planet appears to be more complex than has been previously described. Globally, the thermal "continents" of low-inertia material probably represent deposits of airborne dust and are determined by the wind

patterns. Intermediate thermal inertias appear to be heavily crusted materials. The occurrence of the highest-thermal-inertia materials, and their moderate to strong correlation with local geology and geomorphology, has not been discussed in detail before.

The highest-inertia materials are located predominantly in local topographic lows, including crater interiors, catastrophic flood channels and chaos regions, and the troughs of Valles Marineris. The lack of general correlation with elevation indicates that they are not likely to be an artifact of the radiative effects of airborne dust. These materials also are not simply the high-end tail of the high-inertia mode of the distribution of thermal inertia. Rather, they represent a separate class of material in and of themselves.

At these high values of thermal inertia, there is an inherent ambiguity as to whether the values are determined by the abundance and properties of the rocks, blocks, or crusts. Increased abundance of any of these features can increase the thermal inertia. If due to crusts, the crust would need to be very well developed in order to have such a high thermal inertia; the highest values would correspond to a thermal conductivity only an order of magnitude lower than that of solid granite or dense sandstone. Similarly, the average or effective thermal conductivity would need to be 5-10 times higher than that of the Viking landing sites. If the high thermal inertia were produced by there being a high rock abundance on top of a dusty surface, roughly 3/4 of the surface would need to be covered with large rocks. If the high values were obtained by adding rocks to a surface that had a duricrust similar to that at the Viking sites, it still would require that half of the surface be covered with rocks.

Although we should fold in the information on surface structure obtained from the Viking and Pathfinder sites in order to understand these high-inertia surfaces, we cannot use them for specific guidance as they probably represent a different type of surface.

Although the places we have examined in detail were selected for the specific reason of looking for regions that might be suitable for finding present or past life (and therefore as potential future landing sites), they include a broad range of places of geological interest and help us to understand the global distribution of surficial geological features and processes. Many of the places show a strong correlation between surface thermal properties and the local geology and geomorphology. In essentially every instance in which there is such a correlation, it occurs where the feature of interest has high thermal inertia (both high relative to the high-I mode and high relative to their surroundings).

Other places show essentially no correlation of I with the local geology or geomorphology. In these

cases, both the feature of interest and the surrounding terrain have low to intermediate thermal inertia values. These surfaces are likely to have been modified substantially or blanketed by deposits subsequent to the time that they originally formed. As a result, it is likely that the decimeter- to meter-scale features in these areas will not reflect the same processes that were responsible for forming the 10- to 100-m-scale features.

In the high-inertia regions, the lack of blanketing suggests removal or non-deposition of aeolian materials. The surface materials may be remnant of the original processes that formed the features. In this sense, these sites may be the best sites at which to land, as we are likely to find materials at the surface that really do represent the types of materials that we expected to find based on orbiter-scale imaging.

There is an inherent conflict in choosing sites for *in situ* analysis and sample return, between enhancing the science return and enhancing the spacecraft safety. The safest sites are those with few rocks and blocks, which have been blanketed by aeolian or other materials; these are of less interest scientifically, as the materials of most interest may not be exposed or identifiable at the surface. The most interesting sites scientifically are those that remain unblanketed, with the surface materials left over from the original geological processes that formed the surfaces; these may be the least-safe sites, however, due to the absence of mantling materials and the likely high abundance of rocks and crusts, as indicated by the thermal inertia and by the strong correlation of I with geology.

Ongoing analysis. We are continuing our mapping efforts using a second-generation data base of thermal inertia. This data base incorporates data from a larger fraction of the mission, with a corresponding increase in coverage at each site. In addition, we will be comparing thermal inertia results with other data sets, including MOC imaging at high resolution and radar analysis of reflectivity and abundance of roughness elements. Results will be made available to the landing site working group as they become available.

ATMOSPHERIC CONSTRAINTS ON LANDING SITE SELECTION. D. M. Kass, J. T. Schofield, 169-237 *Jet Propulsion Laboratory, California Institute of Technology, 4800 Oak Grove Drive, Pasadena, CA 91109* (David.M.Kass@jpl.nasa.gov, John.T.Schofield@jpl.nasa.gov).

The Martian atmosphere is a significant part of the environment that the Mars Exploration Rovers (MER) will encounter. As such, it imposes important constraints on where the rovers can and cannot land. Unfortunately, as there are no meteorological instruments on the rovers, there is little atmospheric science that can be accomplished, and no scientific preference for landing sites.

The atmosphere constrains landing site selection in two main areas, the entry descent and landing (EDL) process and the survivability of the rovers on the surface. EDL is influenced by the density profile and boundary layer winds (up to altitudes of 5 to 10 km). Surface survivability involves atmospheric dust, temperatures and winds.

During EDL, the atmosphere is used to slow the lander down, both ballistically and on the parachute. This limits the maximum elevation of the landing site to -1.3 km below the MOLA reference aeroid. The landers need to encounter a sufficiently dense atmosphere to be able to stop, and the deeper the landing site, the more column integrated atmosphere the lander can pass through before reaching the surface. The current limit was determined both by a desire to be able to reach the hematite region and by a set of atmosphere models we developed for EDL simulations. These are based on TES atmospheric profile measurements (Conrath *et al.*, JGR, 2000), Ames MGCM results (Haberle *et al.*, JGR, 1993), and the 1-D Ames GCM radiative/convective model by J. Murphy. The latter is used for the near surface diurnal cycle. The current version of our model encompasses representative latitude bands, but we intend to make specific models for the final candidate landing sites to insure that they fall within the general envelope.

The second constraint imposed on potential landing sites through the EDL process is the near surface wind. The wind in the lower ~ 5 km determines the horizontal velocity that the landers have when they land. Due to the mechanics of the landing process, the total velocity (including both the horizontal and vertical components) determines whether or not the landers are successful. Unfortunately, the landing system has no easy way to nullify any horizontal velocity imparted by the wind, so the landing sites selected need to have as little wind as possible. In addition to the mean wind velocity, the landing system is sensitive to vertical wind shear in the lowest kilometer or so. Wind shear can deflect the retro rockets (RADs) from their nominal vertical orientation producing unwanted horizontal spacecraft velocities. Both mean velocity and wind shear are dominated by the local topography and other surface properties (in particular albedo and thermal inertia which control the surface temperature). This is seen even in simplified 2-D mesoscale models (Savijarvi and Silli, JAS, 1993). The effects in a fully 3-D model are expected to be even more topographically dependent. In particular there is potential for wind channeling in canyons and other terrain features. Boundary layer winds and wind shear are currently being mod-

eled based on terrestrial data and boundary layer scaling laws modified for Martian conditions. We hope to supplement this with mesoscale model results (from several sources) once the number of landing sites is reduced to a manageable number.

MER uses the Pathfinder airbag landing system, but the rovers are landing at mid-day (~ 2 pm for MER-A and ~ 12:40 pm for MER-B) compared with ~ 3 am for Pathfinder. In addition they land at the Spring equinox instead of the Fall equinox. This results in an approximately 1 mbar higher surface pressure, but are otherwise similar dynamically. The change in landing time makes the lower atmosphere during EDL more of an issue. The warmer daytime temperatures tend to make the atmosphere less dense, requiring lower landing altitudes. This effect is compensated for by design changes (larger RADs) to allow landing at higher elevations than considered for Pathfinder. At night the surface-cooled lower atmosphere is stable and, at least in flat regions, there is relatively little wind. During the mid-day, the boundary layer is strongly warmed by the surface and is usually convectively unstable. This leads to both stronger and more variable winds, as demonstrated by features like dust devils.

In addition to atmospheric constraints on potential landing sites due to EDL issues, the atmosphere also affects the landed portion of the mission. On the surface, atmospheric dust affects the rover's solar power supply and temperature and wind affect the thermal environment. Both will have to be evaluated to make sure the rovers can function for the duration of the mission at the desired landing sites.

Atmospheric dust affects rover power by attenuating the radiation falling on the solar panels. This attenuation can be caused by atmospheric dust and by the accumulation of dust deposited on the panels. Atmospheric attenuation can be a problem if the rover finds itself in a local or especially a regional dust storm. Although visible opacities are unlikely to exceed two (unless a major global dust storm is in progress during the early part of the mission), this is sufficient to hinder operations significantly for several days. It should be noted that TES has seen several dust storms in equatorial regions during this season (Smith *et al.*, JGR, 2000) and the Viking landers also saw such storms (Zurek *et al.*, *Mars*, 1992). Unfortunately there is no good dataset to determine which regions are more likely to have regional or local dust storms. The deposition rate of dust on the solar panels depends on the background dust opacity. As dust appears to be well mixed (at least in the lower atmosphere), the lower the landing site, the higher the opacity and the more deposition. Also, certain regions, in particular inside the large canyons, are often seen to be dustier than others (but not at dust storm levels). It is not clear whether this is just an altitude effect or site specific effect (Ivanov and Muhleman, GRL, 1998).

Near surface temperature and wind directly affect the lander thermal environment. This is especially an issue for ex-

ATMOSPHERIC CONSTRAINTS: Kass and Schofield

posed items. Both the wind and atmospheric temperature the lander experiences are controlled by the local and regional topography and diurnal ground temperature variations. In particular, depressions (such as craters and canyons) and slopes can generate significant winds due to day/night temperature contrasts and the corresponding pressure and density changes. The atmospheric temperature at the height of interest is controlled by the heat exchange with the surface. The surface temperature is dominated by the insolation, local albedo and thermal inertia. At the height of the rovers, the atmosphere will tend to respond to the surface on time scales of minutes. For the low nighttime wind speeds seen by Pathfinder (1 to 3 m/s, Schofield *et al.*, Science, 1997), this means the air temperature is only affected by the surface properties within a few hundred meters of the lander. We hope to obtain results from

mesoscale models for a few sites of interest, but at present it is not possible to cover all the possibilities. Furthermore, while mesoscale models should be able to simulate regional scale effects, the data (topography, albedo and thermal inertia) required to study so of the more local effects are not available.

Part of the difficulty with landing on Mars is that we have relatively little atmospheric data about the regions of importance for EDL and surface operations. There is the meteorological information from the three previous landers, but they were all landed in "safe" sites so are not necessarily representative more interesting ones. Each successful lander has also created a single atmospheric profile, but the landing systems tend to interfere with good atmospheric measurements at the most critical near surface altitudes. Furthermore, these are some of the most difficult locations to study from orbit.

EOS CHASMA AS A POTENTIAL SITE FOR THE MER-A LANDING

R.O. Kuzmin¹, R. Greeley², D.M. Nelson², J.D. Farmer², H.P. Klein³, ¹Vernadsky Institute, Russian Academy of Sciences, Kosygin St. 19, Moscow, 117975, GSP-1 Russia (rok@geokhi.ru), ²Arizona State University, Dept. of Geology, Box 871404, Tempe, AZ 85287-1404, ³SETI Institute, 2035 Landings Dr., Mountain View, CA 94043

Introduction: The key science goals for the Mars 2003 Rover mission include the study of the climate and water history of Mars at sites favorable for life. The regions for the MER-A landing site are confined to the latitudes of 5°N-15°S [1]. We focus on Eos Chasma, a region characterized by long-term hydrologic processes related to underground water release resulting from Hesperian magmatic and tectonic activities. Surface sediments include fluvial, paleo-lacustrine, and possible hydrothermally-derived materials. In addition, the sediments could contain a chemical and mineralogical signature reflecting a hydrologic and climate history in which the conditions could have been favorable for pre-biotic and biotic processes.

Location: The proposed region for MER-A is in northeastern Eos Chasma (12°-15°S; 40°-42°W) on the smooth plain of a fluvial channel (~ 120 km in length and from 60 to 30 km in width). This channel joins chaotic terrain to the west with Aureum Chaos to east. Two landing ellipses are placed on the channel floor (Figure 1) at: 13.4°S, 41.4°W, and 13.95°S, 41.7°W.

Geologic background: Geologic mapping from Viking images [2,3,4,5] suggests that the ancient plateau surface was resurfaced throughout the Hesperian period from releases of huge volumes of subsurface water from the eastern part of Valles Marineris (Capri Chasma and Eos Chaos). The water mass could have resulted from melting of ground ice [4,6]. It is possible that the liquid phase of CO₂ and its gas hydrate (which could be part of the permafrost volatiles [7,8,9]) might be part of the powerful and catastrophic processes of the highland plateau resurfacing.

Resulting geomorphic features from flooding include fragments of eroded channels, chaos terrain, and terraces etched into the eroded plateau surfaces around Eos Chasma and its walls. A temporal paleo-lake formed within the large collapsed depression of the chaotic terrain and its later drainage resulted in formation of erosional channels and fluvial sedimentation. Multiple erosional levels are evident as distinct terraces along the Chasma walls and plateau surfaces. These features formed by successive drainage from the main system of Valles Marineris, Ganges and Capri Chasmata, which passed through Eos Chasma and eventually northward to form the Xanthe Terra outflow channels. Orientations of eroded ridges and grooves on the terraces indicate that local direction of the water flow changed with time.

As a result of outflow events, sediments on Eos Chasma floor could consist of fluvial and paleolake deposits, including ancient crustal fragments, and possible hydrothermal products related to volcano/magmatic processes within Valles Marineris. [2]. Therefore, the past conditions of the area could be favorable for preserving evidence of possible pre-biotic or biotic processes within the sediments of Eos Chasma.

Depending on the final position of the lander within the landing ellipse, the walls Eos Chasma could be viewed by the PanCam at a feature a few hundred pixels high.

Conformity To Engineering Constraints: The proposed landing site at Eos Chasma fulfills the engineering requirements for the MER-A mission. The site is well within the latitude limitation and landing ellipses with long axes of 56 km and azimuths of 66° can be accommodated. The areas of the ellipses are relatively flat and free from known topographical hazards. MOC images show that the floor of Eos Chasma is significantly smoother than the Viking-1 and MPF landing sites (Figure 1). The elevation of the ellipses is approximately -3.5 km below the MOLA defined elevation reference [10].

Analysis of MOLA profiles across the Eos Chasma channel [11] shows that at the surface resolution of the data (footprint ~300 m) the channel's surface is relatively smoother than the surface in the regions of the Viking and MPF landing sites. The topographic surface variations (across the area of the ellipses) range from 20-70 m over 10-30 km.

TES thermal inertia values of the surface at the proposed site range from 7 to 12 x10⁻³ cal/cm² s^{0.5} K of cgs units (equivalent to 293-502 J/m² s^{0.5}K) derived from 3-km pixel resolution data [12]. Effective particles sizes corresponding to the values of thermal inertia [13] indicate values which are interpreted as medium and coarse sand (particles ranging from 350-1000 μm). The relatively high thermal inertia values suggests small amounts of dust on the surface layer and supports evidence for a sufficiently high load bearing soil essential for the rover transportation. The rock abundance of the landing site region is 10-20%, based on Viking IRTM data [14]; this is similar to values found at the Viking and MPF sites [15]. The albedo values measured within the landing site ellipse are between 0.13-0.20, which is lower than the average value of Mars (0.24). This also implies low dust cover on the surface. The lack of dust could reduce the eventual covering of fine material on the rover's solar panels during its active mission and extend the lifetime of the rover operations.

By reviewing the correlation between thermal inertia and radar properties [16], we determined that the site is sufficiently radar reflective for the descent radar altimetry to perform effectively. The values of the proposed site ranges from 0.05-0.08 and 0.05-0.06 at 13.6 cm 3.5 cm wavelength respectively (at scattering low exponent $n=1.5$). This information was obtained from global mapping of radar reflectivity (absolute depolarized reflectivity) of the Martian surface [17] which was created from Arecibo/Goldstone observations at 12.6 and 3.5 cm wavelengths. These values are sufficiently consistent with the engineering constraints for the surface radar reflectivity (>0.05).

Conclusion. Analysis of the proposed landing site in Eos Chasma channel reveals a elevation with a good load bearing and smooth surface, a moderate rock abundance, and a very rich and long-term history of fluvial processes resulting from multiple ground-water release and paleo-lake drainage.

References: [1] mars.jpl.nasa.gov/mep/mslides/index.html; [2] Luchitta, B.K., et al., 1992, In *Mars* (Kieffer H.H., et al., eds) Univ. of Arizona Press, pp. 453-492; [3] Baker, V.K., et

al., 1992, In *Mars* (Kieffer H.H., et al., eds) Univ. of Arizona Press, pp. 493-522; [4] Carr, M.H., 1996, *Water on Mars*, Oxford Univ. Press, NY, pp. 229; [5] Carr, M.H., 1981, *The surface of Mars*, Yale Univ. Press, New Haven, pp. 232; [6] Rotto, B.S., and K.L. Tanaka, 1995, Geologic/Geomorphic map of the Chryse Planitia Region of Mars, *USGS, Misc. Inv. Map*, 1:5M, I-2441; [7] Milton D.J., 1974, *Science*, 183, pp. 654-656; [8] Kuzmin, R.O., 1977, In *Problem of Cryolithology*, Moscow Univ. Press, 6, 7-25; [9] Kuzmin, R.O., 1983, *Cryolithosphere of Mars*, Moscow: Nauka Press; [10] Smith, D.E., et al., 1999, *Science*, 284, pp. 1495-1503; [11] marsweb.nasa.gov/landingsites/mer2003; [12] Mellon, M.T., et al., 2000, *Icarus* (in press); [13] Christensen P.R., 1986, *Icarus*, 68, pp. 217-238; [14] Edgett, K.S., and P.R. Christensen, 1994, *J. Geophys. Res.*, 99, pp. 1997-2018; [15] Golombek, M.P., et al., 1999, *J. Geophys. Res.*, 104, pp. 8585-8594; [16] Christensen, P.R., and H.J. Moore, 1992, In *Mars* (Kieffer H.H., et al., eds), Univ. of Arizona Press, pp. 686-729; [17] Harmon, J.K., et al., 1992, *Icarus*, 98, pp. 240-253.

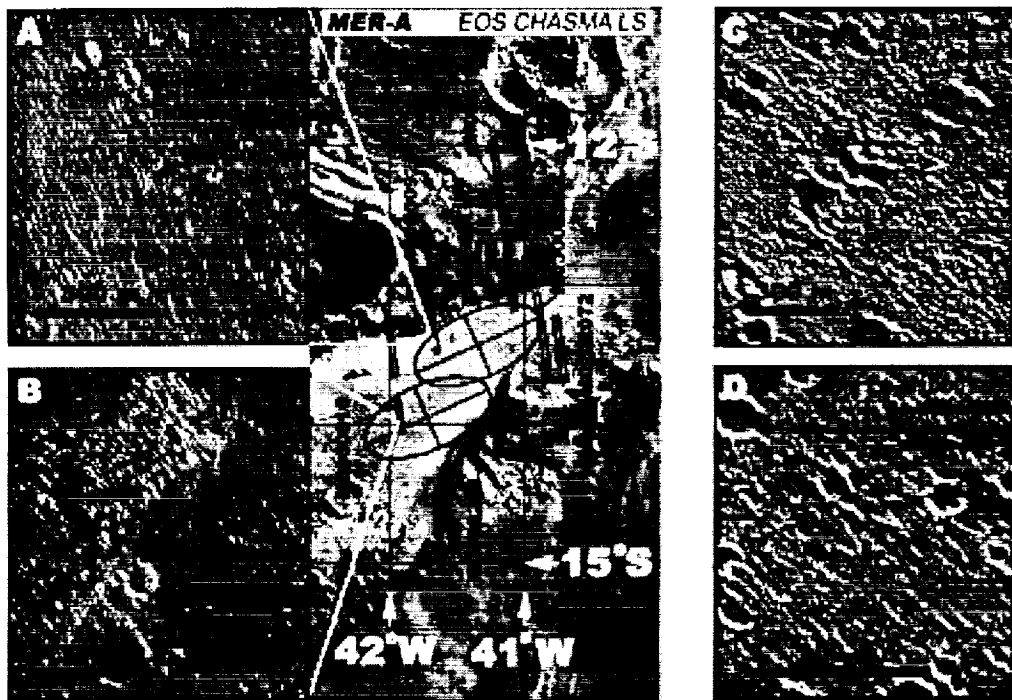


Figure 1. Photomap of proposed landing sites in Eos Chasma. MOC image subframes are used to compare the surfaces of the candidate landing sites (A, B) with Viking-1 (C) and MPPF (D). Available MOC images across this Chasma are identified.

MELAS CHASMA: MAJOR SCIENTIFIC OPPORTUNITY FOR MER 2003. N. Mangold, F. Costard, P. Masson and J.-P. Peulvast, Equipe Planétologie, UMR 8616, Bat. 509, Univ. Paris-Sud, 91405 ORSAY Cedex, France, mangold@geol.u-psud.fr.

Introduction: The two Mars Exploration Rovers (MER) of 2003 will give the opportunity to explore several parts of the Martian geology never studied before by in-situ analysis. The geographic locations of the two landing sites are disconnected because of the different orbit insertion of the two missions. The MER-A is supposed to land between 15°S and 5°N and MER-B between 5°S and 15°N. The possible landing sites for MER-B only cover northern volcanic plains and outflow channels. This kind of site has already been explored by Viking or Pathfinder in the past, but such regions will assure a safe and hazard-free landing site. At the other hand, MER-A has the opportunity to land in unexplored regions, like the lower part of Noachian highlands, impact crater paleolakes or Valles Marineris. Such landing site would be clearly more hazardous than those for MER-B. However the scientific goals of such region are so challenging that we recommend to take the risk to land in regions like Melas Chasma.

Geological setting: Melas Chasma takes place in the central part of Valles Marineris (Lat: 10°S, Long: 73,5°W). The nature of the deposits blanketing the bottom of Valles Marineris is uncertain. Several hypotheses were proposed including aeolian deposits, landslide debris, alluvial, lacustrine or volcanic origins [2, 3, 4]. Lacustrine or alluvial deposits would improve our knowledge on climate evolution and exobiology. Debris coming from landslides may present a large variety of materials with different ages that would be useful for geochemical purposes. Such landing site would help to the understanding of Valles Marineris formation and evolution, and therefore the evolution of the whole Tharsis region. The scientific implications of a rover inside Valles Marineris are then multiple.

Technical constraints:

- Lat/Long: 10°S- 73°
- Elevation (MOLA): -2.0km/-3.5km
- Viking Orbiter Image coverage:

HR	915a13-25	60 m/pix
	914a13-25	60 m/pix
	915a53-64	42 m/pix
	914a51-62	44 m/pix
MR	058a81-92	125 m/pix
LR	608a73	232 m/pix
- Several MOC pictures (see next paragraph).
- Thermal Inertia (IRTM): >4 cgs units.
- Rock abundance: 5-15%
- Stratigraphy:
 - Avf Valles Marineris Interior deposits.

Hvl Layered outcrops of Valles Marineris. Possible landing ellipse are mapped as VM49A to VM52A (Fig. 1) on the map of the USGS web site [1].

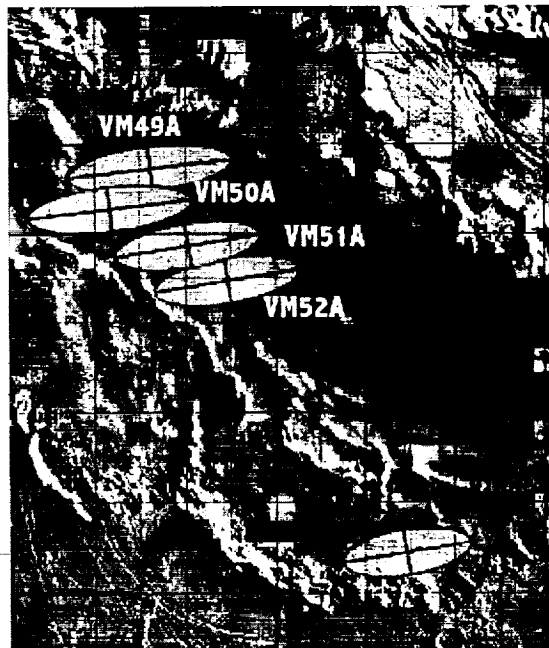


Fig.1: Location of the potential landing sites in Melas Chasma from the USGS web site.

MOC picture interpretation: Landing in Melas Chasma has been proposed by our team for the canceled Surveyor 01 mission [5]. This site was chosen as a preferential site by the French community. However no MOC data of this region were available at this time. Now, new MOC data permit to study the practicability of such landing site for both technical purposes and scientific goals. MOC pictures available in the bottom of Melas Chasma are still sparse in comparison to all pictures taken on the flanks of the chasmata. However, they show the occurrence of a great number of layered units. These layers are cut by erosion and present typical thickness of several tenths of meters or less (Fig. 2 and 3). They also display tectonic deformation in several regions (Fig. 2). The origin of these layers is unknown but they do not have the same properties than the upper scarps of Valles Marineris which are supposed to be volcanic. Sedimentary deposits on the floor of Melas Chasma are highly possible [3]. The tilt and deformation of these layers are possibly due to the tectonic evolution of Valles Marineris. The bottom of

Melas Chasma does not show great variations in elevation, because of the strong erosion of these layered units. The origin of this erosion remains also unknown but liquid water may have been involved to explain the efficiency of erosion. The Rover could analyze several of these layers along short displacements (i.e. few tenths of meters). Melas Chasma then represents one of the most attractive landing site because it is one of the few regions where a variety of layers can be analyzed in a single site.



Fig.2: Part of MOC picture M09-02145 (74.5°W, 8.8°S). 2 km wide.

Technical restrictions to land in layered units: Two difficulties are expected for such landing. Firstly, layers seem to be eroded at the hundred meters scale but they probably show small rocky scarps at the limit between soft and hard layers. Secondly, this region is not only affected by outcrops of layered terrain but also by dunes fields (Fig. 3) and pitted terrain. So this landing site cannot be considered as completely hazard-free. At the present time, the number of MOC pictures available is not sufficient to conclude whether the distribution of dunes fields or pitted terrains covers a negligible surface or not.



Fig.3: Part of MOC picture M03-01869 (74.6°W, 10.3°S). 5 km wide.

Conclusion: Melas Chasma displays eroded layered units that give an unique opportunity to study different stratigraphic levels with a Rover. The technical constraints are in agreement with those needed for MER-A landing site, but they do not rule out the possibility of hazard due to the large variety of geological processes and landforms of this region. More MOC data of sites VM49A to VM52A should be acquired in order to solve this problem.

References: [1] Mars 03 Landing Site Website, webgis.wr.usgs.gov/mer/ [2] Nedell S. S. *et al.* (1987), *Icarus*, 70, 409-441 [3] Lucchita B. K. (1987), *Icarus*, 70, 411-429. [4] Peulvast J.-P. and P. L. Masson (1993), *Earth, Moon and Planets*, 61, 191-217, 1993. [5] Costard F. *et al.* (1999). Melas Chasma: Potential landing site for the Mars 2001 mission, *Workshop on Mars 2001*, LPI Houston.

POTENTIAL 2003 LANDING SITES IN THE CERBERUS PLAINS, SE ELYSIUM PLANITIA. A. McEwen¹, P. Lanagan¹, R. Beyer¹, L. Keszthelyi¹, and D. Burr², ¹Lunar and Planetary Laboratory, University of Arizona, Tucson, AZ 85721, USA, (mcewen@lpl.arizona.edu), ²Department of Geosciences, University of Arizona, Tucson, AZ 85721, USA.

Summary: There are spectacular and well-preserved volcanic, fluvial, and sedimentary features in the Cerberus plains region, but the surfaces are often extremely rough at the scale of meters to tens of meters, unsafe for landing and impractical for the Athena rover. However, several sites (EP71A, EP74A, EP77A, EP61B, EP62B) appear reasonably smooth over much of the terrain seen in MOC images. All of these sites are just north of the contact between finely-layered sedimentary deposits mapped as part of the Medusae Fossae Formation and very young flood lavas (1 N, 212 W to 5 N, 221 W). Landing in this region could enable study of well-preserved lava flows, possible phreatic cones, finely-layered sedimentary strata, possible shoreline features, and patterned ground. We could answer questions about recent volcanic and fluvial activity, the origin of the layered sedimentary deposits, and whether ground ice is present within the upper tens of meters of the surface.

Background: MOC images have revealed well-preserved volcanic and fluvial features on or near the Cerberus plains (~5 S to 10 N, 180-220W) [1]. Recent (Upper Amazonian) flood lavas in this region were first described by Plescia [2]. Finely-bedded sedimentary deposits similar to those described in [3] overlie or reside near portions of the Cerberus plains, especially in the SE areas. The Cerberus plains comprise the largest region on Mars with well-preserved volcanic and fluvial morphologies, with primary features preserved at the scale of meters. Much of the plains are covered by lava flows with a distinctive platy/ridged morphology similar to portions of lava flows on Iceland [4]. Some of the lava flows appear to be younger than 10 Ma based on counts of small craters [5]. Marte Vallis (~10 N, 180 W) and channels near 8 N, 205 W reveal terraces, longitudinal grooves, and streamlined islands, similar to large paleoflood

channels on Earth and elsewhere on Mars [6]. The channels near 8N, 205 W originate from Cerberus Rupes (actually fossae) and/or ancient highland terrains, but disappear to the south beneath the very young Cerberus lavas. The channels in Marte Vallis become recognizable at ~10 N, 180 W in spite of embayment by lava flows, and continue to the NE into Amazonis Planitia. Based on these relations and the MOLA topography, the channels near 8N, 205 W probably continued south and then west into Marte Vallis, but are completely buried by thick lavas in the central Cerberus plains [6]. These channels are probably younger than 500 Ma [2], and may be much younger if we can correctly interpret the size-frequency distributions of small craters.

In southern parts of the the Cerberus plains, some lava flows are being exhumed from beneath weakly indurated sediments of the Medusae Fossae Formation (MFF). Some of these sediments are finely layered [e.g., 3]. Most previous workers have interpreted the age and stratigraphy of the MFF as Upper Amazonian, although [3] have interpreted the layered sediments as Noachian. Sedimentary units of the MFF (not necessarily like those described by [3]) overlie sparsely cratered lava flows in places, so the crater distributions may date the exhumation rather than emplacement of the lava flows. However, a Noachian or Hesperian age for the lavas would require some improbable assumptions about the geologic history, i.e. that an erosion-resistant layer covering a huge area was only very recently breached but left few remnants. In other places lava clearly embays the MFF.

Many origins for the MFF have been proposed. The association with flood lavas suggests that some of these sediments may be volcanic tephra from basaltic lava fountains or from phreatomagmatic explosions where the magma

interacted with ice-rich terrains [4, 7]. If so, then the lava and MFF have nearly the same emplacement age, but the tephra has been eroded by wind over the past $\sim 10^7$ - 10^8 yrs. The best evidence for volcano-ground ice interactions in this region are the many (100s) of cones interpreted as phreatic or rootless cones [8]. Such cones suggest the presence of shallow ground ice (< 10-20 m) at the time of lava emplacement, perhaps only $\sim 10^7$ yrs ago. The ground ice could have been recharged within $\sim 5 \times 10^8$ yrs via fluvial floods. Patterned ground is also common over portions of these plains, probably from cooling and contraction of ponded lava but perhaps due to shallow ground ice.

Potential Landing Sites: About 20 potential landing sites on the Cerberus plains have been identified by Golombek and Parker [9] on the basis of various datasets, not including MOC. MOC high-resolution images show that terrains nearby and contiguous with the landing sites are usually dominated by platy/ridged lava, MFF eroded into a rough wind-sculpted surface, or moderately cratered plains. Both the platy/ridged lava and MFF are extremely rough surfaces at the scales of 1-100 m and should be ruled out as feasible landing sites. Note that many of the very roughest areas as seen by MOC correspond to some of the very smoothest areas seen by MOLA or Viking at larger scales. The moderately cratered plains appear geologically uninteresting.

The most promising sites on this list are EP71A at 1.2 N, 212 W and EP77A at 4.5 N, 220.5 W, and perhaps other sites that lie between these locations (EP74A, EP61B, EP62B). All 5 of these sites have a similar geologic setting, north of the contact between MFF and the Cerberus lavas. EP77A is covered by several MOC images; these and MOC images near the other sites often reveal relatively smooth surfaces. Typical terrains include extensive areas that we interpret as inflated pahoehoe lava flows and patterned ground (probably lava), both of which appear fairly smooth (but this needs to be quantified). There are also regions of platy/ridged lava, which we

interpret as rubbly pahoehoe, inflated lavas that have been remobilized and the crust broken up into a chaotic and extremely rough surface. Care must be taken to find a landing ellipse that minimizes this terrain and other rough surfaces. Also present near these sites are hundreds of cones of potential phreatic origin, finely-layered sedimentary strata, and possible small-scale shoreline strands. Exploration of this region could answer questions about recent volcanic and fluvial activity, the origin of the layered sedimentary deposits, and whether ground ice is present within the upper tens of meters of the surface (via composition of phreatic deposits). Such shallow ice in the more accessible and hospitable equatorial region would have important implications for future exploration. The scenery should be quite spectacular from the viewpoint of Athena.

MOC images covering EP77A include M0701753, M0802926, and M0902230; MOC images near the other sites include FHA01586, M0203479, M0001046, M0001434, M0201183, M0305363, M0702180, M0703125, M0703643, M080090 and M0902816.

References:

- [1] McEwen, A. et al. (1999) LPSC XXX, #1829, on CD.
- [2] Plescia, J.B. (1990) *Icarus* 88, 465-490.
- [3] Malin, M., and Edgett, K. (2000) *Science* 290, 1927-1937.
- [4] Keszthelyi, L., McEwen, A., Thordarson, Th. (2000) *JGR* 105, 15027-15050.
- [5] Hartmann, W. and Berman, D. (2000) *JGR* 105, 15011-15026.
- [6] Burr, D. and McEwen, A. (2000) IAHS proceedings, The Extreme of the Extremes conference, Reykjavik, July 2000, in press.
- [7] McEwen, A. et al. (2000) abstract for conference on Volcano-Ice Interactions on Earth and Mars, <http://www.flag.wr.usgs.gov/USGSFlag/Land/IcelandMeeting/>
- [8] Lanagan, P., et al. (2000) submitted.
- [9] Golombek, M. and Parker, T. (2000) <http://marsweb.nas.nasa.gov/landingsites/mer2003/memorandum.html>

HUBBLE SPACE TELESCOPE VISIBLE TO NEAR-IR IMAGING AND SPECTROSCOPY OF MARS IN SUPPORT OF FUTURE LANDING SITE SELECTION. R.V. Morris¹ and J.F. Bell III², ¹NASA Johnson Space Center, Code SN3, Houston TX (richard.v.morris1@jsc.nasa.gov), ²Cornell University, Department of Astronomy, Ithaca NY (jfb8@cornell.edu).

Since 1990, the Hubble Space Telescope (HST) has been obtaining high-quality visible to near-IR imaging and spectroscopic measurements of Mars. The most recent observations, obtained during the 1999 opposition [1,2], are the highest spatial resolution Earth-based data of Mars ever obtained, providing resolution of 20 to 30 km/pixel for regions near equatorial latitudes. Examples of 1999 HST images are shown in Figure 1. The HST data cover up to 12 discrete diagnostic wavelengths (~255 to 1042 nm) that were not measured by the Mariner, Viking, or MGS Orbiters and they approach the spatial resolution of existing orbital spectroscopic measurements by Phobos-2 (22 km/pixel ISM data) and MGS (~3x6 km to ~10 km/spectrum TES data). HST's ability to image the planet at these visible to near-IR wavelengths would only have been exceeded by the multispectral investigation planned by the MARCI instrument on the failed Mars Climate Orbiter mission [3]. Some of MARCI's capabilities may be recoverable from measurements by the VIS channel on the Mars 2001 Orbiter's THEMIS instrument, if that instrument is successfully launched and delivered to Martian orbit. However, with the failure of MCO and prior to the potential acquisition of THEMIS/VIS data, HST provides the best available capability for studying Mars at visible to near-IR wavelengths.

Observations in the visible to near-IR can provide unique and diagnostic information on the abundance, oxidation state, crystallinity, and cation ratios of iron-bearing minerals. Specifically, as discussed previously [4-7], these wavelengths can provide constraints on the presence of relatively unweathered surface components like pyroxene as well as highly altered components like nanophase and well-crystalline hematite and other ferric oxide/oxyhydroxide phases. Examples of the quality of typical 12-color Mars spectra obtained using multispectral imaging with the HST Wide Field Planetary Camera-2 (WFPC2) instrument are shown in Figure 2.

In addition to compositional information,

HST data also provide the ability to assess temporal variability on the Martian surface associated with aeolian redistribution of windblown dust. Long-timescale variations in the appearance of classical albedo features have been noted in historical telescopic observations [8]. More recently, HST has provided quantitative information on variations in surface albedo features during a time period (1980s through arrival of MGS) that was not well studied by spacecraft [9]. These observations show that the albedo and wavelength-dependent reflectivity of the Martian surface today are not identical to that observed during the Viking era.

In this presentation, we will focus on the compositional and mineralogic interpretations being obtained from our 1999 HST/WFPC2 images, the comparison of results being derived from HST to those being derived from MGS/TES in the mid-infrared, and the potential implications of our HST measurements on the landing site selection process.

References: [1] Farrand, W.H., J.F. Bell III, R.V. Morris, and M.J. Wolff, *Bull. Amer. Astron. Soc.*, 32, 1119, 2000. [2] Bell III, J.F. and M.J. Wolff, *Lunar and Planet. Sci. XXXI*, Abstract #1223, 2000. [3] Malin, M. *et al.*, *JGR*, in press. [4] Soderblom L.A., in *Mars* (H. Kieffer *et al.*, eds.), pp. 557-593, 1992. [5] Roush T.L., Blaney D.L., and Singer R.B., in *Remote Geochemical Analysis: Elemental and Mineralogical Composition*, (C. Pieters and P. Englert, eds.), pp. 367-393, 1993. [6] Bell III, J.F., in "Mineral Spectroscopy: A Tribute to Roger G. Burns," *Geochemical Society Special Publication 5* (M.D. Dyar, C. McCammon, and M.W. Schaefer, eds.), 359-380, 1996. [7] Morris, R.V., D.C. Golden, J.F. Bell III, T.D. Shelfer, A. Scheinost, N.W. Hinman, G. Furniss, S. Mertzman, J.L. Bishop, D.W. Ming, C. Allen, and D.T. Britt, *J. Geophys. Res.*, 105, 1757-1817, 2000. [8] Martin, L.J. *et al.*, in *Mars* (H. Kieffer *et al.*, eds.), pp. 34-70, 1992. [9] Bell III, J.F., M.J. Wolff, T.C. Daley, D. Crisp, P.B. James, S.W. Lee, J.T. Trauger, and R.W. Evans, *Icarus*, 138, 25-35, 1999.

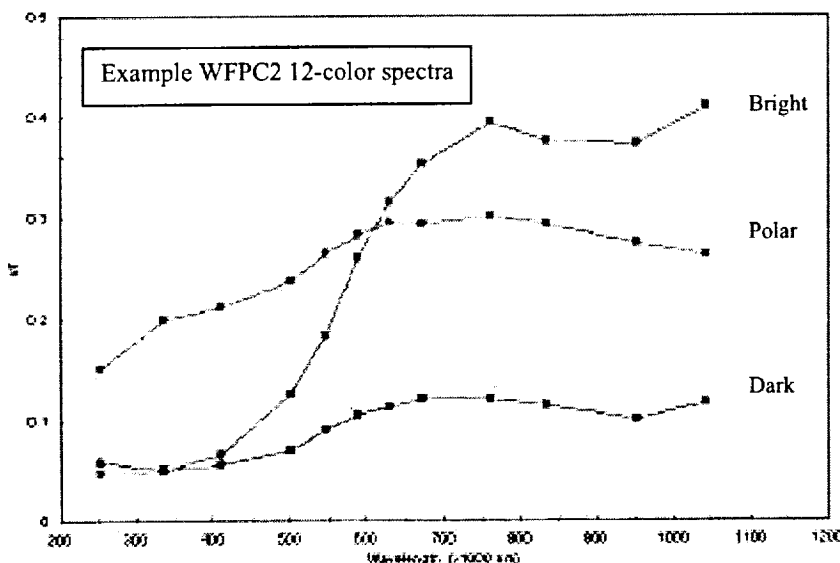
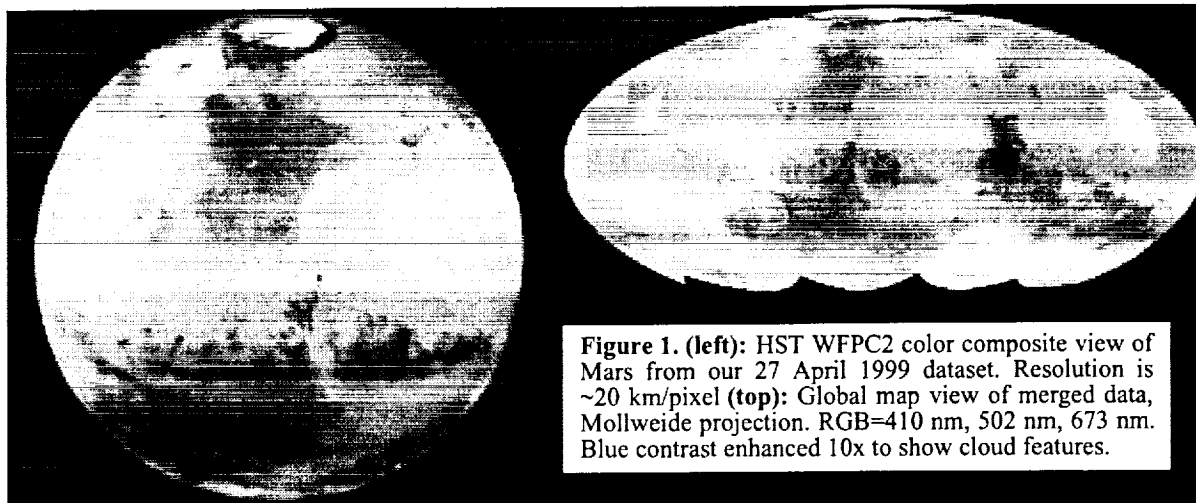


Figure 2. Spectra extracted from the 27 April 1999 HST/WFPC2 12-color multispectral dataset, after mapping and coregistration of the individual images. Uncertainties in the absolute I/F calibration are from 2% to 5% for all channels except 763 nm and 835 nm, which have absolute calibration uncertainties of 10-15%.

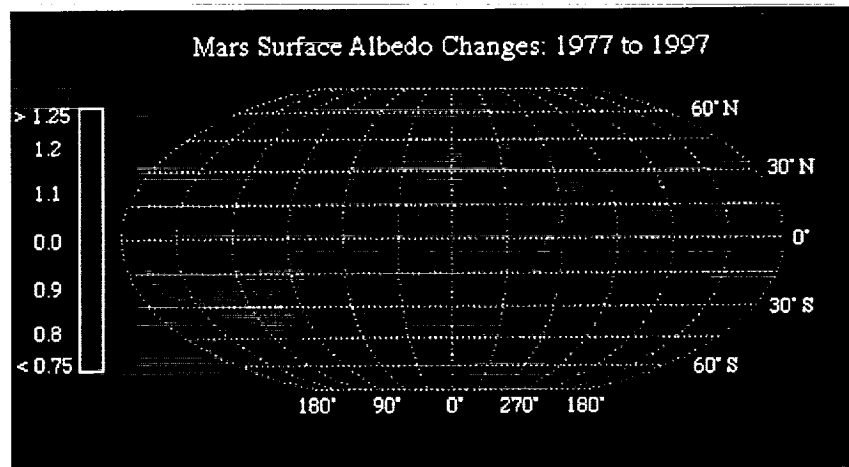


Figure 3. Albedo changes on the Martian surface over a 20 year period [8]. This is a ratio image of a 1997 1042 nm HST global mosaic to the Viking Orbiter 1977-era IRTM albedo map. Surface regions that have brightened more than 5% since 1977 are shown in shades of red. Surface regions that have darkened more than 5% since 1977 are shown in shades of blue.

DURIUS VALLES OUTFLOW BASIN, MARS: PROPOSED SITE FOR MER-A

D.M. Nelson¹, J.D. Farmer¹, R. Greeley¹, R.O. Kuzmin², H.P. Klein³, ¹Arizona State University, Dept. of Geology, Box 871404, Tempe, AZ 85287-1404 (nelson@dione.la.asu.edu), ²Vernadsky Institute, Russian Academy of Sciences, Kosygin St. 19, Moscow, 117975, GSP-1 Russia, ³SETI Institute, 2035 Landings Dr., Mountain View, CA 94043

Introduction: The primary goals for future landed Mars missions include: 1) the search for past or present life, and/or evidence of prebiotic chemistry, 2) understanding the planet's volatile and climatic history, and 3) determining the availability and distribution of mineral resources on Mars. Determining the history of water is essential in accomplishing all of these goals. On Earth, microbial fossilization only occurs under specific circumstances, including entombment by rapid burial of fine-grain sediments and precipitation of dissolved minerals (e.g., carbonates, etc.) [1]. Therefore, in addition to targeting sites where liquid water might have been present, the next step is to locate paleoenvironments that were most favorable for the capture and preservation of fossil biosignatures. Astrobiologically important sites on Mars are: hydrothermal, lacustrine, and "grab-bag" (e.g., a locale that had a variety of geologic processes acting upon it). An emphasis on lander safety and surface accessibility is also vital in landing site selection. Surfaces must have little accumulation of dust and yet be relatively smooth with a low degree of rock abundance. The landing ellipse must lie on a flat surface, eliminating areas with irregular or heavily cratered surfaces. Visiting sites where natural geological processes (e.g., outflows, impacts, etc.) have transported a variety of materials to a single site is vital. The aim in site selection is to ensure access to a variety of aqueous deposits of differing ages.

Site Location: The proposed landing site for MER-A is located 50 km to the northeast of the mouth of Durius Valles, where the channel drains into the south end of Elysium Basin at the highland-lowland boundary (Figure 1). The landing ellipse is centered on a relatively flat surface of sedimentary material at 14.6°S, 187.6°W. Similar sites in this area have been previously proposed [2,3,4]. Rocks sampled at this site would include Noachian age materials, which had been modified and transported by fluvial processes, and possibly volcanic materials from a small volcanic construct at the head of Durius Valles. Possible exobiologic material from the highlands, if present, could have been preserved in the fine-grained sediments on the depositional plain.

General Geology: Durius Valles consists of four flat-floored tributaries which have incised the cratered highlands of Terra Cimmeria and converged into a single channel before debauching into De Vaucouleurs basin, an ~300 km diameter extremely degraded impact basin.

The southwest tributary incises Noachian terrain, passing through a ~50 km diameter crater, and smooth plains before joining the main tributary. Two smaller channels join the main channel near the mouth of Durius, one crossing dissected terrain from the west and the other through similar terrain from the east. At the head of the main channel of Durius Valles is a small volcanic construct. To the northwest of the cone is a shallow depression with dissected margins from which the main tributary of Durius Valles flows north. The small composite cone sits on the cratered highlands of Terra Cimmeria, suggested to be an Early Hesperian age

volcano (see MOC image M03-07208). Materials from this area were transported north into the lowland depositional basin. Stratigraphic correlation of materials in the basin and terraces within the channel indicate that at three main outflow events deposited materials in De Vaucouleurs. The first event deposited a thick layer of sediment; the last remnants of which are visible as a plateau of severely eroded material in the west end of Figure 1. The second outflow passed ~100 km into the basin, eroding the older deposit, and leaving a thin smooth layer of sediment. The proposed landing site sits on this second deposit. The last event extended a lobe of material ~60 km into the basin [5].

Moderate resolution Viking images (431S11-13, and 432S05-08; ~71 m/pixel), clearly reveal the surface of this site. At this scale, the surface is relatively smooth on the outflow plain with some hummocky material at the west end and the north central part of the ellipse. The ellipse contains three small (<5 km diameter) craters, and several shallow linear valleys. The origin of the valleys is uncertain: they do not appear to be fluvial in origin, but are more likely to be tectonically derived. No MOC images exist within the landing site ellipse, although four images were obtained nearby and several images in DeVaucouleurs basin are available. M00-00565 is a MOC image of the first sedimentary deposit ~70 km west of the proposed ellipse. The surface appears etched and pitted with dune-filled depressions indicating a highly erodable material. To the west of the ellipse, MOC image M02-1037 reveals an irregular north-south trending ridge of hummocky material, interpreted as the margin of the last outflow material. To the northeast, the terrain in image M03-03358 consists of smooth, blocky mesas interspersed with sediment-filled depressions. MOC image M07-00408, northwest of the ellipse, shows a relatively flat surface with scattered mesas and small patches of linear dune-like features. The last two images depict the margins of the second sediment deposit from Durius Valles. Although some areas within the landing site ellipse appear somewhat uneven, the mesas, craters, and valleys should pose little hazard for the airbag descent.

Scientific and exobiologic significance: This site is located at the end of an outflow channel where it empties into a broad, low-lying plain. Lobes of material on the plain suggests the presence outflow deposits. Because the plain does not appear to have been a lacustrine environment but an outwash area, biotic processes probably could not have been established here. However, possible exobiologic material from the highlands, transported from subsurface water sources, could have been transported downstream to the depositional area. Proximal coarse grains within the delta could contain fossiliferous clasts, whereas the fine-grained distal sediments could have entombed microbial organisms within shales. Other materials sampled at this site would include rocks derived from Noachian outcrops in the highlands. Also, minerals that had been hydrothermally altered within springs at the small composite volcano, as

Nelson, et al., Durius Valles: Potential Site For MER-A

well as basaltic or pyroclastic materials erupted from the volcanic center, could have been transported to the site.

Engineering Constraints: The proposed site falls within the engineering constraints for the MER-A mission [6]. It is near the southern margin of the latitude limitation of 15°S, but the entire ellipse lies north of this latitude. Review of the MOLA data places the site at -1.6 km below planetary datum [6,7]. Four MOLA tracks cross the ellipse (10330, 10832, 10917, 11003) and re of approximately equal value, suggesting that there is little east-west slope variation.

The TES defined thermal inertia value within the landing ellipse is $\sim 200 \text{ J/m}^2 \text{ s}^{0.5} \text{ K}$, which is above the minimum constraint of 165. This value is derived from 3-km pixel resolution data [8]. IRTM models of the surface indicate a moderate but acceptable amount of dust at the surface with a fine component value of $\sim 5.9 \times 10^{-3} \text{ cal/cm}^2 \text{ s}^{0.5} \text{ K}$ [9,10]. Block abundance is low, with a surface coverage of only 2-3% [9,10,11,12]. However, the maneuverability of the rover should make interesting nearby rocks accessible. The albedo values measured in the ellipse is ~ 0.256 [13,14,15], slightly above the planetary average, but this is probably a result of the small number of rocks. Global mapping of radar reflectivity of the surface by Arecibo/Goldstone observations (12.6 and 3.5 cm wavelengths) [16,17] indicated values greater than 0.05 (scattering exponent: $n=1.5$).

Conclusions: The outflow plain beyond the mouth of Durius Valles is proposed as a candidate landing site for the MER-A 2003 mission. It is a high to moderate priority target with respect to astrobiology. The characteristics of the site, fulfill the engineering constraints imposed on the mission. Dust coverage is moderate, but acceptable. Rock abundance is

low, but samples will be accessible because of the long-range capabilities of the rover. Low slopes and few obstacles will provide good trafficability at the site. The primary consideration for this site is the accessibility to Noachian rocks which might preserve information on the early climate of Mars. Fine-grain, fluvial materials are present which could include Early Hesperian volcanic rocks, and possible hydrothermally altered minerals. The information gained from the materials analyzed at this site could provide insight into the viability of life on the surface or near surface of Mars during its early history.

References: [1] Farmer, J.D., and D.J. DesMarais, 1999. Exploring for a record of ancient Martian life. *J. Geophys. Res.*, **104**, 26,977-26,996; [2] Cabrol, N.A., J.D. Farmer, R. Landheim, 1994. Site 079 Aeolis Southeast. In *Mars Landing Site Catalog*, eds. R. Greeley and P.E. Thomas, NASA Ref. Publ. 1238, 2nd ed., 218-221.; [3] Landheim, R., 1995. *Exobiology sites for Mars exploration and geologic mapping of Gusev crater—Ma'adim Vallis*. Master Thesis, Ariz. State Univ.; [4] Nelson, D.M., J.D. Farmer, R. Greeley, H.P. Klein, R.O. Kuzmin, 1999. Geology and landing sites of the Elysium Basin-Terra Cimmeria region, Mars. *Proc. 2nd Mars Surveyor Landing Site Workshop*, SUNY, Buffalo (June 22-23), 71-73; [5] Kuzmin, R.O., et al., 2000, USGS Misc. Inv. Map, 1:500K, I-2666; [6] marsweb.nas.nasa.gov/landingsites/mer2003/; [7] Smith D.E. et al., The global topography of Mars and implications for surface evolution, *Science*, 284 1495-1503, 1999; [8] Mellon M.T., et al., 2000, High resolution thermal inertia mapping from the Mars Global Surveyor Thermal Emission spectrometer, *Icarus* (in press); [9] Christensen, P.R., 1986, *J. Geophys. Res.*, **91**, 3533-3545; [10] Golombek, M.P., et al., 1997, *J. Geophys. Res.*, **102**, 3967-3988; [11] Christensen, P.R., 1982, *J. Geophys. Res.*, **87**, 9985-9998; [12] Christensen, P.R., 1986, *Icarus*, **68**, 217-238; [13] Pleskot, L.K., and E.D. Miner, *Icarus*, **45**, 179-201, 1981; [14] Christensen, P.R., 1988, *J. Geophys. Res.*, **93**, 7611-7624; [15] Kieffer, H.H., et al., 1977, *J. Geophys. Res.*, **82**, 4249-4291; [16] Christensen P.R. and H.J. Moore, 1992, In *Mars* (Kieffer H.H., et al., eds.) Univ. of Arizona Press, 686-729; [17] Harmon, J.K., et al., 1992, *Icarus*, **98**, 240-253.

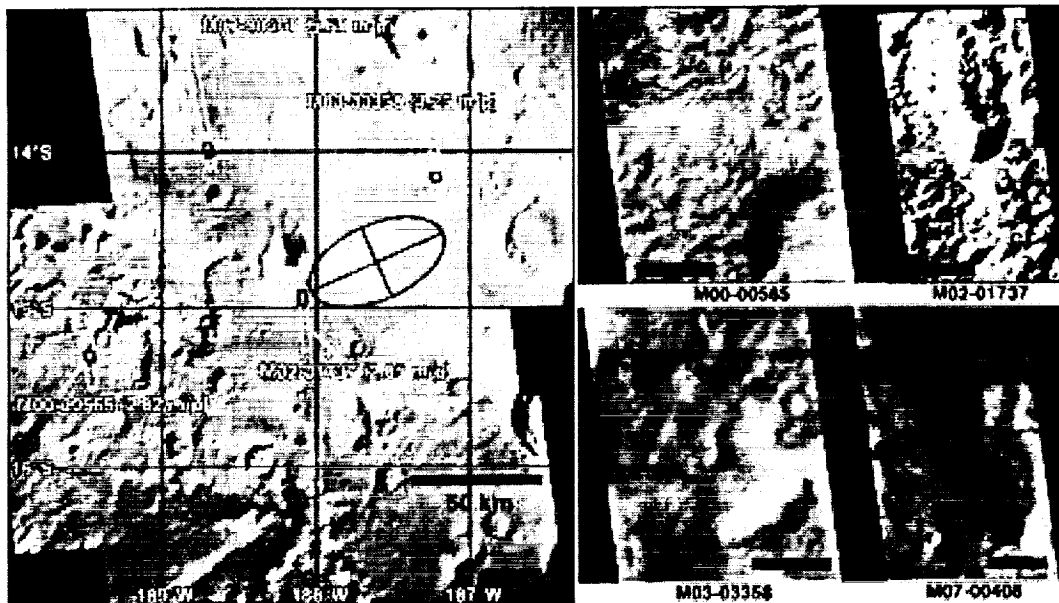


Figure 1. Photomosaic of Durius Valles from mid-resolution MOC images. MOC subframes depict sample surface areas of the terrain surrounding the proposed site. Scale bars on the subframes are 1 km wide.

IMPACT CRATER LANDING SITES FOR THE 2003 MARS EXPLORER ROVERS – ACCESSING LACUSTRINE AND HYDROTHERMAL DEPOSITS H. E. Newsom, University of New Mexico, Institute of Meteoritics, Dept. of Earth & Planetary Sciences, Albuquerque, NM 87131 U.S.A. E-mail: newsom@unm.edu.

Introduction: Five craters larger than 100 km diameter, including Gale with its spectacular lake deposits, have been identified as possible landing sites for the Mars Explorer Rovers (MER) 2003 missions [1]. These craters are important locations where lacustrine, fluvial, and hydrothermal processes occurred on Mars, they have exciting landscapes, and these missions represent the first chance to visit a large crater on another planet [2,3,4]. Lakes probably formed in these craters, with water supplied from aquifers or surface sources, resulting in deposition of water-lain sediments and evaporites [3,5,6,7]. Lake waters derived from broad regional aquifers, can potentially collect biological material from a wide region and provide environments for possible life forms to flourish. Hydrothermal systems, which formed in the craters due to heat from impact melt and uplifted basement, are highly sought after targets because terrestrial life probably originated in such systems. Studying hydrothermal and aqueous processes in large craters on Mars will allow us to:

- Identify and characterize environments for the origin and evolution of life on Mars.
- Understand the history of water at the Martian surface, including hydrothermal systems, lake formation, and the nature of ancient climates.
- Study the contributions to the Martian soil from hydrothermal and evaporite processes [8].

The location of fluvial and lacustrine deposits are often evident from geomorphic evidence, such as layering and delta structures, but the location of hydrothermal deposits is less obvious. However, continuing research including study of MGS MOC imagery (Fig. 1), hydrothermal modeling, and terrestrial analogue studies provide strong guidance on where such deposits can be found, and on the processes that may have exposed or delivered this material to the landing sites.

MER impact crater landing sites: Possible landing sites on the floors of five craters were identified during early assessment of MER landing sites. These craters include Gusev (EP55A, -1.9 km elev., 160 km diam.), Gale (EP82A, -4.5 km elev., 170 km diam.), Boeddicker (EP64A, -2.1 km elev., 110 km diam.), an unnamed crater in Elysium Planitia (EP69A, -1.7 km elev., 100 km diam.), and an unnamed crater in Terra Meridiana containing two sites (TM15A, north site, TM16A, south site, -1.9 km elev., 150 km diam.). Unfortunately, there are virtually no MOC high-resolution images of the landing sites on the floors of these craters. Evidence for fluvial and lacustrine deposits have been identified in Gale (Viking and MOC), and the

unnamed EP crater (Viking data) [4,6,7], and such deposits have a good chance of being present at the surface in their landing sites. Gusev crater was thought to be a good candidate, but unreleased MOC images do not reportedly show evidence of lake deposits or evaporites on the crater floor [9]. For the Unnamed TM crater, there appears to be a channel leading into the crater from the south, however no deltas have been identified, and no evidence for sedimentary layering is obvious in the two released MOC images. Evidence for lacustrine activity has not been reported for Boeddicker, but there are no released MOC images.

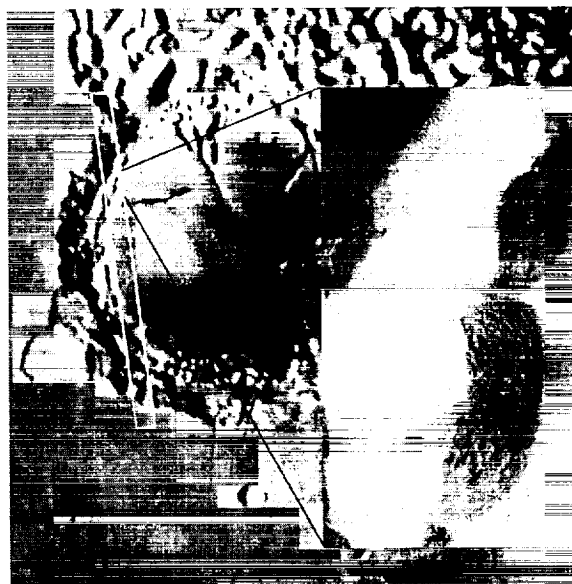


Figure 1. This picture illustrates the high permeability at the rim of a buried crater on Mars. This chaos region formed in a buried 50 km diameter crater at 1° N, 26° W, due to erosion of blanketing deposits by emerging groundwater. The localization of the outflow was probably due to bedrock fracturing, and hydrothermal alteration due to focusing of fluid flow around an impact melt sheet following crater formation. The inset image is a portion of a high resolution MOC image. (Context image M0307651, picture width 85 km, inset M030750, width 2.1 km).

Location of hydrothermal deposits: In large craters the nature and geometry of the heat sources and the zones of higher permeability controls the location of hydrothermal deposits. The heat sources are the impact melt sheet on the crater floor, and the uplifted

basement [2,10,11]. Recent results by Thorsos et al. [11] indicate that these two sources of heat were approximately equal during the formation of large craters in the southern highlands. Numerous studies of terrestrial hydrothermal systems and theoretical studies of Martian systems by Gulick [12] and Rathbun and Squyres [13] shows that focusing of hydrothermal fluids occurs at the edge of planar heat sources. Both geological evidence and modeling suggest that the flow of hydrothermal fluids in large craters will be concentrated at the edges of the melt sheets in zones of higher permeability present in the crater rim and central uplift.

Terrestrial geological evidence for the concentration of hydrothermal fluid flow at the rims of craters comes from the Ries crater, where evidence exists for intense hydrothermal alteration of suevite associated with nearby carbonate spring mounds of probable hydrothermal origin on the western rim [14]. Evidence from the Sudbury structure includes the occurrence of hydrothermal ore deposits at the contact of the basement rim material with the crater fill. Evidence from Mars for the high permeability of central uplifts consists of the images of recent channel formation on pole-facing slopes of the central uplifts of large craters [15]. Evidence for permeability in the rims of large craters on Mars comes from the circular pattern of erosion in the cover of preexisting craters in chaos regions (e.g. Fig 1).

The hydrothermal potential for the candidate craters can be estimated from the total heat available from impact melts and uplifts. The smallest crater, the 100 km diameter Unnamed EP crater, will have 3,000 km³ of impact melt, corresponding to a layer almost 400 m thick on the crater floor, while the largest craters, Gale and Gusev nearly 170 km in diameter may have as much as 20,000 km³ of impact melt, corresponding to a layer almost 900 m thick. The total heat available in these craters, assuming equal amounts from uplift and impact melt, ranges from 2×10^{22} up to 2×10^{23} Joules. In terms of possible volcanic hydrothermal activity, Gusev is the only crater with a near-by large volcanic construct, Apollinaris Patera., and a near-by area of chaos.

Discussion: Of the crater landing sites, Gusev at 14.2° S, 184.8° W, and Boeddicker at 14.8° S, 197.5° W, are only accessible to MER A, while the other craters are accessible to either lander. Only one of the craters in the Elysium Planitia area, can be targeted because landing sites must be located 37° from each other. Because the MER B lander has a larger footprint, it would be logical to send this lander to the Western Hematite location at 0.5° to 0.8° west, and use MER A for one of the five craters in Elysium Planitia.

Some conclusions can be drawn regarding the potential accessibility of hydrothermal deposits from the

central uplifts and crater rim materials based on the probable geometry of the landing site ellipses and the available imagery. With the possible exception of Gale, the floors of the large craters are likely to be covered by fluvial and aeolian deposits, making access to the underlying melt sheets very unlikely. The ejecta blankets of superimposed craters provide a way to distribute samples from the rim and central uplift onto the floor of the craters. A superimposed crater, 18 km in diameter, is present on the rim of the Boeddicker crater adjacent to the EP64A site, and a 16 km diameter crater is located on the floor of the unnamed TM crater, adjacent to the southern, TM16A site. Unfortunately, none of the five candidate craters have the combination of strong evidence for lacustrine activity, and ejecta from a large superimposed crater, although the released MOC imagery is limited or nonexistent. Alternative mechanisms for delivering material to the floors of the craters include ejecta from small craters and fluvial transport. In terms of proximity, landing sites in Boeddicker and Gale may have material from both central peaks and rims that have been transported to the landing sites, but high-resolution MOC images are needed to verify this.

Summarizing, the Gale landing site (EP82A) may have outcrops of lacustrine deposits, and hydrothermal deposits transported from the central uplift and crater wall. The landing sites in Boeddicker (EP64A) and the unnamed TM crater (TM16A) contain ejecta from large superimposed craters, providing the best chance of finding impact melt and crater wall material, but they have no evidence of lacustrine material in the limited available imagery. Landing in a large crater has a great potential for addressing the goals of the MER missions, but acquisition of better imagery is essential.

References: [1] <http://marsoweb.nas.nasa.gov/> [2] Newsom H.E. (1980), *Icarus*, 44, 207. [3] Newsom H.E. et al. (1996) *JGR* 101, 14951. [4] Malin, M.C. and Edgett, K.S. (2000) *Science* 290. [5] Cabrol, N. et al. (1996) *Icarus* 123, 269. [6] Cabrol N. et al., (1999) *Icarus* 139, 235. [7] Cabrol N. and Grin E. (2000) *Icarus*, in press. [8] Newsom H.E. et al. (1999), *JGR* 104, 8717. [9] Edgett K.S. and Malin M.C. (2000) *EOS Transactions AGU*, Suppl. #P52C-09, F774. [10] McCarville, P.J. and L.J. Crossey (1996) *G.S.A. Special Paper*, 302, 347. [11] Thorsos I.E. et al. (2000) *AAS Bulletin*. [12] Gulick V. (1998) *JGR*, 103 19365. [13] Rathbun, J.A. and Squyres, S. W. (2000) *Lunar and Planet. Sci. XXXI*, # 1111. [14] Graup, G. (1998) personal communication. [15] Malin, M.C. and Edgett, K.S. (2000) *Science* 288, 2330.

TES HEMATITE LANDING SITES IN SINUS MERIDIANI FOR 2003 MARS EXPLORATION ROVER.

E. Noreen¹, K. L. Tanaka², and M. G. Chapman², ¹Cal. State Univ. at Los Angeles, 2460 Meadow Valley Terrace, Los Angeles CA 90039 (ericnoreen@yahoo.com), ²USGS, 2255 N. Gemini Dr, Flagstaff, AZ 86001-1600.

Introduction: The Thermal Emission Spectrometer (TES) on the Mars Global Surveyor (MGS) has detected large concentrations of bulk crystalline hematite within the western equatorial region of Mars. The hematite represents a unique and enigmatic spectral signature as one of surface rock distinct from basalt or basaltic andesite. Analysis of the spectral data also suggests that the hematite grains are axis-oriented [1], increasing the mystery.

The largest accumulation of hematite has been found within Sinus Meridiani (SM) centered near 2°S latitude between 0 and 5°W longitude covering an area >500 km² [2]. Within the hematite area in SM there are several locations suitable as landing sites for the 2003 Mars Exploration Rover (MER).

This area has been proposed as a candidate for a landing site before because of its hematite signature [2,3], and our further analysis indicates even more possible origins and implications for its presence. In SM and other areas of hematite, we find direct associations with fluvial/groundwater and volcanic geomorphology that may be indicative of the formative processes. Given the generally bland mineralogic landscape of Mars, the concentrated crystalline hematite locales are the only known areas in which we confidently expect to find rock and mineral types dissimilar to that of the Viking and Pathfinder landing sites [3].

Areal Extent of Hematite: Although SM has the largest signature of hematite, numerous other occurrences have been found in the equatorial region, including: Aram Chaos [4], Ares Valles [5], Margaritifer Chaos, in the interior layered deposits within central Valles Marineris (VM) [5] and Eos Chasma [5]. The hematite is restricted to a ~1200 km band trending N80°E from VM to SM. The confinement of the hematite to one relatively linear region rather than dispersed planetwide suggests that all of the bulk crystalline hematite may have formed by the same process.

Proposed Landing Sites: We favor four landing sites within SM: TM22B, TM23B, TM10A, TM11A [6, Table 1]. These sites all are below the -1.3 km Mars Orbital Laser Altimeter (MOLA) geoid required for safe atmospheric entry. MOLA data also show that they are all on gentle slopes of less than one degree. MGS Mars Orbital Camera (MOC) context and high-resolution images (see images listed in Table 1) show a lack of fresh craters within SM. TES data shows that the ellipses of the sites are relatively hazard free seen in the low total rock coverage (>11%.) TES also data

shows that the SM sites are relatively free of dust, inferred from their relatively high thermal inertia (7-8 x 10⁻³ cal cm⁻² s^{-0.5} K⁻¹.)

...With engineering requirements [6] for safety met, we favor a landing site with high concentrations of hematite. TM23B, and to a lesser extent TM10A, are therefore favored due to their having significant concentrations of hematite evident in the TES data. TM23B more than meets all of the engineering requirements and has a very high concentration of hematite, low total rock coverage (6-9%), and a very gentle slope over the ellipse. The only drawback to TM23B is the elevation (-1.4 km) being close to the required -1.3 km required for safe atmospheric entry. TM10A, while being well below the required elevation, has a higher rock coverage and slightly lower hematite concentration, which may hinder the pursuit of the science objectives. Based on the above, TM23B is the preferred landing site for SM.

Regional Geologic Context of Hematite: The hematite signatures have been found on several different geologic units. In SM the hematite is confined to unit *Npl2*, a subdued cratered unit thought to be thin interbedded lava flows or eolian deposits partly burying weathered cratered terrain [7]. At a larger scale the subdued cratered unit was remapped as unit *sm* [8], a smooth, layered friable surface variously interpreted as eolian/volcanic deposits [7], paleopolar deposits, and wind eroded sedimentary deposits [8].

The other, smaller occurrences of hematite appear on units *Hch*, *Hcht*, *Hvl*, and *Avf* [7]. In central VM the hematite is confined to a single unit, *Airs*, interpreted to be eolian deposits or airfall tuff [9]. High-resolution MOC images show that the hematite in central VM occurs within a unit similar in appearance to the hematite area in SM (SM- M0400568, M0300764; VM- M0201705.)

MOLA data revealed that the occurrences of hematite exist in a variety of topographic terrains. Within unit *sm* it occurs on a gentle slope downtrending to the NW; in the eastern area of *sm* a high concentration is on a local topographic high. In Aram Chaos it occurs on the floor of the eroded crater in between small mesas. In VM and the remaining areas it occurs on relatively gentle slopes and troughs.

In many areas the hematite is associated with volcanic features. TES data shows an intimate relationship between the hematite and possible basalts seen in basaltic spectral compositions found within or surrounding the hematite areas [10]. Within central VM

most of the hematite signatures are found adjacent to unit *Ahd*, a unit interpreted to be young mafic volcanic material [9]. One occurrence in central VM is ~2 km upslope from a feature interpreted to be a caldera [9]. Within SM, unit *sm* appears consistent with ignimbrite deposits, based on localized layering and mantling of topography, and numerous mounds that can be interpreted as fumarolic [3].

All of the hematite areas show some evidence of near-surface water activity in nearby fluvial, ground-water, or lacustrine features. South of unit *sm* there are extensive ancient channels within *hc*, a heavily cratered unit, that terminate at the contact of the units [8,3].

ment of volcanic materials, based on the volcanic associations and geomorphology of SM and VM.

Potential Instrument Utilization at SM Sites:

Each instrument on the rover will be brought to bear on the question of the hematite formation in the western equatorial region of Mars as well as the general geology of the landing site. They will be utilized to this end in the following ways: (1) The PanCam will take panoramic images to focus the search for hematite-bearing rocks and visually describe their geologic context. (2) The Rock Abrasion Tool will expose fresh surfaces on rocks for study. (3) The Miniature Thermal Emission Spectrometer will gather mineralogic

Table 1: Selected hematite landing sites for 2003 Mars Exploration Rovers

Site	Lat. (°)	Long. (°)	Elev. (km)	Geologic units [7,8]	MOC high-resolution images
TM22B	-3.2	7.1	-1.7	<i>Npl2, sm</i>	SP240604, M0300371
TM23B	-3.4	3.1	-1.4	<i>Npl2, sm</i>	M0403468, M0200446, M0002022, M0002021, M0204225, M0401900
TM10A	-2.2	6.6	-1.7	<i>Npl2, sm</i>	M0001660, M0301632, M0201539
TM11A	-3.4	6.9	-1.6	<i>Npl2, sm</i>	SP240604, M0300371

Directly northeast of unit *sm*, in MOC image M0401289, there is a 1-km-diameter feature that could be interpreted as thermokarstic or lacustrine. Aram Chaos contains chaotic terrain, possibly caused by near-surface water activity. VM is the source area for the massive outflow channels in the region.

Possible Formation Processes: Using the spectral, geologic/geomorphic and topographic relationships, we are able to develop some constraints on the possible formation processes. Spectral evidence indicates that the grains are large (≥ 10 microns) [2] and axis oriented [1], limiting the formational processes to those that can produce the preferred growth and size. Although all hematite sites have possible lacustrine features nearby, the topography of unit *sm* indicates that the hematite, if geologically recent, did not form in standing water. The topography of SM also shows that a metamorphic origin of the hematite, i.e. schistose hematite, is unlikely, as it does not reflect the necessary range of elevation required to produce an overburden pressure that would produce re-crystallization of nano-phase hematite and orientation of the resulting grains.

Using the above constraints to exclude, at least tentatively, several formation processes, those that remain become more probable. The remaining processes that fit all available data are: hydrothermal alteration or replacement of a parent rock with an existing orientation of minerals, thermal oxidation of magnetite-rich lavas [4], and primary mineralization within the cooling unit of an ignimbrite [3,5]. We favor a volcanogenic formation, either mineralization within the welded zone of an ignimbrite or hydrothermal enrich-

information at an outcrop scale of the landing area facilitating the search for hematite host rocks at a finer scale than MGS-TES. (4) The Mössbauer Spectrometer will gather information on the oxidation states of iron-bearing minerals, which will determine the extent of alteration, if any, in the hematite host rocks. (5) The Alpha Proton X-Ray Spectrometer will determine the composition of rocks and soils in the landing area and will be able to classify the hematite host rock type. (6) The Microscopic Imager will obtain extremely high resolution images of rocks and soils which will give clues to the formation of the hematite and may determine the nature of the alignment of the hematite grains.

References: [1] Lane, M. D. et. al., (2000) *LPSC XXXI*. [2] Christensen, P.R. et. al. (2000) *JGR, 105*, 9623-9642. [3] Chapman M. G. (1999) 2nd Mars Surveyor 2001 Landing Site Workshop. [4] Christensen, P.R. et. al. *LPSC XXXI*. [5] Noreen, E. et. al. (2000) Mars Tharsis Workshop; [6] Golombek, M. and Parker, T. (2000) *MER Engineering Constraints and Potential Landing Sites Memo*. [7] Scott, D. H., and Tanaka, K.L. (1986) *USGS Map I-1802-A*. [8] Edgett, K.S., and Parker, T.J., (1997) *GRL 24*, 2897-2900. [9] Lucchitta, B.K. (1999) *USGS Map I-2568*; [10] Banfield, J. L. (10/2000) TES Team Member. Personal Comm.

GANGES CHASMA LANDING SITE: ACCESS TO LAYERED MESA MATERIAL, WALL ROCK, AND SAND SHEET. James W. Rice, Jr., Arizona State University, Tempe, AZ 85287, rice@east.la.asu.edu

Introduction

The floor of Ganges Chasma offers an ideal landing site for the MER A/B rovers (Figure 1). This site is exquisite both in terms of engineering constraints and science objectives.

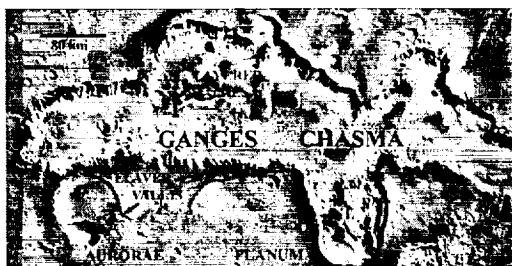


Figure 1. Ganges Chasma Region.

The floor of Ganges Chasma is mantled with an extensive low relief sand sheet (Figure 2). This maximizes landing site safety issues and allows us entrance into Valles Marineris. Other floor regions of Valles Marineris (e.g., Candor, Capri, Melas) appear very rough and hazardous in MOC imagery.

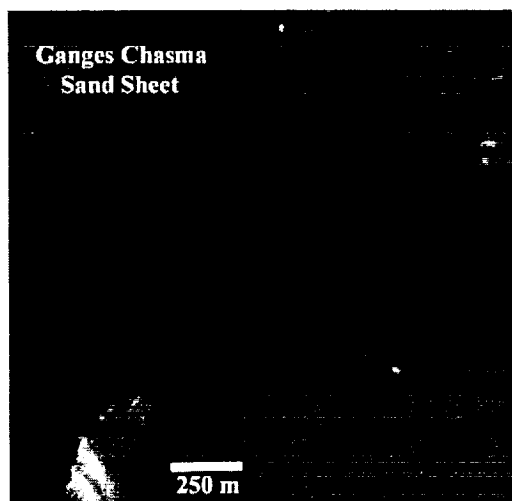


Figure 2. Ganges Chasma Floor (MOC image AB-1-028/02, 4.98 m/p).

Recent work by Malin and Edgett [1] suggest that the layered mesa material and wall rock of Ganges Chasma are composed of lacustrine sedimentary rock layers. This is where to go in order to investigate the exobiologic and geologic history of early Mars (Figure 3).

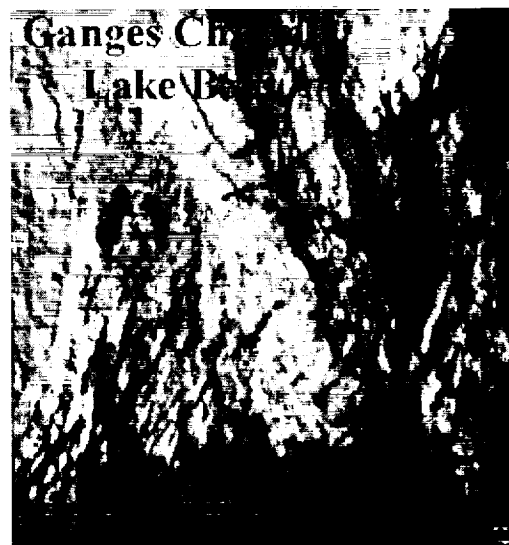


Figure 3. Lakebeds Exposed in Ganges Chasma (MOC image AB102802, 5.9 m/p).

Science Objectives:

- *What is the nature and composition of the layered mesa material (lacustrine, aeolian, volcanic, other)?
- *What is the nature and composition of the canyon wall material?
- *What is the nature and source of the sand?
- *What is the composition, grain size, shape, sorting, and stratigraphy of the sand?
- *Is the sand monomineralic, lithic fragments, ice or salt cemented dust?

The philosophy for selecting this site is that it would allow analysis of Chasma floor material which should be composed of wall material and the layered mesa material, there is also abundant evidence of channels emptying into the canyon thereby providing a source for aqueous sediments.

Geologic Setting:

Ganges Chasma is located south of Shalbatana Vallis and north of Capri Chasma. Ganges Chasma is the type area for the Layered Material (interior layered deposits) located on the floors of the Valles Marineris. The walls are mapped as Noachian/Hesperian material with Hesperian layered material 100's m thick located on the floor of Ganges: this enigmatic material

has been interpreted to be lacustrine, volcanic, aeolian deposits or remnant wall material. Amazonian alluvial deposits, landslides, sand sheets and dune fields are also found on the floor.

Numerous channels also empty into Ganges Chasma, the largest is Elaver Vallis. Elaver Vallis flows 160 km across the upper surface of Aurorae Planum before emptying onto the floor of Ganges Chasma, 4 - 5 km below, forming the largest waterfall in the Solar System. The source of Elaver Vallis is a 77 km diameter crater. The source crater is breached by an outlet channel 5 km wide, located on its southeastern flank. The crater rim height is calculated (shadow measurement) to be 450m above the crater floor. Using this as the upper limit for the water level in the crater yields a volume of water nearing 2,100 km³ that would have drained into Ganges Chasma. This crater also contains what appears to be a sinkhole (40 km diam) located on its southern floor. The source regions of Shalbatana Vallis also appear to display a karst topography. This "karst topography" begs the question: what is the composition of the underlying layered plateau rock?

Engineering Concerns:

Sand sheets provide an extremely safe landing site and have very low relief. Sand sheets develop in conditions which are unfavorable for dune formation. These may include a high water table, periodic flooding, surface cementation, and coarse grained sands [2]. The most extensive sand sheets on Earth are located in the eastern Sahara. These sheets have a relief of less than 1m over wide areas and total thick-

ness ranges from a few cm to 10 m. The surfaces of sand sheets are composed of granule to pebbly lag deposits.

The safety concerns regarding slopes, rocks, and dust would be alleviated by the sand sheet. Furthermore, this vast sand sheet would allow the Rover to travel 'maximum traverse distances' and allow it to reach the layered mesa material and wall rock brought down by mass wasting processes. Rover navigability on the sand sheet would be very easy compared to the tedious rock avoidance maneuvers that Sojourner had to execute. Dust should not be a problem: Thermal inertia is 7.7 to 8.9 cgs units. This site satisfies all engineering constraints.

Ganges Chasma Landing Site Characteristics:

Site ID: VM42A

Location: 7.7S, 50.7

Elevation: -4.5

Geologic unit: Avf

Rock Abundance: 8 to 10 % (Floor and Mesa)

Thermal Inertia: Floor: 7.7 to 8.8

Mesa: 8.8 to 8.9

Fine Component: Floor: 7.0 to 8.3

Mesa: 7.2 to 7.8

Albedo: Floor: 0.1530 to 0.1740

Mesa: 0.1650 to 0.1700

Slopes: Floor: 0° to 3°

Layered Mesa Material: 0° to 5°

Layered Mesa Material: 100 X 45 km

Hazards: Minimal on the Sand Sheet

Exobiologic Potential: Region contains lacustrine sediments, thus an excellent locale.

References:

- [1] Malin, M.C. and K.S. Edgett, 2000, *Science*, 290, 1927-1937. [2] Lancaster, N., 1995, *Geomorphology of desert dunes*, 290p..

A SPECTRALLY-BASED GLOBAL DUST COVER INDEX FOR MARS FROM THERMAL EMISSION SPECTROMETER DATA. S. W. Ruff¹ and P. R. Christensen¹, ¹Department of Geological Sciences, Arizona State University, Tempe, AZ, 85287-1404, ruff@tes.asu.edu

Introduction: One of the greatest problems with any form of spectral measurement on the surface of Mars is dust that obscures the surface of rocks. This was clearly demonstrated with the Pathfinder mission and its visible/near-infrared and alpha proton x-ray measurements. In both cases, interpretations of the data measured from rocks at the landing site were confounded by the presence of the fine dust coating many of the rock surfaces. The 2003 Mars Exploration Rovers will carry a set of spectrometers that also will be affected by the presence of dust. An assessment of surface dust cover is thus an important consideration for landing site selection.

Currently, thermal inertia and albedo data from the Viking IRTM and MGS TES form the basis for the assessment of surface dust. However, thermal inertia measurements are insensitive to a dust layer less than a few centimeters thick and albedo is not a definitive indicator of dust occurrence. An alternative means of sensing the presence of dust is to exploit the spectral particle-size effects produced by fine particles.

The effect on thermal infrared spectra of decreasing particle size is well known and reasonably well understood. A reduction in spectral contrast accompanies the decrease in particle size down to $\sim 60 \mu\text{m}$. Below this threshold where the diameter of particles approaches the wavelength of thermal-IR light, a phenomenon known as volume scattering begins [1]. The apparent effect is the appearance of spectral features unique to fine-particulate materials. Recognition of these features in TES spectra and mapping of their geographic distribution across the planet forms the basis for a global map of surface dust.

Evidence of Particle-size Effects: The evidence of particle-size effects in TES spectra is displayed most clearly by comparing spectra from representative areas on the planet that are recognized as dust-covered and dust-free based on thermal inertia and albedo considerations. An example of a dust-covered region is central Arabia Terra while central Syrtis Major likely is free of any significant dust accumulation. Figure 1 shows emissivity spectra from these two regions that have not been atmospherically corrected. Included in this figure are laboratory spectra intended to demonstrate the spectral appearance typical of silicate materials in coarse and fine particulate form. The TES spectra are dominated by atmospheric absorption features, especially in the 1300 to $\sim 560 \text{ cm}^{-1}$ range, but outside of this range surface spectral character is evident. Be-

low 560 cm^{-1} the Syrtis spectrum has lower emissivity than the Arabia spectrum, closely paralleling the behavior of the coarse- and fine-particulate basalt spectra. Above 1300 cm^{-1} the emissivity behavior is reversed, with Syrtis showing higher emissivity than Arabia, consistent with the trend of the laboratory spectra. A thorough analysis described elsewhere [2, 3] demonstrates that an average emissivity value from 1350 to 1400 cm^{-1} is a robust indicator for the presence of fine-particulate silicates in spite of the known atmospheric absorptions that effect this spectral region. This index can be mapped globally to identify surfaces on Mars that are dominated by fine particulates, i.e., dust (Figure 2).

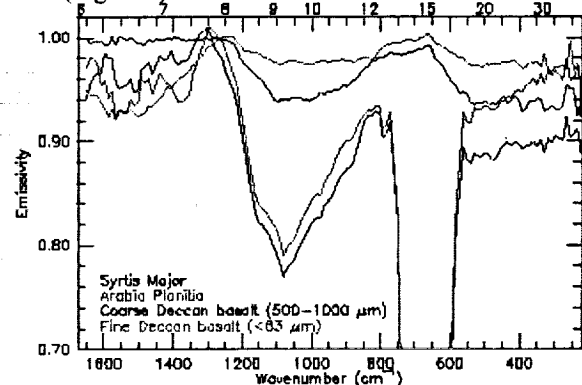


Figure 1. Evidence of particle size effects in atmospherically-uncorrected TES spectra of bright and dark regions.

Discussion: The index produces a spatially coherent map that clearly is related to albedo. Unlike albedo (and thermal inertia), this spectral index is a direct indicator of the presence of dust layers a few 10s of microns or more in thickness. Orange, red, and white areas on the map likely are completely dust mantled, while blue and minor purple areas likely are dust-free. Yellow, green, and cyan likely represent surfaces that are partially dust covered. All three previous lander sites are within the intermediate colors. Sites chosen within the blue regions likely will have the most dust-free surfaces on the planet.

References: [1] Salisbury, J.W. and A. Wald, (1992) *Icarus*, **96**, 121-128. [2] Ruff, S.W. and P.R. Christensen (1999) *The Fifth International Conference on Mars.*, Abs. #6230, LPI Houston (CD-ROM). [3] Ruff, S.W. and P.R. Christensen, (2001), *J. Geophys. Res.*, submitted.

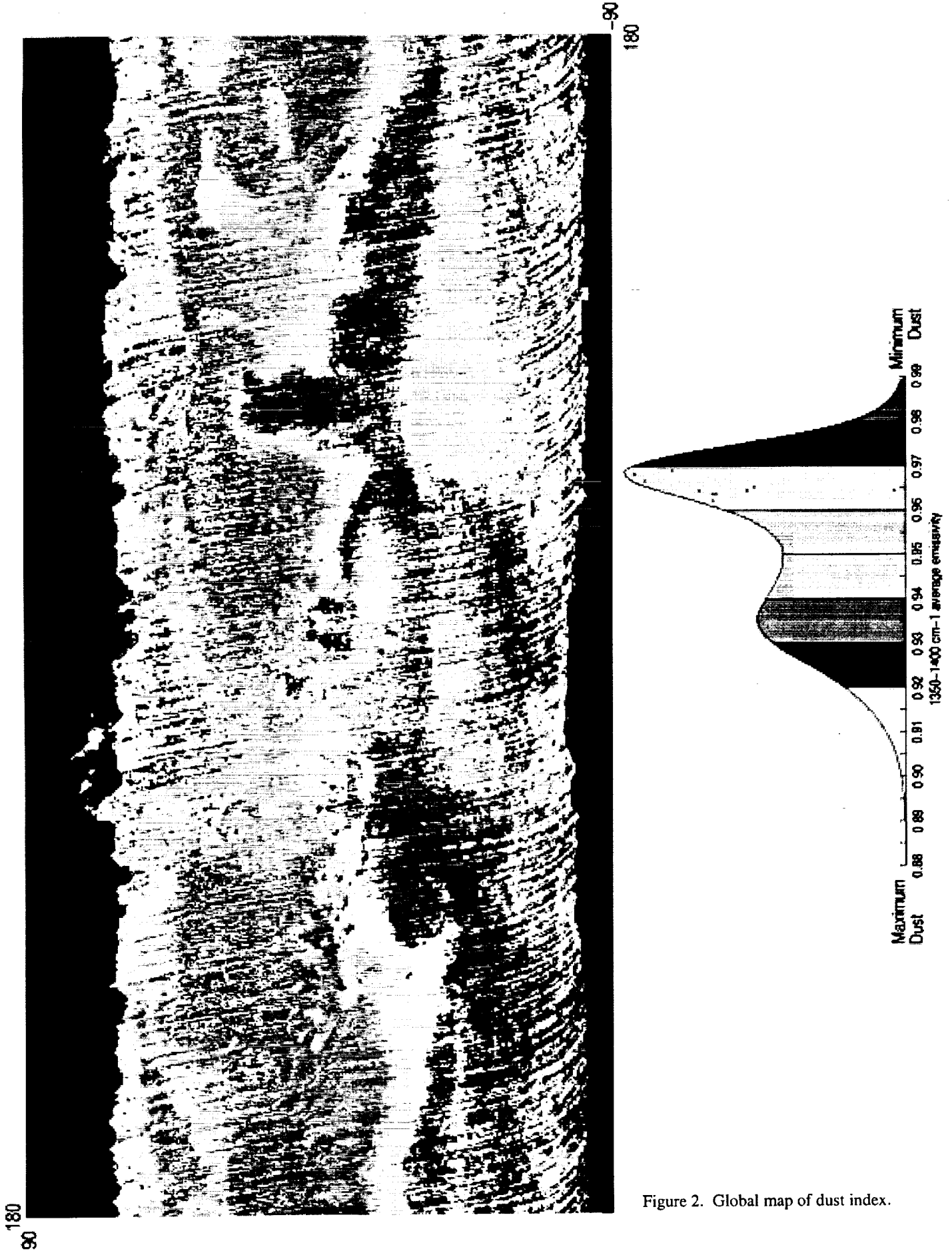


Figure 2. Global map of dust index.

The Athena Science Payload for the 2003 Mars Exploration Rovers. S.W. Squyres¹, and the Athena Science Team (R.E. Arvidson, J.F. Bell III, M. Carr, P. Christensen, D. Des Marais, T. Economou, S. Gorevan, L. Haskin, K. Herkenhoff, G. Klingelhöfer, A. Knoll, J.M. Knudsen, A.L. Lane, V. Linkin, M. Malin, H. McSween, R. Morris, R. Rieder, M. Sims, L. Soderblom, C. d'Uston, H. Wänke, T. Wdowiak) ¹Cornell University, Ithaca NY 14853.

Introduction: The Athena Mars rover payload is a suite of scientific instruments and tools for geologic exploration of the martian surface. It is designed to: (1) Provide color stereo imaging of martian surface environments, and remotely-sensed point discrimination of mineralogical composition. (2) Determine the elemental and mineralogical composition of martian surface materials, including soils, rock surfaces, and rock interiors. (3) Determine the fine-scale textural properties of these materials. Two identical copies of the Athena payload will be flown in 2003 on the two Mars Exploration Rovers. The payload is at a high state of maturity, and first copies of several of the instruments have already been built and tested for flight.

Imaging and Remote Mineralogy: The topography, morphology, and mineralogy of the scene around the rover will be revealed by *Pancam* and *Mini-TES*, which are an imager and an IR spectrometer, respectively, integrated with a single mast. *Pancam* views the surface around the rover in stereo and color. The detectors are 1024×1024 CCDs, and the electronics provide 12-bit analog-to-digital conversion. Filters provide 14 color spectral bandpasses over the spectral region from 0.4 to 1.1 μm . Narrow-angle optics yield an angular resolution of 0.28 mrad/pixel. Image compression is performed using a high-performance wavelet compression algorithm.

The Mini-Thermal Emission Spectrometer (*Mini-TES*) is a point spectrometer operating in the thermal IR. It produces high spectral resolution (10 cm^{-1}) image cubes with a wavelength range of 5-29 μm , a nominal signal/noise ratio of 450:1, and angular resolution modes of 20 and 8 mrad. The wavelength region over which it operates samples the diagnostic fundamental absorption features of rock-forming minerals, and also provides some capability to see through dust coatings that could tend to obscure spectral features. The mineralogical information that *Mini-TES* provides will be used to select from a distance the rocks and soils that will be investigated in more detail. *Mini-TES* is derived from the MGS TES instrument, but is significantly smaller and simpler. The instrument uses an 6.3-cm Cassegrain telescope, a Michelson interferometer, and uncooled pyroelectric detectors. Along with its mineralogical capabilities, *Mini-TES* can provide information on the thermophysical properties of rocks and soils. Viewing upward, it can also provide tem-

perature profiles through the martian atmospheric boundary layer.

Elemental and Mineralogical Composition: Once promising samples have been identified from a distance using *Pancam* and *Mini-TES*, they will be studied in more detail using two compositional sensors that can be placed directly against them by an instrument arm. These are an *Alpha Particle-X-Ray Spectrometer (APXS)* and a *Mössbauer Spectrometer*. The APXS is derived from the instrument that flew on Mars Pathfinder. Radioactive alpha sources and two detection modes (alpha and x-ray) provide elemental abundances of rocks and soils to complement and constrain mineralogical data. The Athena APXS has a revised mechanical design that will cut down significantly on backscattering of alpha particles from martian atmospheric carbon. It also includes a target of known elemental composition that will be used for calibration purposes. The Athena Mössbauer Spectrometer is a diagnostic instrument for the mineralogy and oxidation state of Fe-bearing phases, which are particularly important on Mars. The instrument measures the resonant absorption of gamma rays produced by a ^{57}Co source to determine splitting of nuclear energy levels in Fe atoms that is related to the electronic environment surrounding them. The Mössbauer Spectrometer (as well as the other *in-situ* instruments) will be able to view a small permanent magnet array that will attract magnetic particles that settle from the martian atmosphere.

Fine-Scale Texture: The instrument arm also carries a *Microscopic Imager* that will obtain high-resolution images of the same materials for which compositional data will be obtained. Its spatial resolution is 30 $\mu\text{m}/\text{pixel}$ over a 6-mm depth of field. It uses the same CCD detectors and electronics as *Pancam*.

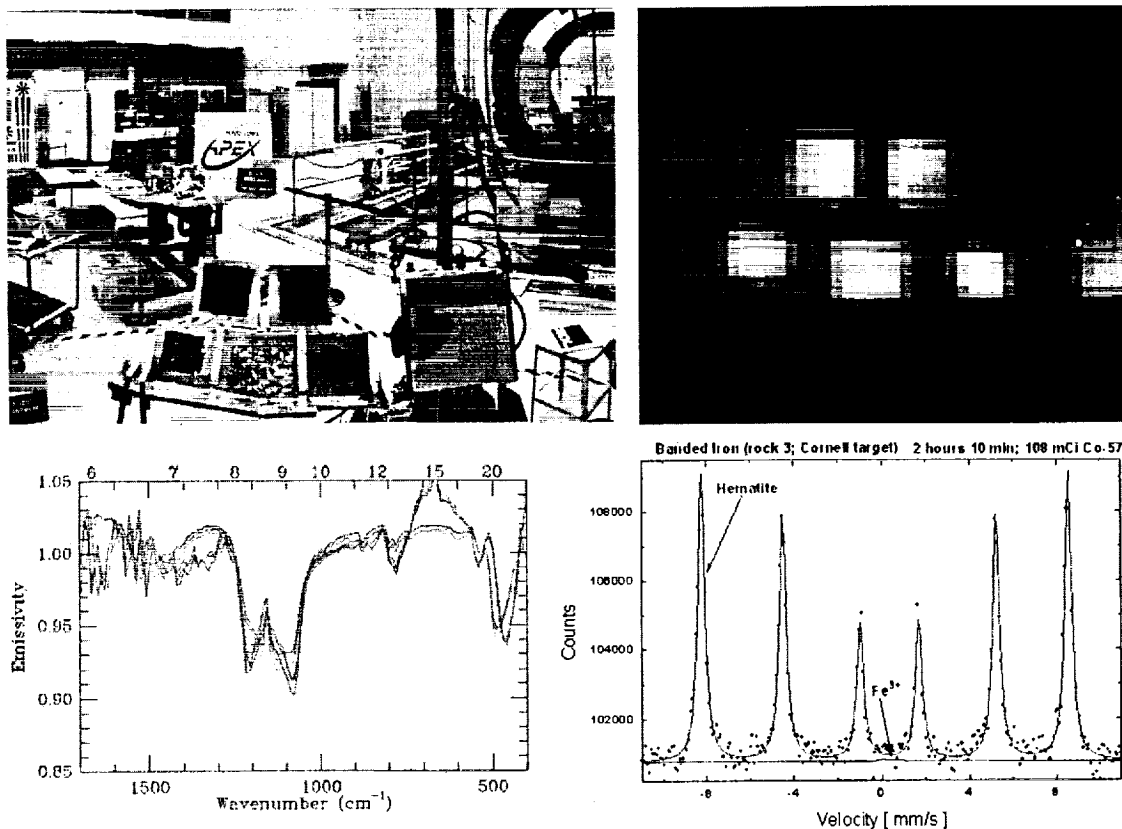
Sample Preparation: Some martian rock surfaces are likely to be dust-covered, coated, weathered, or otherwise unrepresentative of the rock's interior. For this reason the Athena payload includes a Rock Abrasion Tool (RAT). The RAT is also carried on the rover's instrument arm. When placed against a rock, it uses two mechanical grinding wheels to remove 5 mm of material over a circular area 45 mm in diameter. The resultant exposed region is large enough to be investigated in detail using all of the instruments on the payload.

Payload Status: The Athena payload was originally selected for flight in November of 1997, and has been in development since that time. Flight-qualified versions of Pancam, Mini-TES, APXS, and the Mössbauer Spectrometer have been built, calibrated, and tested for survival and operation in key flight environments. The existing Mini-TES and Mössbauer Spectrometer will be flown on one of the MER rovers, and identical copies of these instruments are being built for the other rover. The MER Pancams and Microscopic Imager will use a camera body design similar to that of the existing Pancams, but with an improved CCD; the other cameras on the rover will also use this same design. The RAT is a new development, but its design

has some heritage from a rock coring drill also developed as part of the Athena payload.

Payload Synergy: The Athena payload is specifically designed to be used as an integrated instrument suite. As the rover explores, the in-situ instruments perform detailed analyses of promising samples that are identified from a distance with Pancam and Mini-TES. Selected rocks and soils can then be examined with the three *in-situ* instruments. When desired, the RAT can be used to expose fresh subsurface rock that can be examined by all the instruments. Recent tests have demonstrated the capabilities of the Athena flight instruments. Figure 1 shows some example data.

Figure 1: Data from recent tests of the Athena flight instruments. Clockwise from top left: (1) Part of a Pancam panorama, showing a rock target in the foreground. (2) A Mini-TES image of the rock target (with a person sitting to the left of it); colors denote mineralogy. (3) A Mossbauer spectrum of one of the targets, showing the signature of hematite. (4) A Mini-TES spectrum of the same target, showing signatures of hematite and quartz.



SCIENTIFIC RATIONALE FOR MARS EXPLORATION ROVERS A AND B LANDING SITES: OUR BIASED VIEW. K. L. Tanaka¹, L.S. Crumpler², M. S. Gilmore³, E. Noreen⁴, Trent M. Hare¹, and J.A. Skinner¹.
¹U.S. Geological Survey, 2255 N. Gemini Dr., Flagstaff AZ 86001; ktanaka@flagmail.wr.usgs.gov, ²New Mexico Museum of Natural History and Science; ³Wesleyan University; ⁴California State University at Los Angeles.

Introduction. The dual Mars Exploration Rovers (MER), A and B, planned for launch in 2003, provide the planetary science community with an exciting opportunity to investigate two equatorial sites of scientific interest. Selection of key sites that will help decipher the geologic history of Mars and address the question of life on this planet is desired. Here we suggest that down-selection of sites for the MER's might lead to similar sites selected for the now-scuttled 2001 lander mission: Noachian highland material (such as Libya Montes) and the Sinus Meridiani hematite deposit.

Down-Selection Rationale: Fluvial/lacustrine Noachian rocks. No doubt a variety of down-selection approaches will be offered and debated by the planetary science community at the workshop and in other venues. This debate involves potential scientific advances, rover and payload capabilities, engineering constraints, and mission operations. We describe here our geologically biased view for down-selection, with some attention given to the other areas of concern.

The next landing sites for Mars exploration obviously should be chosen to afford investigations of completely different types of landscapes than those of the bland northern plains as seen by the Viking and Pathfinder landers. Broad expanses of Hesperian ridged plains material presumably made up of widespread sheet lavas should be reserved for future landers that may have geochronologic capabilities to pin down the global crater flux [1]. Because of the prevailing, current interest in understanding Noachian geology, climate, and possible biology, sites that investigate the highlands should have the highest priority for the MER 2003. In particular, sites should show obvious evidence for the activity of water.

What constitutes a Noachian outcrop? We have performed a preliminary re-evaluation of the crater-density boundary between Noachian and Hesperian rocks within the equatorial region using the crater database of Barlow [2], which is complete for crater diameters >5 km. Ridged plains material, defining the Early Hesperian [3], in the equatorial region ($\pm 15^\circ$ latitude) has an $N(5)$ density of 202 ± 5 (craters/ 10^6 km²) and $N(16) = 32 \pm 2$. These values are slightly higher than the boundary defined by Tanaka [3] of $N(5) = 200$ and $N(16) = 25$. The Late Noachian subdued cratered unit (unit Npl₂) has $N(5) = 383 \pm 11$ and $N(16) = 115 \pm 6$. Somewhere between these counts should be the Noachian boundary [3]. The unit Hr crater densities are very similar to counts of fresh highland craters by Craddock and Maxwell [4].

Thus the Noachian/Hesperian boundary seems to represent both the termination of ubiquitous crater degradation and the onset of widespread ridge plains material emplacement. This boundary may not be precise in time, for crater degradation may have ceased (or slowed) over time, perhaps as a function of elevation [4]. Also, outcrops of Noachian ridged plains material have been identified [5-6]. Further analysis of crater densities as a function of crater preservation and specific rock outcrops will likely result in a more clearly defined Noachian/Hesperian boundary.

Evidence for the geologic activity of water at a potential MER site may come from imaging (Viking and MOC), topographic (MOLA and MOC and Viking stereo), and spectral mineralogic and grain-size data (Viking thermal inertia and TES). Geomorphic indicators are notoriously ambiguous, so these must be interpreted with caution. For example, although valleys may have a fluvial appearance, little may be understood about their discharge history. Topographic catchments may be filled with layered material and steep-sided fans may occur at the mouths of channels, but their appearance does not prove that they resulted from standing bodies of water, even though this may be the most common explanation in a terrestrial setting. When compared to Earth, Mars has exotic environmental conditions, and therefore exotic geomorphological processes may predominate. Still, maps of valleys and basins [7-8] from image and MOLA data provide useful starting points to search for Noachian water channels and their deposits. Finally, the only mineralogic signature from Mars that seems to indicate abundant water in certain locales is hematite [9].

To make a case for a landing site, digital datasets, including detailed geologic and thematic maps [e.g., 10-11], would profit from synthesis into a GIS database [12]. This approach permits statistical spatial analysis of the datasets in relation to the landing-site ellipse.

Another essential consideration in down-selection is that some of the potential landing site regions [13] will likely fail some of the engineering safety criteria as more data and analysis techniques become available [e.g., 14]. This may mean that some of the sites with little room for shifting (e.g., Valles Marineris) may eventually have to be removed from consideration. It will thus be wise to start with a broad selection of sites at this stage that meet the science objectives of Noachian rocks and evidence for surface water activity.

Suggested sites. Having two landers allows for the selection of diverse sites. For prudence sake, one site should be relatively safe, with more easily achieved main scientific goals. The other may be more adventurous within acceptable terms of risk, with the potential for more scientific return.

Given the down-selection rationale described here, we suggest that the "safe" site should be the hematite-rich material associated with a mappable geologic unit in Sinus Meridiani [9, 15]. Previously proposed for the 2001 Lander [16], this unit has four landing-site ellipses that fit the current engineering criteria for the 2003 MER landers as well as potentially fulfilling all science objectives [17]. Further work can be performed to constrain this unit's relative age and possible origins with Mars Global Surveyor data.

The second, more adventurous site should have, if possible, geologic outcrops in distant view that potentially can be associated with local outcrops and loose rocks within reach of the lander. The ring of massifs along the southern margin of Isidis basin exposes some of the most ancient crust of Mars [3]. However, because of the much larger ellipses for the MER's compared to that of the 2001 lander, landing cannot be made in the rocks of the intermontane plains and piedmont. Instead, the adjacent Isidis Planitia would have to be selected, assuming that it could be demonstrated that Isidis rim rocks are at the surface of these areas. This setting would potentially provide an opportunity to examine a grab-bag sampling of rocks with the rover and possibly correlate

them with outcrops seen in the surrounding massifs.

Also, potential Noachian sites occur in Xanthe Terra, as well as sites that include a contact between Noachian units [18]. These require further analysis to define their suitability for safe landings and meeting key science objectives. Acquisition of more MOC images, especially stereo pairs, would permit more detailed geologic mapping and terrain analysis of these locations.

References. [1] Doran P.T. et al. (2000) *EOS* 81, 533. [2] Barlow N.G. (1988) *Icarus* 75, 285-305. [3] Tanaka K.L. (1986) *PLPSC 17, JGR 91 suppl.*, E139-E158. [4] Craddock R.A. and Maxwell T.A. (1993) *JGR* 98, 3453-3468. [5] Scott D.H. et al. (1986-87) *USGS Maps I-1802A-C* [6] Dohm J.M. et al. (in press) *USGS Map I-2650*. [7] Carr M.H. (1995) *JGR* 100, 7479-7507. [8] Scott D.H. et al. (1995) *USGS Map I-2461*. [9] Christensen P.R. (2000) *JGR* 105, 9623-9642. [10] Crumpler L.S. et al. (2000) *LPSC XXXI*, #2057. [11] Crumpler L.S. et al. (2001) this volume. [12] Hare T.M. et al. (this volume). [13] Golombek, M. and Parker, T. (2000) *MER Engineering Constraints and Potential Landing Sites Memo*. [14] Grant J. and M. Golombek (2000) *Second Announcement, First Landing Site Workshop, 2003 MER*. [15] Edgett K.S. and Parker T.J. (1997) *GRL* 24, 2897-2900. [16] Chapman M. G. (1999) 2nd Mars Surveyor 2001 Landing Site Workshop. [17] Noreen E. (2001) this volume. [18] Gilmore M.S. et al. (2001) this volume.

LANDER DETECTION AND IDENTIFICATION OF HYDROTHERMAL DEPOSITS. M. L. Urquhart¹ and V. Gulick², ¹NRC/NASA Ames, MS 239-20, Moffett Field, CA 94035 (murquhart@mail.arc.nasa.gov), ²SETI Inst./NASA Ames, MS 239-20, Moffett Field, CA 94035 (vgulick@mail.arc.nasa.gov).

Introduction: The role of hydrothermal activity on Mars in altering crustal materials and sequestering volatiles is a critical component in understanding the interactions between the atmosphere, surface, and hydrosphere of Mars. In turn, these interactions are key elements in understanding the martian climate history, surface geology, and potential for past life on Mars. Identification of hydrothermal deposits at the surface of Mars, especially within a region in which the geologic context is clear (e.g. a volcanic region such as a Apollinaris Patera), would provide valuable information about the geologic history of the planet, and would be indicative of a potential site for the search for evidence of life on Mars.

Specific hydrothermal mineral assemblages will be dependent on the environmental conditions under which the country rock was altered. Mini-TES, however, has the capacity to identify a wide range of alteration products, and Mössbauer Spectrometer will be able to identify both altered and unaltered iron-bearing minerals, and will yield information on the environment in which iron oxidation has occurred. The instruments on the 2003 rover will have the capability to identify hydrothermal deposits present at the surface of the landing site, potentially yielding information about the nature of the environment in which hydrothermal alteration occurred.

Environments of interest: Sites where hydrothermally produced minerals may be present at the surface range from volcanic regions and impacts craters to sites of

ground water outflow channels and smaller water-carved features such as gulleys. In some terrestrial environments where the bulk of hydrothermal activity occurs in the subsurface, the surface expression of alteration products such as carbonates may be minimal in comparison with the overall extent of the region hydrothermal activity. Such is the case of Yellowstone's Mammoth Hot Springs [1]. The release of ground water may also carry alteration products onto the surface, or exposed rock may contain veins of altered minerals. Hydrothermal deposits may be located at sites where their presence was not detected from orbit.

Identification of hydrothermal vs. other aqueous alteration products: Mini-TES will be able to identify a wide variety of alteration products including carbonates, salts such as sulfates and phosphates, silicates, oxides, and hydroxides. Some minerals resulting from water-rock interactions, such as carbonates, may be produced by both hydrothermal activity and surface aqueous environments such as paleolakes. However, other minerals such as large-grain hematite and quartz [2] are indicative of hydrothermal activity, and can be identified by Mini-TES. The Microscopic Imager may provide contextual information about the minerals within individual rocks, such as the presence of mineral veins indicating water circulation. The Mössbauer Spectrometer can distinguish between individual iron minerals that form in different environments. The data gathered by these instruments will not only have the potential to distinguish between mineral assemblages of

a hydrothermal or surface aqueous origin, but may also give valuable information about the environments under which hydrothermal alteration occurred.

Future Work: We are beginning an investigation of the mineralogies which could be produced by hydrothermal activity on Mars in a variety of environments including volcanic and impact produced hydrothermal systems. Our investigation will include both a comparison of potential Mars environments with terrestrial analogs and a theoretical approach. We will build upon the work of Griffith and Shock [2] who used an aqueous geochemical equilibrium model, EQ3/6, [3] to determine alteration products from a parent rock such as basalt for a range of environmental conditions, each representing a single alteration event. We will use these altered mineralogy as starting points for the same geochemical model, with a new set of environmental conditions. This will serve to simulate changes in the environment within a hydrothermal system. We will examine the affect of different environments and multiple changes in the environment on resulting mineralogies in order to predict mineral assemblages which may be present on the martian surface as well as in the subsurface.

Application: Examining the effect of changing environmental conditions on types of Mars hydrothermal deposits will aid in the search for mineral evidence of long-term or vigorous hydrothermal activity, and potentially the search for evidence of life on Mars. The identification of large-grained hematite by the Thermal Emission Spectrometer (TES) [4], a common terrestrial hydrothermal alteration product shows that hydrothermal deposits are present on Mars.

Hydrothermal systems provide environments in which life may have existed under Mars conditions [5]. If the identification of hydrothermal deposits indicative of long term hydrothermal activity can be located by the 2003 rover or its successors on future Mars missions, then NASA can make a closer examination of the region containing the deposits in its mission to search for evidence of ancient life on Mars.

References: [1] Fournier, R. O. *et al.* (1994) USGS Bull. 2099. [2] Griffith, L. L. and E. L. Shock (1995) *Nature*, 406. [3] Wolery, T. and S. Daveler (1986) *UCRL-MA-110662 PT IV, LLNL*. [4] Christensen *et al.* (2000) *JGR Planets*, 9623. [5] Jakosky, B. M. (1997) *JGR Planets*, 23,673.

POTENTIAL MER LANDING SITE IN MELAS CHASMA. C. M. Weitz¹, T. J. Parker², and F. S. Anderson²,
¹NASA Headquarters, Code SR, 300 E Street, SW, Washington, DC 20546 (cweitz@hq.nasa.gov), ²Jet Propulsion
 Laboratory, 4800 Oak Grove Drive, Pasadena, CA 91109 (Timothy.J.Parker@jpl.nasa.gov;
 F.Scott.Anderson@jpl.nasa.gov).

Introduction: We have selected one area in Valles Marineris as a potential landing site for the Mars Exploration Rover (MER) mission. After 30 years of analyses, the formation of the Valles Marineris system of troughs and its associated deposits still remains an enigma. Understanding all aspects of the Valles Marineris would significantly contribute to deciphering the internal and external history of Mars. A landing site within Melas Chasma could provide insight into both the formation of Valles Marineris and the composition and origin of the interior layered deposits (ILDs). The ILDs have been proposed as: (1) sedimentary deposits formed in lakes [1, 2, 3]; (2) mass wasted material from the walls [2; 4]; (3) remnants of the wall rock [5]; (4) carbonate deposits [5, 6]; (5) aeolian deposits [2, 8]; and (6) volcanic [4, 8, 9, 10, 11]. More recently, *Malin and Edgett* [12] suggest that the fine-scale, rhythmic layering seen in the interior deposits, as well as other layered deposits in craters, supports a sedimentary origin. Because an understanding of the formation of Valles Marineris and its interior deposits is so important to deciphering the history of Mars, we have proposed a landing site for the MER mission on an exposure of interior deposits in western Melas Chasma (Figure 1). Either MER-A and MER-B could land at this same location.

Site Characteristics: The landing site we identified in Valles Marineris meets the current engineering criteria defined by the MER Project. It is located in southern Melas Chasma with an ellipse center at 9.2° S latitude and 76.7° W longitude for the MER-A and 9.1° S and 72.9° W for MER-B. The guided entry ellipse size is 30 km in width and 82 km in length at this latitude for MER-A and 87 km in length for MER-B. The ellipses range in elevation from -1.5 to -4.0 km using the MOLA gridded map, with the highest elevations located in the northeast. Rock abundance ranges from 10-15% based upon Viking IRTM data. Thermal inertias range from approximately 200 to 450 SI. We have picked ellipses that appear hazard-free in both Viking and MOC wide-angle images. A MOLA profile that corresponds to the MOC high-resolution image shows that slopes are <10° along the layered deposit unit at this location (Figure 2).

A MOC narrow-angle image (M0804367) crosses through the western portion of the landing ellipses (Figure 1). The image shows patches of bright deposits with interspersed small sand dunes (Figure 3). MOC

M0702655 crosses through the western portion of the MER-B ellipse. The southern portion of the ellipses appears to have more dunes than in the north based upon the wide-angle MOC images, but MOC narrow-angle images of this area need to be acquired to determine the extent of dunes here.

Geology of the Site: The landing ellipses are located on patchy bright deposits on the floor in western Melas Chasma. From the MOC image in the west, the region consists of oval-shaped patches of layered deposits with dunes interspersed between these deposits. To the northeast is a thicker deposit of ILD but the surface morphology cannot be determined from the lower resolution Viking and MOC images. However, any encountered rocks within the landing ellipses would likely be those of ILDs, making this an exciting place to land in order to study these deposits.

Just to the south of the landing ellipses is the edge of the canyon wall, which would provide spectacular scenery to be imaged by Pancam and mini-TES. We have been careful to position the ellipses to the north of the wallrock in order to avoid the potentially steep slopes associated with the canyon walls. We have also tried to avoid areas in the north and south that may have more dunes and debris. MER-B is the preferred landing ellipse because it avoids the possible dunes in the south and covers more of the ILDs located to the west.

Expected Results: The site we have selected in Melas Chasma would provide much needed insight into the interior layered deposits. Because of the likely possibility that water once existed in Valles Marineris and because the ILDs may be of lacustrine or carbonate origin, analyses at this landing site would have profound implications toward the climatic evolution of Mars. Exploration of Valles Marineris to search for fossil life forms would also be feasible given the likelihood for water and heat sources in the canyon. If the deposits are determined to have a volcanic origin, then analyses of the compositions would shed light on the volcanic history of Mars and have implications toward its tectonic and outgassing history.

The site will permit the rover to study rocks in-situ at outcrop exposures to determine the composition and origin of the interior layered deposits. The rover should be able to traverse and use the Athena science package to analyze rocks from different layers in exposures, thereby determining the causes of the layering seen in the MOC image for this deposit. From this information, it should also be possible to determine the origin of the deposits and obtain important insights into the

history of the Valles Marineris system. Atmospheric exploration could focus on hazes and clouds, which are occasionally observed in the troughs. This site potentially represents one of the few locations on Mars where the MER rovers can land on proposed sedimentary deposits and should therefore be considered a strong candidate as a landing site.

References: [1] McCauley, J. F. et al., *Icarus*, 17, 289-327, 1972. [2] Nedell, S. S. et al., *Icarus*, 70, 409-441, 1987; [3] Komatsu G. et al., *JGR*, 98, 11105-11121, 1993; [4] Lucchitta, B. K. et al., *JGR*, 99, 3783-3798, 1994; [5] Malin, M. C., *Ph.D. Thesis*, Calif. Inst.

Tech., Pasadena, Calif., 1976; [6] Spencer, J. R., and Croft, S. K., *Rep. Planet. Geol. Geophys. Progr.* 1985, *NASA TM 88383*, 193-195, 1986. [7] Spencer, J. R., and Fanale, F. P., *JGR*, 95, 14301-14313, 1990; [8] Peterson, Christine, *Proc. LPSC 12th*, Pergamon Press, 1459-1471, 1981. [9] Lucchitta, B.K., *Icarus* 86, 476-509, 1990; [10] Weitz, C. M., In *Lunar and Planetary Science XXX*, Abstract #1277, 1999; [11] Chapman, M. G., and K. L. Tanaka *Lunar and Planetary Science XXXI*, Abstract #1256, 2000; [12] Malin, M. C., and K. S. Edgett, *Science*, 290, 1927-1937, 2000.

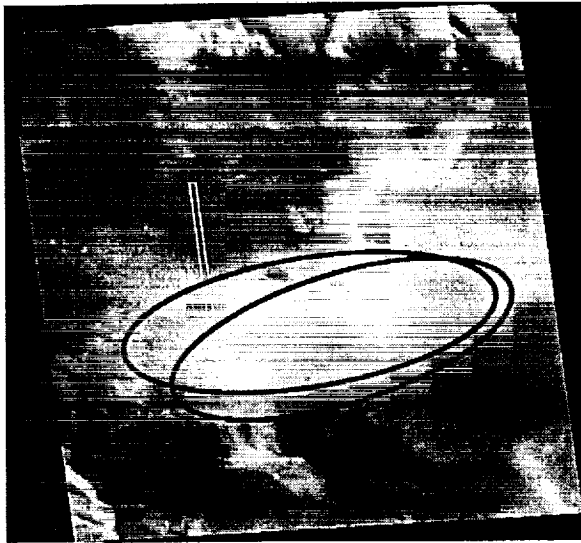


Figure 1. Landing Ellipses in western Melas Chasma shown on MOC M0804368. MER-A landing ellipse is shown in red and MER-B is shown in blue. Also shown is the location of MOC narrow angle image M0804367.

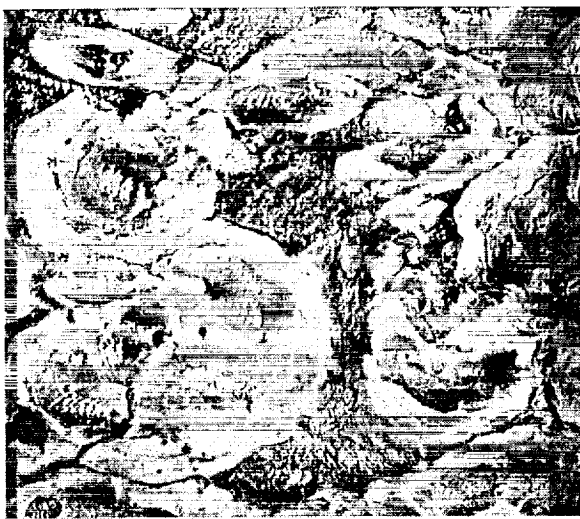


Figure 3. Portion of MOC M0804367 showing the layered unit located in the landing site ellipses. Image is 1.45 km across.

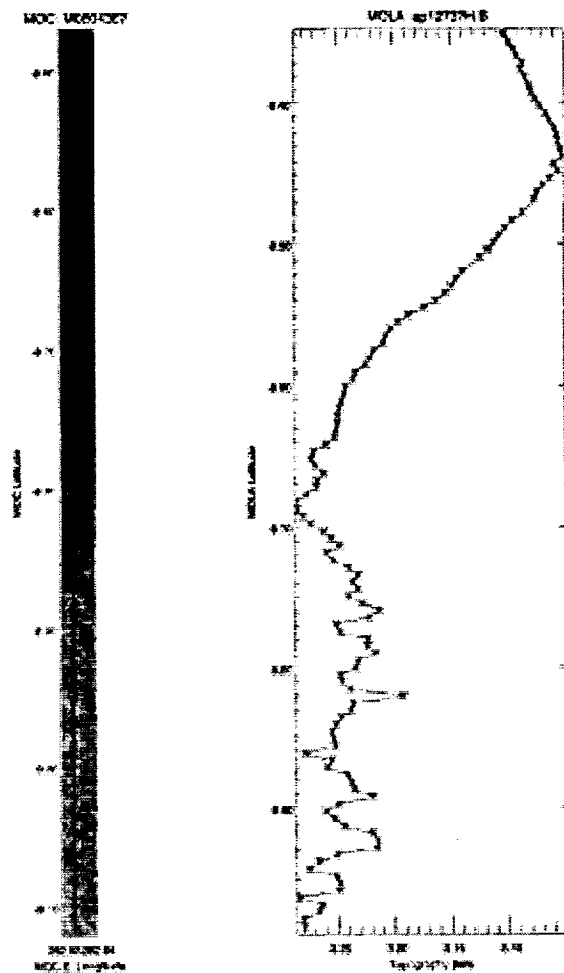


Figure 2. MOC image M0804367 and associated MOLA profile. Slopes at the lower portion of the image, which correspond to the bright deposit in the landing ellipse (see Figure 3), are <math>< 10</math> degrees.